Summer 2017

Evaluation of a prototype inhalable sampler: metal aerosols

Abigail Vonne Tompkins
University of Iowa

EVALUATION OF A PROTOTYPE INHALABLE SAMPLER: METAL AEROSOLS

by

Abigail Vonne Tompkins

A thesis submitted in partial fulfillment
of the requirements for the Master of Science
degree in Occupational and Environmental Health
in the Graduate College of
The University of Iowa

August 2017

Thesis Supervisor: Associate Professor T. Renée Anthony

Graduate College
The University of Iowa
Iowa City, Iowa

CERTIFICATE OF APPROVAL

MASTER'S THESIS

This is to certify that the Master's thesis of

Abigail Vonne Tompkins

has been approved by the Examining Committee
for the thesis requirement for the Master of Science degree
in Occupational and Environmental Health at the August 2017 graduation.

Thesis Committee: _____
T. Renée Anthony, Thesis Supervisor

_____
Thomas M. Peters

_____
Patrick T. O'Shaughnessy

ACKNOWLEDGEMENTS

First, I thank my advisor, Renée Anthony, for her guidance, voice of assurance and for allowing me to work on this project. When I entered her office over a year ago, she asked me what I wanted to gain from my thesis research and I told her that I wanted experience performing personal sampling. Through this project, I have fulfilled my goal and witnessed a side of manufacturing that many people do not see. This research has allowed me to build lasting relationships and gain a vast amount of technical skill. Thank you for being supportive of me in many ways, including funding, and for encouraging and equipping me with the skills I will need to succeed outside of this program.

I am grateful for having Dr. Peters and Dr. O'Shaughnessy not only as professors, but also as my committee members. I thank them for their collaboration, critique and more importantly, for their patience as I encountered multiple timeline setbacks during the formation of this thesis.

I would like to express my gratitude for this program, which brought together an intelligent and vibrant group of people that I will always get to call my friends. Without these friends and my calico cat, I do not believe I would be where I am today. I cannot express how truly grateful and blessed I am to have such supportive, amazing friends.

Lastly, and most importantly, thank you to my family. I have wonderful grandparents who spent their 61st anniversary road tripping from Virginia to see me in Iowa. I will forever be thankful for my mom's continual support provided throughout this phase of my life, even from over 900 miles away and at all times of day. Thank you for allowing me to spread my wings.

ABSTRACT

Occupational exposure limits are generally decreasing and traditional samplers used for quantifying occupational exposures have numerous limitations: cost, disposability, detection of low concentrations, and some even fail to match international inhalable sampling conventions. A low cost, high-flow (10 L min^{-1}) inhalable prototype sampler was developed from the 37-mm cassette and tested in previous studies. These studies called for additional field testing as an area and personal sampler. The sampler was paired with the IOM (2 L min^{-1}), a traditional inhalable air sampler, and deployed in metal working facilities. The samplers were compared to determine whether the prototype matched the IOM and whether the new sampler could improve the sensitivity for detecting lower concentrations of metals. The following processes were sampled: welding, grinding, soldering, pouring, sawing, tending and shooting guns. A total of 21 out of 28 paired samples had detectable metals out of 15 possible metals. There were seven out of eight personal samples and 14 out of 20 area samples with detectable metal concentrations. The average sample time was seven hours, but ranged from 4.2 – 8.3 hours. The most common metals that were detected on 10 or more samples were iron, manganese, zinc, copper, and lead. Metal concentrations collected by the two samplers were not statistically different for the aggregate metal concentrations collected ($p = 0.67$), metals collected by sample type, personal or area ($p = 0.52$) or by particle "sizes," small or large ($p = 0.40$), collected from the processes. While the samplers were not statistically different, linear regression equations to assess the sampler relationships showed that there were significant differences between the two samplers. Over the total metal concentrations collected, the prototype collected about 71% of what the IOM collected. By sample type, the prototype performed better during area sampling as opposed to personal sampling and by particle size, the prototype performed better in the collection of smaller, heat generated particles, as opposed to larger, mechanically generated particles. Though minor differences were found between concentrations detected on the prototype and IOM, it was determined that in general, these differences were negligible in their interpretation and comparison to occupational exposure limits. Plots also indicated that the prototype sampler performs well at sampling low concentrations of metals, however, only a small amount of metals were detected on the prototype that were not found on the IOM, therefore, the improvement of sensitivity was not assessed. High-flow sampling was hindered by the ability of air sampling pumps to maintain the required operation flow rate of 10 L min^{-1} for

the duration of a work shift. Additional field studies are needed to determine whether the sensitivity for detecting lower concentrations of metals can be improved.

PUBLIC ABSTRACT

Air samplers to measure inhalable dust have been found to under sample in comparison to international inhalable sampling criterions. Occupational exposure limits to substances, particularly metals, have become smaller over time and, therefore, there is a need to be able to detect lower concentrations of metals present in the occupational environment. A new, high-flow inhalable prototype sampler was developed and tested. The purpose of this study was to field test and collate the prototype sampler as an area and personal sampler with the IOM inhalable air sampler in metal-working facilities. This study also hoped to determine whether collecting more mass on the prototype due to the higher flow rate would increase sensitivity in the detection of lower concentrations of metals.

Four metal-working sites were studied, and multiple metals with severe health effects were found. Metal concentrations detected by the prototype sampler were not statistically different from the IOM. However, minor differences in metal concentrations collected were found, indicating that the prototype sampler generally collected a little bit less than the IOM. While these minor collection differences were found between the two samplers, in comparison and interpretation of metal concentrations to occupational exposure limits, differences found were generally negligible. This study also found a few metals on the prototype that were not detected on the IOM, indicating potential for improved sensitivity with the new prototype sampler.

Future research will examine the prototype sampler's performance over shorter sampling periods and for inhalable metals that require increased sensitivity for detection, such as beryllium.

TABLE OF CONTENTS

LIST OF TABLES

LIST OF FIGURES

CHAPTER I

LITERATURE REVIEW

Metal-Work Occupational Injury and Illness Data

In the United States alone there are more than 12.3 million workers that comprise the manufacturing industry, with over 3 million involved directly in metal work (North American Industry Classification System) NAICS sector codes 31-33, 332, 333, and 339 (BLS, 2017). As of May 2016, more than 300,000 workers in the U.S. were employed in metals manufacturing, including foundries, and more than 400,000 workers were employed in welding, soldering and brazing operations (Standard Occupational Classification System, SOC 51-4070, 51-4050, 51-4190 and 51-4120) (BLS, 2016). In 2011, the Occupational Safety and Health Administration (OSHA) created a new National Emphasis Program (NEP) directed at the primary metals industries and their large workforce (OSHA, 2011). The NEP followed a review of the Bureau of Labor Statistics (BLS) Census of Fatal Occupational Injuries (CFOI) and was created to address and attempt to reduce or ideally eliminate metal worker exposures to harmful chemical and physical agents. Previous OSHA inspection records had revealed an array of occupational hazards posed from metal dusts and fumes, carbon monoxide, lead and silica, as well as heat and noise (OSHA, 2011).

The BLS revealed consistently high injury and illness rates in metal industries. Specifically, foundries have remained on the BLS list of industries with the highest nonfatal injury and illness rates every year for just over two decades, from 1994 to 2015 (BLS, 2015). In 2012, foundry nonfatal injury and illness rates peaked, yielding one of the top five highest rates of nonfatal injuries and illnesses out of all industries in the United States. The national average incidence rate was 3.7 nonfatal injuries and illnesses per 100 full-time workers, whereas that for ferrous metal foundries was 10.5 per 100 full-time workers in 2012 (BLS, 2012). Iron foundries in that sector had the highest rate at 11.4 per every 100 full-time workers (BLS, 2012).

While there is no breakdown of injury and illness rates by welding, cutting and brazing operations, an OSHA archived document stated that just over half a million workers were at risk for exposure to chemical and physical hazards of these processes (OSHA, 2002). In 2008, welding, cutting and brazing fatalities peaked with 65 fatal injuries attributable to contact with hazardous objects and equipment (BLS, 2008). As of 2014, the number of welding, cutting and brazing fatalities was reduced by half, with fires and explosions emerging as top fatal events or exposures (BLS, 2014).

Metals Process Descriptions

Foundries

Sand casting is a common metal casting process performed by foundries (Stellman, 1998). Casting begins with preparing sand and forming the sand into a mold, which is typically comprised of a mix of silica sand, coal dust, clay and organic binders (Stellman, 1998). A core is also created out of a similar sand and binder mix, which is then placed inside of the mold. Simultaneously, metal/alloy "pigs" or ingots are placed into a furnace and are melted at a high heat dependent upon metal type, and then the molten metal is poured into pots or ladles and transferred to a pour station. At the pour station, molten metal is poured into the molds and allowed to cool. The metal solidifies in the form of the mold, with a hollow area left where cores were positioned. This resulting metal cast is removed from the mold, following transport to a shakeout facility either by an open-belt conveyor or with a shaker-conveyor belt. Shakeout releases the sand molding from the metal cast. The cast is then cleaned, which involves further process by sawing, grinding, and often a chemical dip. The processed sand mix can either be reused in the facility or shipped out and reclaimed at another site. Foundries that create casts by this process are known as "greensand" foundries.

Welding and Soldering

Welding and soldering similarly involve coalescing of metals once they are heated to their melting point. Two common welding methods use a gas-shielded arc: metal- and tungsten-inert gas welding (MIG and TIG) (Stellman, 1998). These types of welding are categorized under gas metal arc welding (GMAW). In TIG welding, a non-consumable tungsten electrode is used to establish an arc to heat the workpiece and a filler rod (Burgess, 1995; Stellman, 1998). The filler metal is melted along a seam or surface of the workpiece as the arc is drawn and, eventually, the metal from the work piece and filler rod pool and cool to form the weld (Burgess, 1995). The MIG welding process is similar to TIG welding, but alternatively, the electrode is a consumable material that serves both to generate the arc and to fill the weld.

Both MIG and TIG welding use inert gases such as argon, helium, nitrogen, or carbon dioxide which are fed to the space around the electrode to prevent oxidation and contamination of the weld (Burgess, 1995; Stellman, 1998). TIG welding is typically used for stainless and low-alloy steels, nickel alloys, as well as copper-nickel, brasses, silver and bronze metals (Burgess, 1995). In MIG welding, the electrode is a hollow consumable wire, which may be shielded by carbon dioxide, or an inert gas shield may be generated by the flux core itself (Burgess, 1995).

The consumable wire composition is usually similar to the parent metal, with a coating of copper to prevent rusting (Burgess, 1995; Stellman, 1998). In general, welding is used for metals with higher melting points, whereas soldering binds metals with lower melting points.

Metal-Working: Hazards

Foundries

Both historical and current hazard assessments as well as OSHA citations indicate that foundry workers are exposed to a variety of hazards, majorly dependent upon the metal composition. Foundry hazards range from silica dust (Gomes, Lloyd, Norman, & Pahwa, 2001; NIOSH, 1985; Rosenman et al., 1996), metal fumes and chemicals (Westberg, Lofstedt, Selden, Lilja, & Naystrom, 2005) to noise (Gomes, Lloyd, & Norman, 2002; NIOSH, 1985), high heat (Gomes et al., 2002; NIOSH, 1985; Rodahl, 2003), nonionizing radiation (NIOSH, 1985), mechanical equipment, vibration, and repetitive motion (Gomes et al., 2002; NIOSH, 1985).

Foundries are generally classified as ferrous or nonferrous dependent upon metal used. Historically, ferrous metal foundries made up the largest foundry sector, melting and manufacturing gray ductile iron, malleable iron, and steel (Burgess, 1995; Stellman, 1998). Nonferrous foundries use metals such as aluminum, copper-based alloys, brass, bronze, zinc, and magnesium (Burgess, 1995; NIOSH, 1985).

Common dust or fume exposure compositions and their respective health effects from foundry melting and pouring processes are listed in Table 1. While foundries work with base metals, they also use metals such as titanium, chromium, nickel and magnesium and these metals may have a significant composition of more hazardous metals, including beryllium, cadmium and thorium (Stellman, 1998). Acute adverse health effects frequently include metal fume fever (MFF) from prolonged or elevated fume exposures (Cheng et al., 2008). In particular, foundries that work with brass and bronze metalloids regularly report lead exposures exceeding occupational exposure limits, especially during melting, pouring and finishing processes (Stellman, 1998). The presence of lead in brass and bronze foundries is one example of how alloys and contaminants contribute to airborne exposures in foundries.

Welding and Soldering

Metal exposures during soldering and welding processes are a function of the welding materials and the base metal used. Hazardous exposures during MIG and TIG welding include metal fumes, fluorides, infrared and ultraviolet radiation, burns, electrical, fire, as well as noise, ozone and nitrogen dioxide (Stellman, 1998). Specifically, during welding, fumes are produced

from the metal being welded, the filler rod, and any metallic coating on welding pieces or the filler rod (*i.e.*, zinc and cadmium from plating, zinc from galvanizing, and copper) (Stellman, 1998). Studies report that as much as 5% of the total electrode mass can appear as fumes during welding (Burgess, 1995).

Some factors that can affect fume concentrations are the current density of the electrode (amperes), wire feed rate, arc time (10-30%), power configuration (direct current or alternating current supply) and straight (electrode negative, work positive) or reverse polarity set up (Burgess, 1995). The most common power usage for welding is direct current (dc), typically with voltages ranging from 10-50 volts (V), with a wide range of current up to 2,000 amperes (A) (Burgess, 1995). The electrode usually contains the parent metal being welded and there are three principal electrodes: cellulosic, rutile and basic. Cellulosic and rutile electrodes contain titanium dioxide metal, while both the rutile and basic electrode contain calcium carbonate metal. The cellulosic electrodes also contain magnesium silicate. In general, coated electrodes have the potential to emit metal fumes containing oxides of potassium, sodium, manganese, iron (II), calcium, aluminum and magnesium (Burgess, 1995).

Similarly to electrodes, filler wire use also affects welding fume composition. For example, steel filler wire typically contains elements like manganese and aluminum, whereas copper and nickel wires can contain titanium; silicon is also found in copper filler wires (Burgess, 1995). In 1990, the International Agency for Research on Cancer (IARC) reported that elements found in fumes from MIG welding were aluminum, nickel, iron, manganese and chromium. An additional concern for MIG welding stems from the use of copper-coated wiring to prevent rust, this copper coating can yield copper oxide fumes. Historically, in comparison of welding oxide fumes emitted from MIG and TIG welding, concentrations of iron oxide were found to be higher in MIG processes (Burgess, 1995).

The acute adverse health effects of welding and soldering are similar to those seen in foundry work. Metal fume fever is commonly observed in workers exposed to zinc and brass processing fumes, however, MFF also arises from exposures to copper, manganese and iron (Stellman, 1998). In 1990, IARC classified welding fumes as “possibly carcinogenic to humans” into Group 2B, but as of April 2017, IARC has confirmed that welding fumes and corresponding UV radiation emitted from welding are carcinogenic to humans and classified them in Group 1 (Guha et al., 2017).

Metal-Work: Aerosol Characteristics

Foundries

Field studies have investigated the particle size distribution for metal fumes in foundries, indicating that most of the activities generate respirable metal aerosols, especially during pouring. In a grey iron foundry, Evans, Heitbrink, Slavin, and Peters (2008) found respirable particles within 0.01 µm to 0.3 µm in size and Cheng et al. (2008) identified particle diameters up to 0.18 µm. In contrast to iron foundries, a study in both a copper smelter and aluminum foundry were in agreeance with the iron results, finding that 35 and 50% of the dust collected was within the respirable fraction, respectively (Michaud, Baril, Dion, & Perrault, 1996).

Grinding is a common process performed in foundries that has also been found to emit respirable particles of different sizes dependent upon the metal being grinded (Zimmer & Maynard, 2002). Zimmer and Maynard (2002) looked at "coarse mode" particle sizes, which are larger than 2.5 µm, but smaller than 10 µm in size (EPA, 2012). This study reported that the particle count median diameter for grinding was 0.85 µm (850 nm) for steel and 0.6 µm (600 nm) for aluminum.

Specifically, in the analysis of particles emitted from foundry pouring operations, Cohen and Powers (2000) reported that only 2% of the measured aerosol had an aerodynamic diameters smaller than 1 µm and that 70% of the aerosols were larger than 5 µm. Cohen and Powers (2000) also suggested that due to the variety and variability of particle sizes emitted in foundries, air sampling methods that do not discriminate by particle size, (*i.e.,* a 37-mm cassette) should be used as an appropriate screening tool.

Several studies demonstrate the varied particle concentrations that can be emitted from foundry operations. In a grey iron foundry, Evans et al. (2008) found that respirable mass concentrations of particles ranged from 0.001 to 1.07 mg m^{-3}; however, they noted that these concentrations were likely underestimated by a factor of two due to equipment limitations. This same study identified that foundry melt decks, as well as pouring, and core/molding processes generally had the highest mass concentrations of respirable particles.

Further studies identified the foundry process that emitted the most particles, with information on particle compositions. In iron foundries, Zhang, Billiet, and Dams (1985) found that coarse particles in dust were primarily generated during pouring processes and Cheng et al. (2008) found the highest concentration of particles from 0.01 to 0.1 µm was 0.07 particles m^{-3}.

Zhang et al. (1985) identified sodium, potassium, manganese, cadmium, and aluminum in dust from iron metal pouring.

Welding and Soldering

Welding and soldering processes generally emit small particles, similar to those sizes identified in foundries. Some of the first studies of welding in shipyards from the American Welding Society (AWS) identified that over half of the fume particles were smaller than 0.25 µm, and that of those, almost all were smaller than 0.05 µm (AWS, 1979; Burgess, 1995). In agreeance with the AWS study, the IARC 1990 study states that for MIG welding, fumes were generally smaller than 0.2 µm, but have aerodynamic diameters that range from 0.11 to 0.23 µm. Research by Glinsmann and Rosenthal (1985) stated that ~90% of welding fume particles are smaller than 1 µm .

Further evaluation of welding fume particle sizes characterized relatively larger fume particles. Malmqvist, Johansson, Bohgard, and Akselsson (1986) studied fumes that were emitted from low hydrogen welding using basic electrodes and concluded that most of the welding fume particles had mass median aerodynamic diameters smaller than 2 µm. Chung and Scott (1997) identified welding particles with aerodynamic diameters ranging from 0.26 to 0.56 µm using a micro-orifice uniform deposit impactor (MOUDI).

Several other welding and soldering studies identify particle size distributions and some characteristics of the emitted aerosols. In a steel foundry and laboratory setting, the background concentration of ambient aerosols were characterized as mostly 0.05 µm (50 nm), but increased to 0.16 µm (160 nm) when MIG welding and soldering processes began (Wake, Mark, & Northage, 2002). In the same study, the count median diameter of welding particles was 0.18 µm, but was smaller (0.072 µm) for soldering operations. The particle geometric standard deviations for these welding and soldering samples were 2.2 and 2.3, respectively, indicating that the particle size distribution of welding fume is likely polydispersed and varying in size as opposed to values closer to 1, indicative of monodispersed aerosols.

Over time, welding fume sampling and corresponding particle characterizations have changed. In 1990, the IARC reported that welding fume concentrations ranged from 2 to 4 mg m^{-3}, but had been decreasing by a factor of two with every passing decade since the 1940's. Hobson, Seixas, Sterling, and Racette (2011) noted that historically, welding fumes were commonly measured as "total" dust (*i.e.,* that measured using a 37-mm cassette) and only recently with inhalable samplers. In the comparison of three inhalable samplers (the IOM, PGP-

GSP and Button), Zugasti, Montes, Rojo, and Quintana (2012), discovered that the IOM sampler, while operating at a lower flow rate (2 L min^{-1}) than the PGP-GSP (3.5 L min^{-1}) and the Button (4 L min^{-1}), collected significantly more welding metal fume than both of the other samplers. Welding fume mass concentrations in these tests ranged from 2 mg m^{-3} to 5 mg m^{-3} .

Lehnert et al. (2012) examined personal exposures of 241 welders: the median mass concentrations for inhalable and respirable concentrations were 2.48 mg m^{-3} and 1.29 mg m^{-3}, respectively. During this study, however, 80 inhalable and 90 respirable particle measurements were found to be below the analytical limit of detection (LOD), especially inside of PAPRs and during TIG welding. TIG welding in general has been found to emit lower concentrations of fumes than other types of welding (Burgess, 1995), however, Lehnert et al. (2012) determined that MIG welding generated more particles in the inhalable range compared to TIG welding. Overall, this study reaffirmed that a welder's exposure was mainly a factor of the welding process and observed that with insufficient LEV, fume concentrations were significantly higher.

Occupational Exposure: Standards and Trends

There are multiple occupational exposure limits that apply to the protection of workers in both foundries and welding and soldering processes. Regulatory agencies such as OSHA and consensus groups such as the American Conference of Governmental Industrial Hygienists (ACGIH) provide occupational exposure limits. OSHA is a federal agency that has regulatory-enforced occupational exposure limits based on an 8-hour time-weighted average (TWA) concentration that a worker should not be exposed to during their shift; these are termed "PELs" or permissible exposure limits. ACGIH is a professional organization of occupational safety and health professionals from both governmental and research organizations that creates threshold limit values (TLVs). OSHA primarily has PELs, ceilings "C," and short-term exposure limit "STEL" designations. A ceiling is an exposure value which may not be exceeded at any time; whereas a STEL is normally a 15-minute TWA not to be exceeded at any time throughout the work day.

Upon initiation in 1970, OSHA had 470 PELs set using the ACGIH and the American National Standards Institute (ANSI) research from the 1950's and 1960's (OSHA, 1996). Since then, OSHA recognized that these earlier limits were outdated and had proved to be insufficient in their purposes of protecting workers health. Nearly two decades later, in 1988, OSHA proposed a rule that lowered existing PELs for 212 toxic air contaminants and established 164 new PELs for previously unregulated contaminants. The final rule set in 1989, however, was

appealed and dismantled in 1992, forcing the Administration's PELs to return to insufficient protection limits that reflected the state of knowledge from 40 to 50 year old research (OSHA, 1996).

Due to the outdated research on which PELs are based, OSHA recognizes that some exposures, while in compliance with the PELs, are hazardous to health, and therefore recommends the reference and use of alternative occupational exposure limits from organizations such as ACGIH TLVs and biological exposure indices (BEIs). ACGIH exposure limit values are not enforceable by OSHA but are based on more recent health effects and toxicological investigations. Under the OSHA Hazard Communication Standard, 29 CFR 1910.1200 part g, OSHA actually requires ACGIH TLVs to be included in "Section 8: Exposure Controls/Personal Protection" of safety data sheets (SDSs), so that workers and health professionals can see both OSHA and these consensus recommendations for exposure limits (OSHA, 2015)

The ACGIH exposure guidelines are published annually and reviewed by professional committees. ACGIH identifies substances that are under current review and those that are proposed to be reviewed in their annual publications. As of 2017, ACGIH has TLVs for more than 650 substances. They are reviewing 109 chemical substances, currently reviewing five, and have 55 that are notified to be under review (ACGIH, 2017). Table 2 lists OSHA PELs and ACGIH TLVs, notations and adverse health effects for common foundry, welding and soldering exposures, using inhalable (I), respirable (R), and "total" (T) size-selective samplers.

Assessing Occupational Metal Exposure

Multiple methods of sampling are available to evaluate occupational exposures to metals, including: wipes, bulk samples, biomonitoring, and air sampling.

Wipes

Wipe sampling can be used to assess the skin of the worker or surfaces in the work environment. In order to take a wipe sample, a wipe is dipped into a solvent or distilled water until moist, then wiped onto the surface being tested (OSHA, 2008). Due to the personal nature of a skin surface sample, it is common to give the wipe to the worker and have them wipe their own skin, typically hands, forearms, faces, and possibly their feet, then return and seal the wipe in a labeled container. The idea is to transfer the surface contaminant onto the wipe, yet not leave any solvent or water on the surface. Wipes are analyzed semi-quantitatively being that

there are no actual surface wipe standards or exposure limits to compare results to (OSHA, 2008)

Lead, however, is one of the few metals that has a direct-read swab, which classifies as a wipe test; the swab changes colors from pink to red if the wiped surface is contaminated (OSHA, 2008). While simple, these direct-read swabs are not without error; if surfaces swabbed were red in color, covered with dark colored dust, or rubbed too hard or long, the color change of the swab can become obscured. Ironically enough, results from said "direct-read" swabs or wipe tests can also be delayed (OSHA, 2008).

Using the wipe method on the skin or clothing of the worker is useful to identify exposures to metals that pose the risk of contact dermatitis (*i.e.,* nickel), irritation, allergic response, or those that can be absorbed directly through the skin, such as beryllium (ACGIH, 2017). Wipe method sampling in the work environment can be used to gauge concentrations of hazardous metals that have deposited on objects such as tools, or stations - a common exposure assessment method for lead (OSHA, 2008). Wipe samples can also be assessed qualitatively by wiping a specified size object, such as a tool handle. Typically, a 10 cm by 10 cm square portion of the tool handle would be wiped, representing an amount of contaminant that would be transferred to the palm of the worker upon contact (OSHA, 2008).

Bulk

Surfaces can be vacuumed to collect dust that may settle onto work areas (OSHA, 2008). Surface samples often provide a secondary analysis of the effectiveness and efficiency of housekeeping procedures on site. If metallic dust settles on equipment or stations within the worker's area, the exposure route of ingestion is presented; ingestion is a primary exposure route for lead. When a worker touches the contaminated surface, the following movements are likely to transfer those metal particles to the eye, nose, or mouth, potentially increasing exposure. Copper in particular is a metal that causes gastro intestinal irritation (ACGIH, 2017).

Biomonitoring

Biological monitoring of exposure focuses on understanding how much of a contaminant or its metabolites is in the worker's body. Human biological samples such as urine, blood, or exhaled breath can be tested for exposure to hazardous metals. Lead biomarkers for example can be detected in blood and bone, whereas cadmium can be identified in both blood and urine (ACGIH, 2017). Finding lead or cadmium in the blood represents recent exposures,

while lead found in bone is indicative of cumulative exposures; a total body burden is reflected upon finding cadmium in urine (ATSDR, 2007, 2012).

Obtaining accurate biological monitoring results is largely a factor of the half-life of the substance and, in some cases, the timing of biological sampling relative to exposure. The half-life is the rate at which the body metabolizes the substance. Lead and cadmium can both have long half-lives in the body, ranging from 30 days to 27 years for lead, and greater than 26 years for cadmium (ATSDR, 2007, 2012). Due to the long half-lives of lead and cadmium, their biological sampling times are not critical; however, hexavalent chromium for example, requires specimen collection at the end of shift at the end of the workweek as its half-life in the body ranges from hours to days (ACGIH, 2017; ATSDR, 2008).

Biological monitoring results provide an indication of the burden of exposure across multiple routes. Inhalation and oral ingestion are primary routes of exposure for both lead and cadmium, providing rational for further air or surface sampling in the workplace (ATSDR, 2007, 2012). For hexavalent chromium, inhalation and dermal routes, or absorption through the skin, are primary entry routes, indicating that air sampling and wiping the worker's skin may be more appropriate assessment methods (ATSDR, 2008).

Air Sampling

In occupational health studies, three key particle size fractions have been developed to evaluate the risk of health effects throughout the human respiratory system. Inspirable/inhalable, thoracic, and respirable particulate mass fractions were developed to represent particle sizes and hazards they pose upon deposition in the three regions of the human respiratory tract (Phalen et al., 1988). The three regions from nose to alveoli are the head airways, trachea-bronchial and gas exchange region. The respirable fraction represents the mass fraction of inhaled particles that have the ability to penetrate to the gas-exchange or alveolar region of the lungs (ACGIH, 2017; CEN, 1993). Particles that penetrate beyond the larynx represent the thoracic fraction, whereas inhalable particles include all particles that can enter the respiratory system from 1.0 to 100 μm, but predominantly represents the upper airways (CEN, 1993). Mass fractions were used to develop equations for ideal size-selective samplers which express sampling efficiency as a function of the particle aerodynamic diameter and specify the fraction of optimal concentrations collected, for example, the inhalable particulate mass fraction is termed "IPM" (Soderholm, 1989).

The particle sizes of aerosols ultimately determine how they will move or deposit within the human respiratory tract, therefore, size-selective sampling for exposure assessments are often necessary (Phalen et al., 1988). An aerodynamic diameter at which 50% of particles larger and smaller than that size are deposited on the collecting filter is used to represent each fraction's sampling criterion and is known as the d_{50}. The d_{50} particle sizes for the respirable and thoracic fractions are 4.0 and 10.0 µm, respectively, but the inhalable fraction does not have a d_{50} particle size, instead, the criterion merely decays to about 50% efficiency for particles 50 to 100 µm in size (ACGIH, 2017; CEN, 1993).

Air sampling is one of the most common forms of metal exposure assessments in the occupational environment. Active sampling requires the use of a pump and tubing to pull air from the room onto a collection media, typically a filter. Sample media for particles may include mixed cellulose ester (MCE), polyvinyl chloride (PVC) or polytetrafluoroethylene (PTFE). The type of filter media used is a function of the analytical method chosen for analysis. Thin MCE filters are typically used for metals digestion, while PVC and PTFE filters are more weight stable and can be used for obtaining gravimetric weights of particles.

The first aerosol sampler used in the U.S. was the 37-mm cassette. The 37-mm cassette was initially a mere filter holder for aerosol sampling and has been referred to as a "total" dust sampler. In the 1980's the Institute of Medicine (IOM) sampler was developed to better reflect how aerosols enter into the mouth and nose of a worker. Later, the Button sampler was found to have similar performance to the IOM. The IOM and Button were introduced respectively and were specifically designed to sample, and reportedly do, the IPM fraction, with both featuring 25-mm filters and differing inlet entries (Aizenberg, Grinshpun, Willeke, Smith, & Baron, 2000; Hauck et al., 1997; Mark & Vincent, 1986). Inlet sizes range from the 37-mm cassette 4-mm inlet, to the IOM inlet at 15-mm and the Button, a hemispherical screen with ~380 µm pores to prevent very large particles from entering (Baron, 2003).

The 37-mm cassette is specified in NIOSH sampling methods for particulates (Method 0500), and by OSHA for particulates not otherwise regulated (PNOR) under OSHA method PV2121 and for metal and metalloid particulates under Method ID-125G (OSHA, 2004). These methods still specify the use of this "total" sampler, even though studies have proven that it does not match the IPM curve. Multiple sampler comparison tests have revealed the deficiencies of the 37-mm cassette in contrast to the IOM. These efficiency tests prove that the 37-mm cassette does not match the IPM curve and in fact, it actually under samples particles

that have an aerodynamic diameter larger than 30 to 45 µm (Aizenberg et al., 2000; L. C. Kenny, Aitken, Baldwin, Beaumont, & Maynard, 1999; L.C. Kenny et al., 1997; Liden, Melin, Lidblom, Lindberg, & Noren, 2000; Mark & Vincent, 1986). Lab studies identified that the IOM collects up to 1.7 times more than the 37-mm cassette (L. C. Kenny et al., 1999; L.C. Kenny et al., 1997) whereas field comparisons of the IOM and 37-mm cassette both open- and close-faced found that the IOM collected 2 to 3 times more than the cassette, depending upon the size of aerosols in the workplace (Liden et al., 2000).

Other studies point out the poor efficiency of the 37-mm cassette in both of its operations, open- and closed-face, and demonstrate the effects of sampler modifications in comparison to the IOM. Liden et al. (2000) reported that 37-mm cassette both open- and closed-face had similar sampling efficiencies, but collected only 10% of the total airborne particle concentrations. Several studies witnessed increased sampling efficiency of the 37-mm cassette when punching a larger inlet hole, which caused oversampling by 35% in comparison to the IOM (Anthony, Landazuri, Van Dyke, & Volckens, 2010; Clinkenbeard, England, Johnson, Esmen, & Hall, 2002).

Particulate losses and wall deposits due to electrostatic properties, bounce and aspiration are of particular concern with both the 37-mm cassette and IOM. Mark (1990) highlighted the attributable error likely produced when internal surface deposits are not included in dust sampling analysis. This study reported that 3 to 44% of the total mass of dust in simulated exposure measurements was deposited on internal sampler surfaces. Liden et al. (2000) similarly identified that ~35% of dust mass deposited in the IOM is actually deposited onto the cassette walls.

Harper and Demange (2007) reviewed metals sampling recovery studies for the 37-mm cassette and IOM. A French study comparing the IOM and 37-mm cassette in three different foundries revealed through gravimetrics that the IOM collected more than the cassette, but upon specific metals analysis, close agreement was found between all of the samplers when wall deposits were accounted for (Demange, Gorner, Elcabache, & Wrobel, 2002). In 2006, a study comparing samplers at a lead mine concentrator mill and lead-acid battery recycler found that considerable particulate was deposited on the interior walls of both the 37-mm cassette and IOM; upon including a wipe method into analysis, this study determined that IOM and 37-mm cassette wall losses were again, similar (Harper, Pacolay, Hintz, & Andrew, 2006).

In specific metals exposure assessments, the 37-mm cassette is primarily used for sampling beryllium. Oddly enough, the ACGIH TLV for beryllium specifically requires a comparison to the inhalable particle fraction (ACGIH, 2017; Brisson & Archuleta, 2009). It is clear that the 37-mm cassette on its own does not collect the inhalable fraction efficiently, especially without the inclusion of wall deposits. In contrast, many sites include policies to follow TLV exposure recommendations, those of which for beryllium are set much lower than most other metals (Brisson & Archuleta, 2009). These facts indicate that the 37-mm cassette is not adequate for sampling beryllium, especially not when comparing exposure values to the ACGIH TLV.

Due to the likelihood of particle wall deposits, wipe and rinse methods for cassette analysis, specifically for metals, have been suggested. OSHA's Sampling and Analytical Methods for Metal and Metalloid Particulates in Workplace Atmosphere by inductively coupled plasma (ICP) Method ID-125G requires that loose dust be transferred from the 37-mm cassette to the digestion vessel and that the inside walls of the cassette be both rinsed and wiped to include all collected material in the analysis (OSHA, 2004) .

Several studies emphasize the particular importance that wiping or rinsing the inside of the cassette plays in obtaining accurate metals analyses (Ceballos, King, Beaucham, & Brueck, 2015; Hendricks, Stones, & Lillquist, 2009). Even with the inclusion of the wipe method during analysis, several studies indicate that the IOM may actually under sample large particles during exposure assessments (Kenny et al., 1999; Kenny et al., 1997). One pharmaceutical study recommended a liquid extraction in 37-mm cassette analysis after the collection of dust revealed only 22% of the dust collected on the filter, with presumed electrostatic properties causing 62% of the dust collected to be adhere to the inside surface of the cassette top (Puskar, Harkins, Moomey, & Hecker, 1991).

Other studies suggest that an internal cassette or cartridge, such as the cassette in the IOM, be used to eliminate wall losses; while this works for analysis, it proves problematic for gravimetric analysis (Hendricks et al., 2009; Mark, 1990). Another solution to the wall deposit problem recommended by NIOSH is to use an internal cartridge or capsule that is actually sealed to the filter, so that the filter and capsule can be analyzed (Baron, 2003; Puskar et al., 1991). Several cartridges that adhere to filters have been designed for the 37-mm cassette, but they are expensive, lack quality control and they come with analytical limitations. The PVC Accu-CAP® and cellulose acetate Solu-CAP® are offered by SKC and cost $182.75 and $224.50 for 60 and 50

caps, respectively (~$3.00 and $4.50 per cap) (SKC, Eighty Four, PA). These caps claim to eliminate the need to wipe or rinse the inside of the cassette during analysis. Alternatively, Zefon offers PVC Gravi Sert™ and cellulose acetate Solu-Sert™ capsules, costing $182.00 and $190.00 for 50 caps, respectively (~$3.60 and $3.80 per cap) (Zefon International, Inc., Ocala, FL). These caps yield a similar SKC claim and apparently capture 100% of particles that are collected by the filter cassette. The Accu-CAP® and Gravi-Sert™ are both suitable for gravimetrics, but not for specific metals analysis. One study that used the Accu-CAPs® observed that the capsules were difficult to remove and about one in twenty capsules varied in both appearance and construction (O'Connor, O'Connor, Feng, & Ashley, 2014). As for metals analysis, the Solu-CAP® and Solu-Sert™ are suitable, but the Solu-Sert™ is only suitable for analysis methods of 12 metal contaminants.

One study specifically notes the tendency for air samplers to be costly and time-consuming to clean, on top of documented performance issues (Brisson & Archuleta, 2009). The 37-mm cassette is considered disposable and therefore has a lower price at around $1.00, but, while inexpensive, again, does not meet the inhalable sampling criteria. The IOM conductive plastic sampler costs $85.00 and the stainless-steel version costs $269.00; the Button (only available in stainless steel) is more expensive yet at $275.00 (SKC, Eighty Four, PA). The 37-mm cassette while following the NIOSH Method for PNOR, is to be operated between 1 and 2 L min^{-1}; the IOM follows suit and samples at 2 L min^{-1} in an ideally low air movement environment. The Button sampler, however, is not as sensitive to air movement and operates at a slightly higher flow rate of 4 L min^{-1}. Both the Button and IOM are reusable, however, there are associated cleaning costs, and the IOM is recommended to be discarded due to contamination concerns after beryllium sampling (Brisson & Archuleta, 2009).

The IOM in particular, needs to be cleaned ultrasonically or wiped with isopropyl alcohol, but its 3 different O-rings need to be individually cleaned with water. The Button has an advantage with no internal walls, yielding no wall deposits, but its performance, while better than the 37-mm cassette, does not completely match the IPM convention as well as the IOM and very large particles can actually clog the entry (Aizenberg et al., 2000; Harper et al., 2006).

Performance differences between the Button and IOM samplers have also been studied for solid and liquid particles and for varying flow rates (Gao, Chen, Baron, & Soderholm, 2002; Koehler, Anthony, Van Dyke, & Volckens, 2012; Zhou & Cheng, 2010). Upon mannequin testing facing the wind, the Button, due to its porous screen entry, aspirated large liquid droplets, while

large solid droplets bounced, affording them the potential enter the sampling air stream again (Koehler et al., 2012). The same study reported that seven times more mass of ~100 um droplets were deposited onto the screened inlet of the Button, as opposed to the filter (Koehler et al., 2012). An earlier study of the Button discovered that in high wind settings, due to the low flow rate of the early version at 2 L min^{-1}, caused aspirated particles traveled back out of the sampler near the outer edges; a suggested remedy was to increase the flow rate to 10 L min^{-1} (Gao et al., 2002). Another study tested an increased flow rate, but with the IOM, at 10.6 L min^{-1} compared to the standard 2.0 L min^{-1} (Zhou & Cheng, 2010). This study found that at a high wind speed, the sampling efficiencies of the IOM at both flow rates were similar, except for with particles of 80 and 100 µm in size.

Continuing with the ease of use of each of the samplers, sample analysis and contamination prevention proves to be a bit more tedious for the IOM. The 37-mm cassette and Button are by far, much more user-friendly for analysis transport after sampling. The IOM cassette needs to be removed from the sampler housing and placed into a "transport clip." The transport clip is one piece of plastic that bends a bit to allow the cassette to slide inside, leaving 3 sides of the cassette open to the environment. Demange et al. (2002) noted that for this transport reason, the risk of polluting or contaminating IOM samples was much higher than that of the 37-mm cassette. After sampling, all of the samples can then be analyzed gravimetrically by mass, or sent into an accredited laboratory for elemental analysis by inductively coupled plasma atomic emission spectrometry (ICP-AES).

For gravimetric analysis, the mass of the filter and capsule, if used, for the 37-mm cassette are measured. For the IOM, the mass of both the filter and cassette are measured, and for the Button, solely the internal filter is weighed. To perform the gravimetric method, weight stable filters and obviously capsules, again, if used, are needed to minimize the influence of hygroscopic and electrostatic properties. Weight-stable filters are generally PVC, Teflon or PTFE in composition. As an extra precaution, the gravimetric method usually involves allowing the filter and cassette to remain in a temperature and humidity controlled room for seven days before weighing and sampling, to stabilize and minimize problematic properties.

The ICP-AES method, such as the NIOSH Method 7300 uses for metals, involves an acid digest of the filters, with MCE filters preferred. Once digested, the sample is introduced into the spectrometer and is atomized into a mist. The mist follows an argon gas stream, exciting the elemental electrons, which are then characterized into corresponding elemental concentrations

dependent upon their light wavelength that is emitted (USGS, 1999). This metals analysis method is influenced by difficulties of trying to include wiped or rinsed particle deposits from the internal walls of samplers.

Two important constraining factors of analyzing sampling results are the analysis laboratory's LOD and limit of quantification (LOQ). The LOD is the mass or analyte at which the analyst can be ~99% confident that the instrument (spectrometer) signal is at or greater than (Kennedy, Fischbach, Song, Elller, & Shulman, 1995). The LOQ is the lowest mass that can be reported with acceptable precision, either corresponding to the mean blank signal or above which analyte recovery is greater than or equal to 75% (Kennedy et al., 1995). Several studies comparing samplers portray that analytical LODs are in fact, limiting, when trying to characterize exposures. A beryllium study on wall deposits denotes the importance and trickiness that the particular metalloid exhibits upon sampling due to its lower exposure values (Brisson & Archuleta, 2009). One study highlighted detection difficulties experienced with the IOM during sampling low concentrations (Cheng et al., 2005). When samplers are operated at lower flow rates, (*i.e*., Button or IOM) the detection limits may not always be met with certainty. In particular, the TIG method of welding was shown to have difficulties achieving laboratory LODs (Burgess, 1995).

With the limitations and alterations that have been made to these traditional samplers in mind, a high-flow prototype inhalable 37-mm cassette sampler was designed using computational fluid dynamics in a simulated wind tunnel (Anthony et al., 2010). This original prototype design was termed the personal high-flow inhalable sampling head (PHISH) and in contrast to the 37-mm cassette, operated at 10 L min^{-1} and exhibited a flat-face with a larger 15-mm screened inlet containing 254 µm diameter pores (Anthony et al., 2010). This sampler however, while designed to match the inhalable particulate mass curve, was not deemed suitable for sampling the inhalable fraction of liquid aerosols due to the larger mesh inlet pore size (Anthony et al., 2010; Koehler et al., 2012). Further sampling efficiency study of the modified prototype samplers compared liquid and solid particle sampling efficiencies of both prototypes against the Button and IOM. The open-faced inlet prototype improved the sampling performance for liquid aerosols, performing better than both the Button and the IOM samplers (Koehler et al., 2012).

Due to the limitations of the mesh inlet, additional design modifications were studied using computational modeling to improve the high-flow inhalable sampler design. The effect of

the inlet diameter, face geometries and perimeter projections were examined using the 37-mm cassette as the baseline dimensions (Anthony, Sleeth, & Volckens, 2016). The study indicated that a second modified prototype featuring the same 15-mm inlet, but open-faced, as opposed to mesh, performed better compared to the other designs (Anthony et al., 2016).

Prior sampler studies emphasize the consideration for particles that deposit on the walls of samplers and this factor was also considered in assessment of the newest prototype sampler (Koehler et al., 2012). Due to the increased flow rate of 10 L min^{-1}, it was thought to be less likely that particles would have enough time to deposit onto the walls of the sampler (Koehler et al., 2012). During testing, the Button experienced particle migration from the filter to the outer rim of the sampler due to rotation and vibration, an event that was mimicked in the PHISH, therefore, an internal capsule similar to the Accu-CAP® was modified and used to recover solid particles collected by the PHISH (Koehler et al., 2012). This study concluded that the Button, IOM and PHISH had the same sampling efficiencies when tested with a 1 µm liquid aerosol, and that the open-faced PHISH did better at sampling solid particles as opposed to liquid.

While the IOM and Button samplers are relatively high in cost, the PHISH sampler upon market introduction would only cost about $10 and it would be disposable. One unique aspect of the PHISH is that due to the inclusion of an internal capsule, this sampler eliminates the concern for particles depositing of the walls. In addition to the capsule, this study and others mention that the high flow rate makes this sampler desirable for shorter sampling durations or in low concentration sampling environments in which the analytical limit of detection needs to be met (Anthony, Cai, Mehaffy, Sleeth, & Volckens, 2017; Koehler & Peters, 2015; Landazuri, Saez, & Anthony, 2016; Stewart et al., 2017).

The new version of the PHISH sampler with the open inlet is pictured in L'Orange, Anderson, Sleeth, Anthony, and Volckens (2016) and was tested similarly to its earlier version in a low-velocity wind tunnel on a manikin (Anthony et al., 2010). The sampler closely matched the IPM criterion and showed potential for sampling low concentrations to reach laboratory LODs (L'Orange et al., 2016). It was determined that the sampler would be capable of evaluating workplace concentrations as low as 15 µg m^{-3} gravimetrically (LOD = < 14 µg) over an 8-hour sampling time period (L'Orange et al., 2016). Along with the improvement to detection limits, the sampler is deemed a simpler alternative to the Button and IOM in both its assembly and transport for analytical purposes (Anthony et al., 2017; L'Orange et al., 2016). Figure 1 depicts the IOM, 37-mm cassette and prototype sampler dimensions.

Due to the performance of the prototype sampler in previous studies, matching the IPM curve on its own and matching it as well as the IOM, it was determined that the operation flow rate of the IOM (2 L min^{-1}) should be lab tested with the prototype (Stewart et al., 2017). Physical prototype samplers with the 15-mm inlet and flat face were positioned on a mannequin in a wind tunnel and operated at both 2 L min^{-1} and 10 L min^{-1} for 45 minutes to avoid overloading (Stewart et al., 2017). Particles tested only ranged from 4.9 to 32.7 µm in size, but ultimately, no significant difference in particles collected or the sampler efficiency at both flow rates was found (Stewart et al., 2017)

Field testing of the prototype performance as an area sampler in a swine farrowing room was also conducted. Paired prototype and IOM samplers were deployed at three fixed locations for 24 hours on 19 days, over a 3-month period; the prototype operated at a flow of 8.2 L min^{-1} (Anthony et al., 2017). By gravimetric analysis of dust collected, an insignificant mean difference between the prototype and IOM sampler was 0.03 mg m^{-3}, indicating that the prototype sampler collected more particles, on average, than the IOM, but an insubstantial amount (Anthony et al., 2017). This study recommended that future work explore the performance of the prototype sampler in dustier environments and as a personal sampler (Anthony et al., 2017).

Objectives

The purpose of this study is to evaluate the performance of the high-flow inhalable prototype sampler in comparison to the low-flow IOM as personal and area samplers in occupational environments that generate metal aerosols. Air concentrations for multiple metals processes will be measured using collocated samplers, comparing concentrations between the prototype and IOM sampler. Field measures will additionally be evaluated to determine whether collecting more mass on the high-flow prototype sampler increases the sensitivity for detecting lower concentrations of metals.

Table 1. Common dust and fume exposures and their respective health effects from foundry melting and pouring processes.

Metal	Dust or Fume	Health Effects	Notations
Iron and Steel	Iron Oxide	Pneumoconiosis	A4
	Lead, leaded steel	Central and peripheral nervous system impairment; hematologic effects	A3, BEI
Bronze and Brass	Copper	General and gastrointestinal irritation; metal fume fever	-
	Zinc	Metal fume fever	-
	Lead	Central and peripheral nervous system impairment; hematologic effects	A3, BEI
	Manganese	Central nervous system impairment	A4
Aluminum	Aluminum	Pneumoconiosis; lower respiratory tract irritation; neurotoxicity	A4
Magnesium	Magnesium	Upper respiratory tract; metal fume fever	A4
Zinc	Zinc	Metal fume fever	-
Cadmium	Cadmium	Kidney damage	A2, BEI
Lead alloys	Lead	Central and peripheral nervous system impairment; hematologic effects	A3, BEI
	Antimony	Skin and upper respiratory tract irritation	-
	Tin	Eye and upper respiratory tract irritation, headache, nausea, central nervous system and immune effects	A4, skin
Beryllium	Beryllium	Beryllium sensitization, berylliosis	A1, skin, DSEN, RSEN
Beryllium-copper	Beryllium	Beryllium sensitization, berylliosis	A1, skin, DSEN, RSEN

*Adapted from Burgess (1995)

A1 - Confirmed human carcinogen.

A2 - Suspected human carcinogen.

A3- Confirmed animal carcinogen with unknown relevance to humans.

A4 - Not classifiable as a human carcinogen.

A5 - Not suspected as a human carcinogen.

Skin - This substance can be absorbed through the skin.

DSEN - This substance has the potential to produce dermal sensitization.

RSEN - This substance has the potential to produce respiratory sensitization.

BEI - Biological Exposure Indice; biological monitoring should be instituted for this substance.

Table 2. OSHA PELs and ACGIH TLVs, notations and adverse health effects for common foundry, welding and soldering exposures, using inhalable (I), respirable (R), and "total" (T) size-selective samplers.

	OSHA PEL (mg m^{-3})			ACGIH TLV (mg m^{-3})				
Metal	**I**	**R**	**T**	**I**	**R**	**T**	**TLV Notations**	**TLV Adverse Health Effect**
Aluminum	-	5	15	-	1	-	A4	Pneumoconiosis, lower respiratory tract irritation, neurotoxicity
Beryllium	-	-	0.002	0.00005	-	-	A1, Skin, DSEN, RSEN	Beryllium sensitization and chronic beryllium disease (berylliosis)
Cadmium	-	-	0.01	-	0.002	0	A2, BEI	Kidney damage
Chromium	-	-	0.5	-	-	0.5	A4	Upper respiratory tract irritation and skin irritation
Copper	-	-	0.1	-	-	0.2	-	General and gastrointestinal irritation, metal fume fever
Iron	-	-	10	-	5	-	A4	Pneumoconiosis
Lead	-	-	0.05	-	-	0.1	A3, BEI	Central & peripheral nervous system impairment, hematologic effects
Manganese	-	-	5*	0.1	0.02	-	A4	Central nervous system impairment
Nickel	-	-	1	1.5	-	-	A5	Dermatitis, pneumoconiosis
Zinc	-	-	5	-	2	10** 10	-	Metal fume fever

*This value is "Ceiling" concentration that should not be exceeded at any time during a workday.
**This is a Short Term Exposure Limit "STEL" value is a 15-minute Time-Weighted Average (TWA) exposure that should not be exceeded at any time during a workday.

A1 - Confirmed human carcinogen.

A2 - Suspected human carcinogen.

A3- Confirmed animal carcinogen with unknown relevance to humans.

A4 - Not classifiable as a human carcinogen.

A5 - Not suspected as a human carcinogen.

Skin - This substance can be absorbed through the skin.

DSEN - This substance has the potential to produce dermal sensitization.

RSEN - This substance has the potential to produce respiratory sensitization.

BEI - Biological Exposure Indices; biological monitoring should be included for this substance.

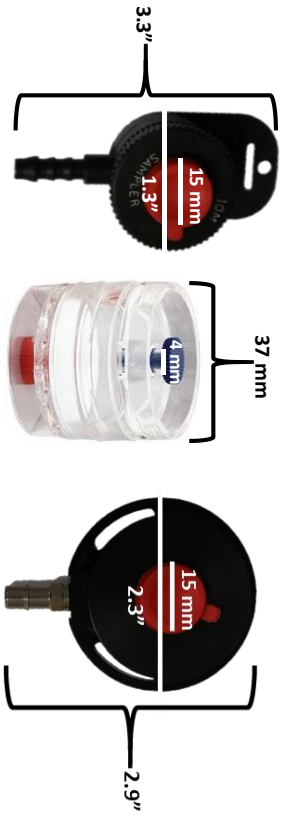

Figure 1. IOM, 37-mm cassette and prototype sampler dimensions.

CHAPTER II

METALS SAMPLING EVALUATION

Introduction

In the United States, more than 12.3 million workers comprise the manufacturing industry and over 3 million are directly involved in metal work NAICS (North American Industry Classification System) sector codes 31-33, 332, 333, & 339 (BLS, 2017). Due to the workplace fatalities documented by the Bureau of Labor Statistics (BLS) in the primary metals industries, the Occupational Safety and Health Administration (OSHA) created a National Emphasis Program in 2011 to address and reduce metal worker exposures to harmful chemical and physical agents (OSHA, 2011). When looking at rates of nonfatal injuries and illnesses in metals industries, for more than twenty years, foundries have remained on BLS charts for industries with the highest rates, OSHA documented that over half a million workers in welding, cutting and brazing operations are at risk for exposure to chemical and physical hazards of these processes (BLS, 2014; OSHA, 2002).

Potential inhalation hazards both in foundries and welding and soldering process are primarily dependent upon the metal composition used during processing. Ferrous foundries typically work with gray ductile iron, malleable iron and steel, whereas nonferrous foundries may use aluminum, copper, brass, bronze, zinc or magnesium metals (Burgess, 1995; NIOSH, 1985; Stellman, 1998). These metals can also be comprised of even more hazardous metals like beryllium and cadmium (Stellman, 1998). In welding and soldering tasks, fumes can contain components of the electrode, metal being processed, filler rod and any metal coatings. Nickel and chromium have been identified in welding fume along with oxides of manganese, iron (II), aluminum, copper and magnesium (Burgess, 1995).

Metal fume fever is a common acute outcome from metals processing in foundries as well as welding and soldering, but is primarily seen from working with zinc (Stellman, 1998). Dependent upon metal fumes generated from these processes, other potential adverse health effects from metals processing include pneumoconiosis, central and peripheral nervous system impairment, sensitization, respiratory or skin irritation and even kidney damage (ACGIH, 2017). In 1990, welding fumes were only considered “possibly carcinogenic to humans” by the International Agency for Research on Cancer (IARC), but as of April 2017, welding fumes and UV radiation from welding have now been moved into Group 1 as confirmed human carcinogens (Guha et al., 2017).

Studies of the particle sizes emitted from foundry, welding and soldering processes have confirmed that a majority of the particles are respirable (AWS, 1979; Cheng et al., 2008; Chung & Scott, 1997; Evans et al., 2008; Glinsmann & Rosenthal, 1985; Malmqvist et al., 1986; Michaud et al., 1996; Wake et al., 2002). In foundries, the highest particle mass concentrations were detected during pouring and melting processes (Cheng et al., 2008). Welding fumes studied by IARC in 1990 found concentrations ranging from 2 to 4 mg m^{-3}, and congruent studies from 2012 identified mass concentrations ranging from 1.29 mg m^{-3} to 5 mg m^{-3} (Lehnert et al., 2012; Zugasti et al., 2012).

In general, three samplers have been used to collect particles and assess respective concentrations produced from metals processes: the 37-mm cassette, which can be operated both open- or closed-face, as well as the Institute of Medicine (IOM) or Button (Brisson & Archuleta, 2009; Hobson et al., 2011; Zugasti et al., 2012). Cohen and Powers (2000) advised the use of the 37-mm cassette "total" dust sampler to assess particles emitted in foundries and stated that it does not discriminate by particle size. Additionally, both the National Institute for Occupational Safety and Health (NIOSH) and OSHA particle sampling methods specify the use of the 37-mm cassette for sampling Particulates Not Otherwise Regulated (PNOR) as well as metal and metalloid particles (OSHA, 2004)

Repeated studies of the 37-mm cassette both open- and close-faced have revealed the sampler under samples particles larger than 30 to 45 µm and accordingly, it does not match the IPM curve (Aizenberg et al., 2000; Kenny et al., 1999; Kenny et al., 1997; Liden et al., 2000; Mark & Vincent, 1986). In evaluation of the 37-mm cassette in both of its forms, open- and closed-face, the sampler only collected 10% of total particulate concentrations, completely invalidating the "total" dust sampler designation as an inhalable size-selective sampler (Liden et al., 2000). Hence, using the 37-mm cassette with large particles in metal exposures assessments may underestimate worker exposure.

In addition to particulate collection deficiencies, both the 37-mm cassette and IOM are affected by particulate losses due to deposition on their inner cassette walls (Ashley & Harper, 2013; Harper & Demange, 2007; Harper et al., 2006; Liden et al., 2000; Mark, 1990; Mark & Vincent, 1986; Puskar et al., 1991). Studies that included a wipe and rinse recovery method into metals analysis determined that the IOM and 37-mm cassette actually have similar particle wall losses, but the difference is that the IOM was specifically designed to include wall deposits into particulate analyses (Demange et al., 2002; Harper et al., 2006). Earlier remedial studies,

however, speculated that even with the incorporation of wipe methods, the IOM still under samples large particles in respect to international inhalable particulate mass (IPM) conventions (Kenny et al., 1999; Kenny et al., 1997). One study indicated that despite equivalent particulate measurements found upon metals analysis, gravimetrics were contradicting, as the IOM was found to collect more particles by weight than the 37-mm cassette (Demange et al., 2002).

The Button sampler is not affected by particulate wall losses due to its lack of internal walls, but the sampler does have limitations. The Button does not match the IPM convention as well as the IOM and the inlet is easily clogged by larger particles (Aizenberg et al., 2000; Harper et al., 2006; Koehler et al., 2012). Some studies even report that the Button design operation at both 2 and 4 L min^{-1} allows particles to reenter the sampling air stream due to bounce off of the screen and leaks near the sampler edges (Gao et al., 2002; Koehler et al., 2012). A suggested countermeasure by Gao et al. (2002) to alleviate leak problems involved increasing the 2 L min^{-1} Button's flow rate to 10 L min^{-1} . A high-flow operation study of the IOM found that the sampling efficiency at 10 L min^{-1} was similar to that of the sampler at 2 L min^{-1} (Zhou & Cheng, 2010).

Modifications to the 37-mm cassette to account for particle losses evolved from the internal cassette featured in the IOM (Hendricks et al., 2009; Mark, 1990; Puskar et al., 1991). However, available internal cartridges and capsules pose further obstacles, including cost and quality control issues coupled with analytical limitations that yield suitability for gravimetrics, but not specific metals analysis (O'Connor et al., 2014)

Additional exposure assessment costs are incurred if samplers are not disposable or reusable (Brisson & Archuleta, 2009). Repurchase of the IOM is required once beryllium is confirmed as a sampled contaminant metal, as the element is particularly difficult to clean and dangerous even in small amounts (Brisson & Archuleta, 2009). Due to its lower flow rate, IOM limitations are accentuated in the sampling of lower concentrations, with samplers notoriously struggling to reach laboratory LODs (Cheng et al., 2005).

In account of exposure assessment hindrances due to traditional sampler designs, a low-cost, disposable prototype high-flow inhalable sampler was designed from the 37-mm cassette (Anthony et al., 2010) and tested in wind tunnels (L'Orange et al., 2016). Further challenge and testing of the prototype with solid and liquid particles led to final modifications which allotted for an open 15-mm inlet and an internal capsule attached to the filter which eliminated deposits concerns observed in other samplers (Anthony et al., 2016; Koehler et al., 2012).

Due to the higher flow rate of this sampler at 10 L min^{-1}, several studies indicate that the prototype sampler yields promise for detecting lower concentrations and potentially for shortening necessary sampling durations (Anthony et al., 2017; L'Orange et al., 2016; Landazuri et al., 2016; Stewart et al., 2017). The 3-piece prototype performance closely matches the inhalable sampling criterion and is therefore deemed a simpler alternative to both the Button and IOM samplers (Anthony et al., 2017; L'Orange et al., 2016).

Actual field testing of the prototype as an area sampler in a swine farrowing room indicated that the IOM did collect more particles than the prototype, but the difference was nonsignificant (Anthony et al., 2017). Anthony et al. (2017) recommended that future work examine the prototype's performance as a personal sampler and in dustier environments.

The goal of this study was to evaluate the performance of the prototype inhalable sampler in comparison to the IOM as both personal and area samplers in occupational environments that generate metal aerosols. These field measures were used in this study to determine whether concentrations collected by the samplers were the same and whether or not the high-flow sampler would increase the sensitivity for being able to detection lower concentrations of metals.

Methods

Sampling Site Information

Once obtaining Institutional Review Board (IRB) approval, four indoor metal-working sites were recruited into this study. The study took place from May 17 through December 8 of 2016. Sampling dates were chosen according to site scheduling availability. Indoor sampling sites included: a foundry, art studio, manufacturing facility, and a shooting range.

Sampler Assemblies

Prototype assembly was followed according to Anthony et al. (2017), but to address the pressure drop across the prototype sampler, the back-up pad was deemed unnecessary per Stewart et al. (2017). The prototype sampler was operated with the largest filter pore size obtainable, an 8.0 µm mixed cellulose ester (MCE) filter (Sterlitech, Kent, WA). However, this filter in 37-mm is not widely available, but was available in a 47-mm diameter. The prototype is 37-mm, therefore a 37-mm (1.5 inch) punch tool was used to create a 37-mm filter, which in-turn contaminated the filters with zinc (min: 1.4 – max: 13 µg/sample). The newly punched 37-mm filter was then bonded to an internal capsule, at 2 points along the perimeter, following the prototype sampler assembly method documented in Anthony et al. (2017).

After filter-capsule assemblies were bonded, they were transferred to an oven and conditioned at 70 °C for 25 hours in order to reach equilibrium, as described in L'Orange et al. (2016). Filter-capsule assemblies were then placed into the prototype sample housings, capped and labeled in preparation for sampling. The plastic IOM samplers were loaded with a standard 25-mm 0.8 µm MCE filter (SKC, Eighty Four, PA).

Sampling Strategies

Sampling pumps were pre-calibrated the night before sampling using a calibration-only prototype or IOM sample in a clean setting with either a Bios DryCal® Defender 520 (Mesa Labs, Butler, NJ) or a BGI tetraCal® (Mesa Labs, Butler, NJ). Prototype samplers were calibrated in an air tight SKC Multi-purpose Calibration Jar Cat No. 225-111 (SKC, Eighty Four, PA). IOM samplers were calibrated using the SKC IOM Calibration Adaptor (SKC, Eighty Four, PA).

For area sampling, paired prototype and IOM (SKC, Eighty Four, PA) sampler setups were affixed on a cart. For the prototype sampler, Sensidyne® Gilian 12 (Sensidyne, St. Petersburg, FL) sampling pumps were operated between 8 and 10 L min^{-1} dependent upon filter loading and resultant pump back-pressure. For the IOM, either the SKC Universal PCXR4 (SKC, Eighty Four, PA) or Gilian GilAir Plus (Sensidyne, St. Petersburg, FL) sampling pumps were used and operated at 2 L min^{-1}.

Upon cart introduction to the area being sampled, samplers were arranged to be as close to the worker as possible. Samplers were activated at the start of the work shift, paused during periods of no-activity (*i.e.,* bathroom, lunch or general breaks), and paused at the end of shift. All sampling pumps were paused and post-calibrated immediately following the end of sampling; respective pre-calibration devices were used. An average of the pre- and post-calibration flow rates was used to determine the sample volume. Acceptable post-calibration flow rates were considered to be within ±5% of the pre-calibration flow rate.

For personal sampling, paired prototype and IOM sampler setups were placed on the lapel of a worker and activated at the start of the work shift. Samplers were paused during lunch breaks and paused at the end of the work shift. Sampling ended at the worker's lunch break if filter overloading was a concern. For personal sampling, the prototype sampler used the Gilian 12 (Sensidyne, St. Petersburg, FL) sampling pumps and operated between 8 and 10 L min^{-1}. Gilian GilAir Plus (Sensidyne, St. Petersburg, FL) sampling pumps were used for the IOM and operated at 2 L min^{-1}. At least one field blank pair was collected at each site; a general rule of

thumb to take one field blank per 10 paired samples was employed (sampling Standard Operating Procedures can be found in Appendix A).

On each sample day, qualitative data were collected to characterize factors that may contribute to or influence metal concentrations at the sites. These factors included ventilation conditions, site and work area occupancy and process speed. For local exhaust ventilation (LEV) a qualitative test was used to assess function, using a plain piece of white paper. The paper was placed in front of the LEV inlet, if the paper was drawn towards or held at the inlet by the ventilation, the LEV was deemed to be functioning.

Type of operation was recorded to broadly categorize the aerosol "size" with heated tasks (welding, pouring, tending, shooting guns) categorized as "small" and mechanical operations (grinding, sawing) as "large."

Sample Analysis

Prior to sampling, samples were transferred back to a clean laboratory and the outsides of the sampler housings were wiped with Curad® Alcohol Prep Pads and allowed to dry to avoid filter contamination from handling the housings. The prototype samples remained in their housings for shipment. After drying, IOM samples were removed from their housings and placed in transport clips for shipment. Samples were sent to an American Industrial Hygiene Association (AIHA) accredited laboratory (101574), (ALS Global, Salt Lake City, UT) and analyzed using the NIOSH Manual of Analytical Methods, modified Method 7300, a 15-metal scan for aluminum, arsenic, beryllium, cadmium, calcium, chromium, copper, iron, lead, manganese, nickel, selenium, sodium, silver, and zinc. A mass measurement of dust collected on the filter was not conducted.

Data Analysis

Sample metal masses were adjusted for field blank sample results for each corresponding sample set. Prototype samples were adjusted for zinc detected in the blanks, due to confirmation that the filter punch process contaminated the filter. Five individual personal samples were also adjusted for 3x zinc dilutions that were performed by the laboratory in order to obtain instrument response within the linear range for zinc. Adjusted concentrations were used for the remainder of the data analysis.

Adjusted paired IOM and prototype data were sorted based upon laboratory "flags." Three types of result flags were reported from the laboratory. A less than sign [<] meant that the testing result was less than the laboratory limit of detection, for the purposes of this study

these results were considered “not detected.” The second flag option was a parenthesis [( )], which signified that the testing result was between the LOD and LOQ and had higher analytical uncertainty than values at or above the LOQ. The last option was for the result to be left unflagged, indicating that the result was above both the LOD and LOQ, or was “detected.”

Paired IOM and prototype individual metal results were sorted by the three laboratory flags into nine categories. Categories were then identified by three markers, a [±] sign, meaning that the result was possibly detected, but was between the laboratory analytical LOD and LOQ, in other words, the metal was detected, but the laboratory could not quantify exactly how much of the metal was on the sample. Detected and non-detected results were identified by [+] and [–] signs, respectively. The nine possible sort categories corresponding with those definitions included: (1) ± Prototype, - IOM, (2) ± Prototype, ± IOM, (3) ± Prototype, + IOM, (4) + Prototype, - IOM, (5) + Prototype, ± IOM, (6) + Prototype, + IOM, (7) – Prototype, - IOM, (8) – Prototype, ± IOM, and (9) – Prototype, + IOM.

A descriptive summary table was created to show the number of paired area and personal samples collected as well as corresponding mean concentrations and standard deviations. Another descriptive table was generated to exhibit the number of pairs collected for each sample process, as well as the number of metals out of 14, detected for each process.

Once individual metal sample pairs were sorted into one of the nine categories, ratios of the paired prototype and IOM individual metal concentrations were calculated. These prototype and IOM concentration ratios were used to create a boxplot to exhibit the distributions and amount of metals sorted into each of the nine possible categories. From the boxplot, paired individual metal concentrations that were detected on both the prototype and IOM (+ Prototype, + IOM) were used for further comparison analyses of the prototype performance. To assess the improvement of sensitivity for detecting metals with the prototype sampler, metals that were detected on the prototype, but not detected on the IOM (+ Prototype, - IOM) were used for further analyses.

To examine the mean difference by metal concentration between the prototype and IOM sampler, a Bland-Altman plot of individual metal concentrations detected on both the prototype and IOM (+ Prototype, + IOM) was generated. Area and personal samples were labeled in the Bland-Altman to display the differences and concentration spread by sample type. If a sample outlier appeared, the outlier was investigated. Upon investigation, if the outlier clearly leveraged the data, further analysis was performed without the outlier.

Concentration ratios of the prototype and IOM were also used to test the normality of each of the nine sort categories as well as the overall data set using Shapiro-Wilk tests. All metal concentrations detected on both the prototype and IOM (+ Prototype, + IOM) were summed to get the aggregate concentrations (mg m^{-3}). Metal concentrations that were detected on the prototype, but not the IOM sampler were also examined to assess the objective on LOD improvement (+ Prototype, - IOM).

To look at the difference between samplers, Wilcoxon Rank-Sum analyses for a two-sided test were performed on concentrations detected on both samplers (+ Prototype, + IOM) with SAS v.9.3. (SAS Institute Inc., Cary, NC). Wilcoxon Rank-Sum analyses were executed for (1) aggregate metals concentrations, and two prototype and IOM concentration ratios: (2) by sample type, personal or area, as well as (3) by particle "size" category, small or large.

To view the relationships between the two samplers, linear regressions between paired samples with detected metals were conducted for (1) aggregate metals concentrations, (2) personal and area samples, and (3) small and large particles. Perfect agreement between samplers would yield a zero intercept and a slope of 1.0.

Results

General Findings

Twenty one out of a total of 28 sample pairs had "detected" metals. Seven out of eight personal samples and 14 out of 20 area samples had detected metals; the average sample time was 7 hours (4.2 – 8.3 hours). The most common metals detected were iron, manganese, zinc, copper, and lead, which were found in more than 10 paired samples. Table 3 shows the number of area and personal samples with corresponding mean concentrations and standard deviations for the prototype and IOM samples.

Table 4 summarizes the number of prototype and IOM pairs collected for each sample process as well as corresponding metals detected from the processes (raw data collected during this study is provided in Appendix C). More welding samples were collected than any other process, but grinding and tending processes collected the most different metals. Figure 2 illustrates the prototype-to-IOM concentration ratios by the nine possible detection categories. Error bars show the highest and lowest ratios achieved for each of the categories, excluding outliers. There were 90 metals detected on both the 21 prototype and IOM paired samples (+ Prototype, + IOM). However, only 11 metals were detected by the prototype sampler and not

the IOM (+ Prototype, - IOM). Sodium outliers were pinpointed in the boxplot and for the purposes of analysis, sodium samples were removed from the data due to minor adverse health effects and excessively higher concentrations (up to 5x) collected on IOM samples compared to the prototype samples.

The IOM collected on average, 0.03 mg m^{-3} more metal concentrations than the prototype, as shown in Figure 3. Only four paired metal concentrations out of 90 were outside of the 95% confidence intervals of sampler difference (-0.23 – 0.16 mg m^{-3}), (SD = 0.20 mg m^{-3}). One zinc sample, (prototype = 0.52 mg m^{-3}, IOM = 2.32 mg m^{-3}) occurring during a metal pouring process sample, was identified as an outlier in the Bland-Altman plot. Further analysis of the metals detected on the prototype and IOM (+ Prototype, + IOM) (N = 90) was conducted without the zinc outlier (N = 89).

Normality Tests

Results of the Shapiro-Wilk normality test on the nine categories of data concluded that most of the data categories were lognormal (6/9 categories), but the category used for analysis, metals detected on both the prototype and IOM, was neither normal nor log normal. Table 5 summarizes normality test results.

Differences between Samplers

The nonparametric test results performed for the 89 metals detected on both the prototype and IOM (+ Prototype, + IOM) showed that there were no statistical differences between the prototype and IOM samplers over aggregate concentrations collected (Wilcoxon p = 0.67), concentration ratios by sample type (p = 0.52), or concentration ratios by particle "size" (p = 0.40). Welding, soldering, pouring, tending and shooting guns involved heat and were therefore determined to emit "small" particles and had 45 paired metals detected. Grinding and sawing were mechanical processes and therefore determined to emit "large" particles, yielding 44 paired metals.

Sampler Linear Relationships

In the examination of the prototype collection performance in relation to the IOM, Table 6 shows the fitted models both with and without the intercepts with corresponding coefficient of determination values (R^2 and adjusted R^2). Intercepts were first fitted, then were removed from models due to nonsignificance ($p > 0.05$). Overall, the prototype collected about 71% of what the IOM collected. In comparison to personal sampling, area sampling yielded the best relationship between the prototype and IOM sampler, with a slope of 1.2 and 98% of the

variability in the IOM accounted for in the prototype. Out of the five regression equations, the prototype undersampled the most in comparison to the IOM for particles that were classified by process to be large. For large particles, the prototype was only collecting just over half of what the IOM was collecting; and the regression only accounted for 73% of the variability in the IOM concentrations.

Discussion

The five most common metals detected during sampling all have the potential to cause severe adverse health effects. The most samples were collected for welding processes while tending and shooting guns had the least pairs collected, only one for each. Even though welding had six paired samples, grinding (five samples) and tending processes (one sample) had the most metals detected, with a total of nine metal species detected out of 14. Interestingly, the one metal detected during the sampling of shooting guns was lead, which is currently trending in terms of its potential to travel from the shooting range to the shooter's household inherently exposing children to leaded dust.

Overall, three trends can be seen in the prototype and IOM concentration ratio boxplot in Figure 2. The first group of three represents where the metal concentration collected by the prototype was possibly detected, or between the laboratory LOD and LOQ (±P), the second indicates that the prototype did detect the metals, or was above the laboratory LOD and LOQ (+P), and the last represents that the prototype did not detect the metals, or was below the laboratory LOD (-P). Only 11 metals from 10 samples were detected on the prototype that were not detected on the IOM (+P, -I). Due to this small number of metals collected and detected on the prototype and not the IOM, the data was not used to assess the sensitivity improvement objective, as 11 results provided insufficient power.

There were 90 metals detected on both the prototype and IOM (+P ,-I). Perfect agreement between samplers would yield a concentration ratio along the y-axis of 1. As can be seen in Figure 2, the plot of the detected metals does center near 1, but there are error bars stretching from about 0.25 to 1.5, indicating substantial variability between concentrations collected by the samplers. The median of the quartiles is also shifted below the dotted line at 1 which indicates perfect agreement between the samplers. This shift implies that the IOM was generally collecting more than the prototype sampler.

In Figure 2, there was a seemingly large amount of metals "not detected" by the prototype or IOM (-P, -I), totaling 184. These values represent values relative to the laboratory

limit of detection and quantification for metals (laboratory LODs and LOQs for individual metals can be found in Appendix B). Again, for each individual sample, 15 metal results were reported and these 184 values are simply due to the fact that the laboratory could not be certain that the respective metals or concentrations were there, and for the purposes of this study, again, these metals were deemed "not detected" (-P) in Figure 2.

The right-most box and whisker plot in Figure 2 indicates that approximately 5 metal concentrations were detected on the IOM that were not detected on the prototype (-P, +I). This is misleading and is solely attributable to prototype blank adjustments for zinc due to filter contamination, which caused those pairs to shift into the last of the nine categories during data sorting processes.

In viewing the Bland-Altman plot in Figure 3, a mean difference between the prototype and IOM sampler was -0.03 mg m^{-3}, indicating that the IOM sampled on average a little more than the prototype sampler. Surprisingly, this mean difference was almost equivalent to previous paired prototype and IOM sampler study in a swine barn, that performed gravimetric analysis of inhalable dust, which found a mean difference of positive 0.03 mg m^{-3} (Anthony et al., 2017). Obviously, the difference found in this study indicated that the IOM collected a little bit more instead of the prototype, which is opposite from what the other study determined, but the finding is still interesting nonetheless.

The Bland-Altman also reveals that while there are a few metal samples outside of the 95% confidence intervals, or two standard deviations of the mean, a majority of the samples are clustered near a mean difference of zero, meaning that the prototype and IOM concentrations actually matched each other quite well, especially when metal concentrations were lower. This adds to study evidence supporting the prototype's applicability for sampling lower concentrations (Anthony et al., 2017; Koehler & Peters, 2015; L'Orange et al., 2016; Landazuri et al., 2016; Stewart et al., 2017).

Lastly, the Bland-Altman revealed a pouring process zinc outlier which appeared to be a legitimate sample after investigation, but upon further analysis without the outlier, it was determined that the outlier was leveraging the data. Upon removal of the one outlier from the 90 samples, the Bland-Altman mean difference between the samplers decreased from -0.03 to only -0.01 mg m^{-3}. The standard deviation also decreased from 0.20 to 0.06 mg m^{-3}. For this reason, the pouring process zinc sample was removed during further analyses.

The Wilcoxon Rank-Sum analyses identified no statistical differences between the prototype and IOM sampler by total metal concentrations collected, sample type, or particle "size" collected. Upon further examination of the sampler relationships by linear regression in Table 6, significant, but not statistical differences were found. From the linear regression analyses, it was clear to see that the prototype significantly under sampled relative to the IOM. These findings further support similar findings from the boxplot and Bland-Altman plot.

Over all metal concentrations collected, the prototype collected 71% of what the IOM collected and this occurrence was also observed for the seven personal samples that were collected. Area prototype samples closely matched IOM area samples, but the prototype actually collected about 20% more than the IOM. In evaluating the sampler relationships by particle size, the prototype generally collected about 80% of what the IOM did for small particles, and only about half of what the IOM collected for large particles.

It is possible that the IOM may have oversampled larger sized particles, which would skew the ratio of the prototype to the IOM to become smaller. If the IOM oversampled larger particles, the equation would portray that the prototype performed poorly in the collection of larger particles, when in reality, the IOM may have been over sampling larger particles. Comparison to the IOM was made because it is the closest widely used sampler in the U.S. that matches the IPM curve, but, the IOM is still not considered "true," or a perfect match to the curve.

In terms of applicability, when using the regression equations for exposure assessments and interpreting sampling results, the differences seen between concentrations collected by the prototype and IOM are not substantial for most metals. For example, in applying the first regression equation for all detected metals, with the IOM maximum detected concentration of 0.87 mg m^{-3} found in Table 6, the prototype detected 0.71 times this value, or 0.62 mg m^{-3}. These differences could potentially by substantial for metals with lower occupational exposure limits such as beryllium (TLV = 0.00005 mg m^{-3}), but prove negligible for metals such as nickel (TLV = 1.5 mg m^{-3}).

Limitations

This study was ultimately affected by its small sample size, being that only 21-paired samples had detectable metal concentrations. Sampling with the prototype at the high flow rate of 10 L min^{-1} was difficult, even with new pumps and batteries. The original filter assembly included a cellulose back-up pad and a smaller filter pore size. Due to the high flow rate, the

back-pressure created by the filter assembly caused the air sampling pumps to repeatedly fault. The filter assembly used to address the pressure drop created by the sampling pumps in-turn contaminated filters with zinc; filter contamination is not desirable for sampling, especially not when hoping to obtain accurate metal concentrations estimations for exposures.

While the high-flow sampling pumps were eventually able to stabilize at 10 or 8 L min^{-1}, the pumps created noise and vibration louder than standard flow personal pumps, which was neither desirable nor feasible for some occupational exposure sampling. Due to the large pressure drop created by the high flow rates, the battery life of the sampling pumps drained much faster than the manufacturer specified, making pumps inoperable after 4 hours of sampling.

Conclusion

The low-cost, disposable high-flow inhalable prototype sampler was not statistically different from the IOM sampler. On average the mean difference of metal concentrations collected between the IOM and prototype was only -0.03 mg m^{-3}, and decreased to only -0.01 mg m^{-3} upon the removal of one outlier from the 90 detected metals found from paired samplers. Sampler performance exhibited by a Bland-Altman plot showed promise for the prototype's ability to sample and detect lower particle concentrations.

Significant differences between the prototype and IOM samplers were identified upon further examining relationships by aggregate metal concentrations collected, sample type (personal or area) and particle size (small or large) through linear regression. Overall, the prototype collected about 71% of what the IOM collected and the prototype best matched the IOM during area sampling in comparison to personal sampling. The prototype performed worse than the IOM for sampling of processes that were thought to emit "large" particles, only collecting about half of what the IOM did, but this difference may be attributable to the IOM tendency to oversample larger particles. For small particles, the prototype generally collected 80% of what the IOM did.

While significant differences were found in the metal concentrations collected by the prototype in comparison to the IOM, these differences were minor and in comparison of the concentrations to occupational exposure limits, the differences found were often negligible.

Additional studies are needed to confirm whether the prototype can provide improved sensitivity for detecting lower concentrations of metals, as only 11 metals from 10 of the 21 sample pairs were detected on the prototype that were not detected on the IOM. This small

number was not deemed appropriate to represent a true sensitivity improvement for the entire study.

Future research may consider sampling for shorter time periods and assess the prototype sampler's performance for metals such as beryllium, which specifically requires lower detection limits and comparison to the inhalable particle fraction in accordance with the consensus group, the American Conference of Governmental Industrial Hygienists (ACGIH) Threshold Limit Values (TLVs).

Table 3. Count and summed metal concentrations of paired samplers, by sampler deployment.

		Pairs	Mean (SD) mg m^{-3}
Area	Prototype	14	0.02 (0.04)
	IOM		0.07 (0.15)
Personal	Prototype	7	0.07 (0.15)
	IOM		0.13 (0.35)
	Total	21	

Table 4. Number of sample pairs and metals detected, by process, sorted into corresponding particle size categories.

	Prototype & IOM		
Process	N-pair(s)	Metals*	Size Category
Welding	6	4	small
Grinding	5	9	large
Soldering	4	2	small
Pouring	2	8	small
Sawing	2	8	large
Tending	1	9	small
Shooting Guns	1	1	small

*Out of 14, Na excluded. Possible metals: Al, Ar, Be, Cd, Ca, Cr, Cu, Fe, Pb, Mn, Ni, Se, Ag, Zi

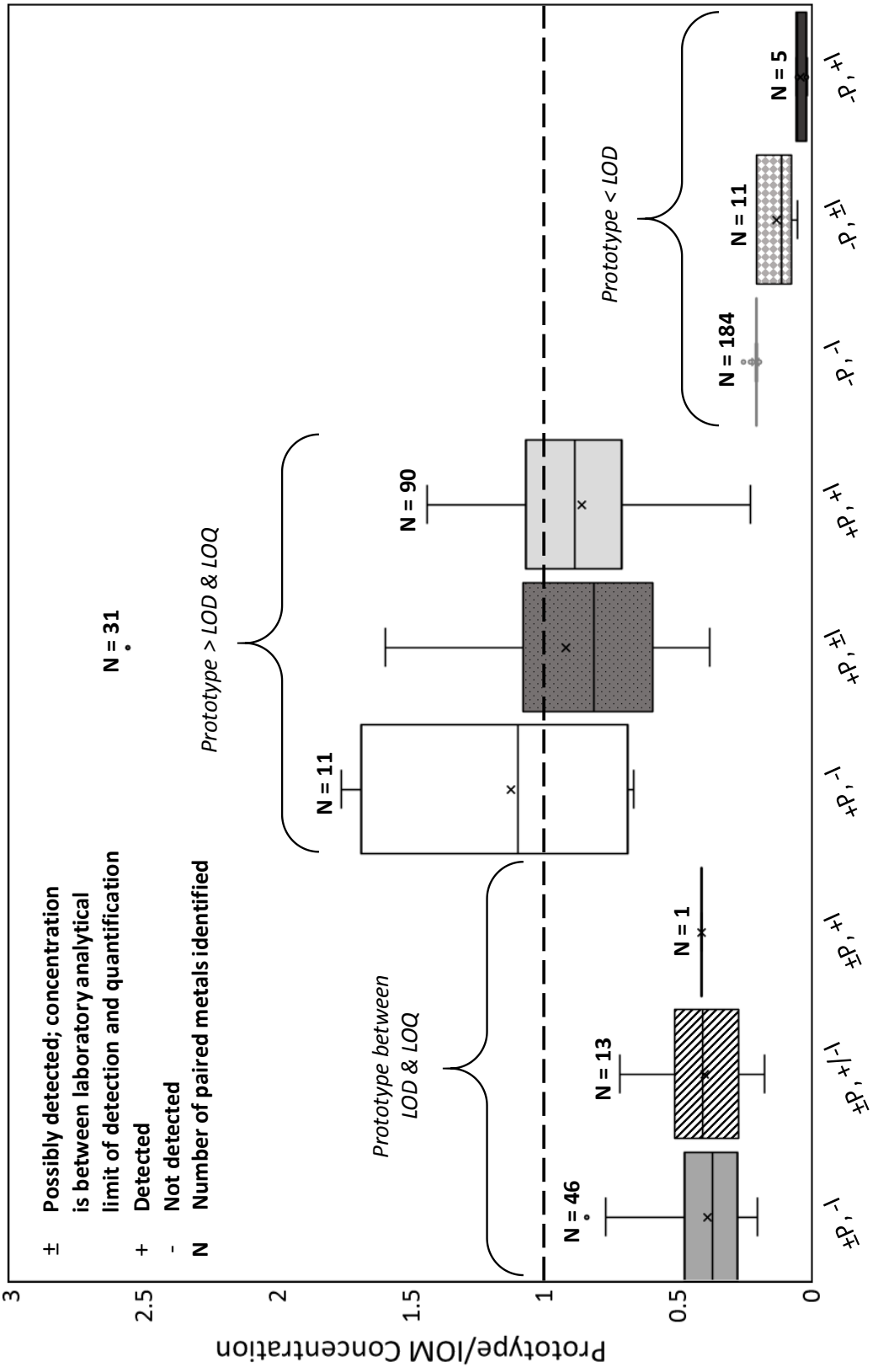

Figure 2. Boxplot of prototype-to-IOM concentration ratio, using nine analytical categories. Error bars are maximum and minimum ratios for each category, excluding outliers.

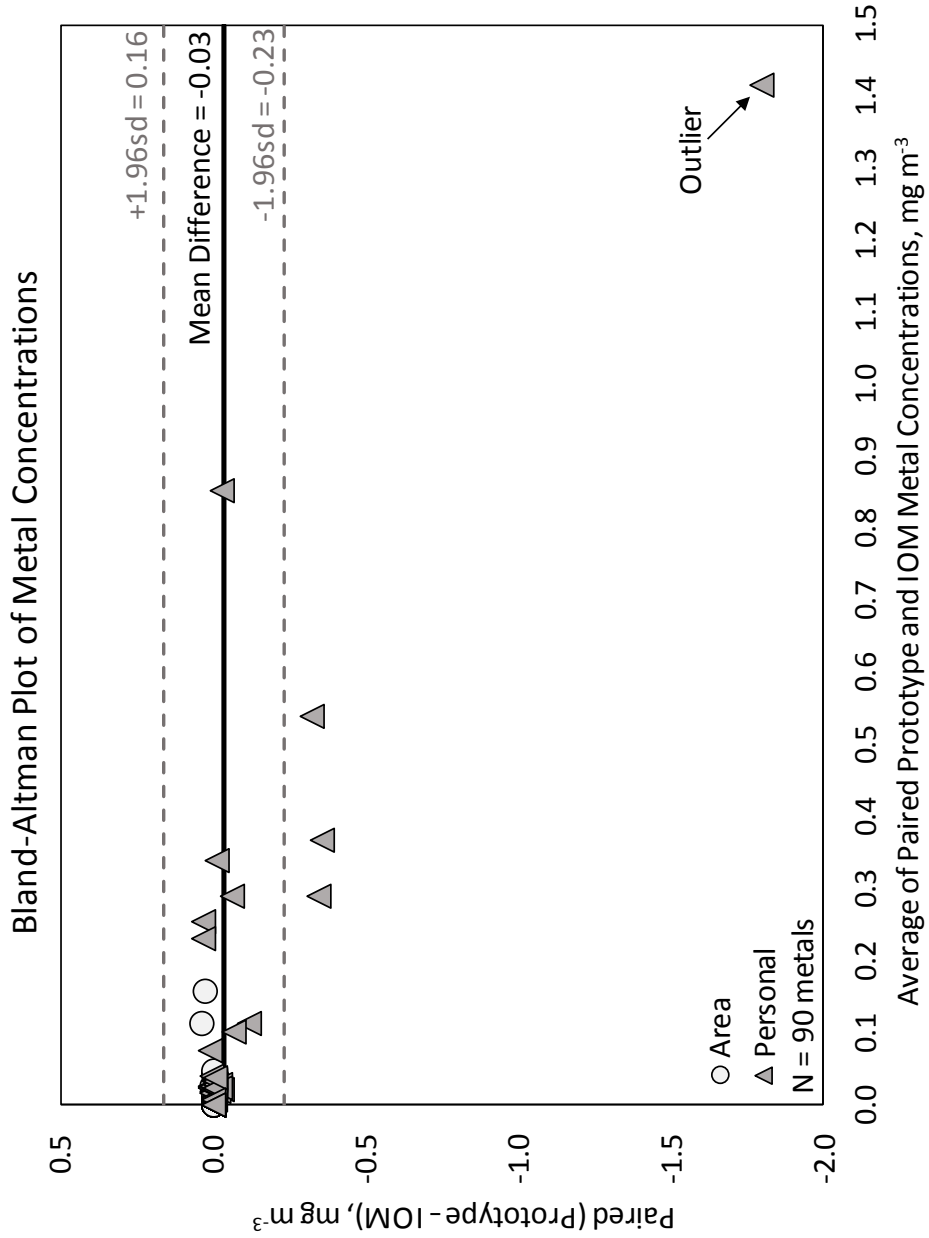

Figure 3. Bland-Altman plot of detected area and personal sample concentrations.

Table 5. Shapiro-Wilk normality test results, using nine analytical categories.

Category	N	Normal p	Lognormal p
±P, -I	46	<0.05	0.31*
±P, ±I	13	0.74*	0.37*
±P, +I	1	-	-
+P, -I	11	0.03*	0.05
+P, ±I	31	<0.05	0.93*
+P, +I	**89**	**<0.05**	**<0.0001**
-P, -I	184	<0.0001	<0.0001
-P, ±I	11	0.02	0.06*
-P, +I	5	0.33*	0.56*

*These data sets were normally or lognormally distributed ($p > 0.05$). Bold indicates the main data set used for analysis.

Table 6. Regression equations to relate metal concentrations between prototype and IOM sampler pairs, fitting the equation: *Prototype = Intercept + Slope (IOM*).

By	N	IOM Max (mg m^{-3})	Intercept	Slope	R^2*	95% C.I. of Slope
All samples	89	0.87	0.0031	**0.70**	0.83	-0.00 - 0.01
			0	**0.71**	0.85	0.64 - 0.77
Personal samples	55	0.87	0.0019	**0.69**	0.82	0.60 - 0.78
			0	**0.70**	0.85	0.62 - 0.78
Area samples	34	0.14	-0.0018	**1.21**	0.98	1.14 - 1.27
			0	**1.18**	0.98	1.12 - 1.25
Small particles	45	0.87	$5.4x10^{-5}$	**0.80**	0.92	0.73 - 0.87
			0	**0.80**	0.93	0.74 - 0.87
Large particles	44	0.55	0.011	**0.53**	0.68	0.41 - 0.64
			0	**0.56**	0.73	0.46 - 0.67

CI = confidence interval

*Adjusted R^2 used for regression equations when intercept = 0

Bolded values indicate $p < 0.05$. No modeled intercept was significant.

CHAPTER III

CONCLUSIONS

This study evaluated a low cost, high-flow prototype inhalable sampler in comparison to the IOM for both personal and area sampling in occupational environments that generated metal aerosols. This study also hoped to determine whether the prototype could improve the sensitivity for detecting lower concentrations of metals. Sampling occurred from May 17 through December 8 of 2016. A total of eight personal samples and twenty area samples were collected with a mean sample time of seven hours, yielding 28 samples. Only 21 pairs out of the 28 sample pairs had laboratory "detectable" metals.

In a boxplot of the detected metals, 90 were detected on both the prototype and IOM and only 11 were detected on the prototype that were not seen on the IOM. A Bland-Altman plot of the mean differences between the samplers showed the in general, the IOM tended to collect a little more than the prototype did, confirmed by an average difference of -0.03 mg m^{-3} found between the samplers. This difference is the opposite of a mean difference identified in an earlier area field-test of the samplers in a swine farrowing barn, which found a difference between the samplers 0.03 mg m^{-3} (Anthony et al., 2017). This mean difference of -0.03 mg m^{-3} was decreased to only -0.01 mg m^{-3} upon the exclusion of a zinc outlier.

The Bland-Altman also exhibited that at lower concentrations, the paired samplers performed similarly, since most of the 90 plotted metal points detected on both sampler pairs were clustered together near smaller concentrations, meaning there was not a large difference between what the two samplers collected.

A ratio of the paired prototype and IOM concentrations was used to perform Shapiro-Wilk normality tests that indicated the data was neither normal nor log-normal. Nonparametric Wilcoxon Rank-Sum analyses determined that there was ultimately no statistical difference between the prototype and IOM by aggregate metal concentrations collected. There were also no statistical differences found when using concentration ratios of the prototype and IOM to assess whether metal concentrations detected from area or personal sampling differed or whether sampler performance differed between the collection of small and large particles.

While no statistical differences between the prototype and IOM were identified, sampler performance equations for personal and area sampling indicated that the prototype and IOM matched best during area sampling, with the prototype collecting about 20% more than the IOM. For personal sampling, the prototype only collected about 70% of what the IOM

did. By particle size, the samplers were more likely to match in their collection of smaller particles, with the prototype only collecting about 80% of the particles that the IOM collected, as opposed to about half of what the IOM collected for larger particles. This difference however may be attributable to the IOM tendency to oversample larger particle sizes, which would make the prototype appear to under sample in comparison to the IOM.

Even though significant differences in the concentrations collected between the samplers were found, it was determined that in interpretation and comparison to occupational exposure limits, the differences found between the samplers were often negligible.

This study was limited due to the small sample size, in which only 11 metals were found on the prototype that were not on the IOM. This number was not deemed sufficient to represent the entire study and prove that the sensitivity was, in fact, improved with the use of the prototype sampler and is a factor for future studies to evaluate. Future research of the prototype samplers may also consider sampling for shorter time periods and sampling for metals that require lower detection limits and comparison to the inhalable fraction, such as beryllium.

Hindrances to this study were experienced majorly due to the high flow rate required by the prototype sampler. Sensidyne® Gilian 12 pumps were not powerful enough to maintain operation at a flow rate of 10 L min^{-1} for full shift, even with the larger pore size filters (8.0 µm) that were used. Even when adjusting the flow rates down to 8 L min^{-1}, pumps faulted frequently, lowering sample time and therefore volume, not to mention that with particulate loading, back pressures caused the pumps batteries to drain completely within four hours. Lastly, the excessive noise and vibration produced by operating pumps are higher flow rates, even though the pumps were specifically designed to operate at higher flow rates, was simply not feasible or desirable for occupational sampling.

In the end, this study allowed me to gain confidence in my knowledge of industrial hygiene sampling and personal protective equipment. I found that through my sampling, I was able to teach others and explain what I was doing, but more importantly, why I was doing it and why air sampling matters. I learned how difficult recruiting facilities into research projects can be and how important it is to maintain relationships and communicate effectively to all parties involved.

I experienced challenges that both required me to react quickly to fix sampling assemblies and to ensure that I was not taking up unnecessary time disrupting the occupational

environments I was in. This project solidified reasons to be prepared for any and everything, from ripped filters, to missing sample covers, backup sampling pumps, and belts for workers who do not wear them as well as people who did not receive a mode of your communication and misconceive what you are doing.

It was important to retain a sense of humor when performing sampling in occupational environments, especially when convincing people to wear multiple sampling pumps and lots of tubing – I found a new appreciation for duct tape. I also realized that no matter how early it was, or how nervous I was to fly solo, a majority of the participants were understanding, and were somewhat used to sampling and were glad to help a student out. Many were interested in knowing a bit about me.

While this project was challenging in recruitment, scheduling, sampling and interpreting, I know that I made a difference in the occupational environments I sampled in. Although the sample size was small, the prototype sampler has the potential to change the way that exposure assessments are performed. If a high flow rate sampling pump can effectively maintain the flow without yielding unreasonable amounts of noise or vibration, it is possible that shorter sampling durations will suffice for analysis and incidentally influence worker participation for personal sampling. Future research of the prototype with metals that require inhalable sampling and lower detection limits such as beryllium should be evaluated.

SOP1602.01 Lab Protocol for Prototype and IOM Samplers

1) Purpose and Applicability

This document outlines the assembly, pre-calibration, and lab analysis for the prototype and IOM samplers for field use.

2) Safety and Operating Precautions

Become familiar with hazards of toluene
Assemble PHISH substrates in laboratory chemical hood
Assemble IOM Samplers in microbalance room
Wear gloves when handling substrates
Take care to avoid exposing substrates to metals

3) Equipment and Materials

Prototype
- 47-mm 8 µm MCE filters
- Back up pads
- Toluene
- Parchment paper
- Oven capable of reaching 70˚ C
- Roll-on adhesive
- Petri dishes

37-mm (1.5”) circle hole-punch
8” x 11” paper (printer paper)
SKC Large Calibration Jar (No. 225-111)
- Personal sampling pumps, 10 LPM (Gilian 12)

IOM
- 25-mm 0.8 µm MCE filters
- Transport cases
- IOM Calibration adapter
- Personal sampling pumps, 2 LPM (Gilian GilAir Plus or SKC 224-PCXR4)

Tweezers
Gloves
Sampler housings
Tygon tubing
Substrate holders - Ziploc bags
Bios DryCal Defender Model 520 calibrator

4) Reference

SOP1612.01 Field Protocol Prototype IOM

5) Definitions

IOM: Institute of Occupational Medicine sampler
MCE filter

6) Procedure

1. **<u>Prototype</u>**

1.1. Preparing filters:

1.1.1. Wipe down the inside of the hole-punch with alcohol wipes to remove any contaminants.

1.1.2. Layer 2 (or more if desired) 8” x 11” pieces of paper (white printer paper).

1.1.3. Place a thin layer of adhesive on the top piece of paper for the 8.0 µm filter to attach to.

1.1.4. Carefully place only the edge of the 47-mm filter onto the adhesive then layer the 2nd piece of paper on top of the other to sandwich the filter.

1.1.5. Line up the 37-mm hole-punch with the filter, careful to avoid including any of the adhesive in the finished product

1.1.6. Use tweezers to remove the filter and paper combination, and then to carefully separate them.

1.2. Preparing substrates:

1.2.1. Use electronic pipette controller and glass pipette to transfer toluene from container into a small beaker.

1.2.2. Lay out petri dishes and place one prototype capsule in each dish, grasping the capsules by the head inlet.

1.2.3. Take apart a cassette and place about 4 back-up pads to the bottom half with back-up support grid.

1.2.4. Place filter on top of back-up pads.

1.2.5. Use tweezers to pick up capsule and gently use Q-tip with toluene to apply on two opposite sides of the PHISH capsule.

1.2.6. Use top half of cassette to push down firmly on filter and capsule with toluene for ~20 seconds.

1.2.7. Remove capsule filter from cassette bottom with tweezers and place in petri dish.

1.2.8. Allow capsules and petri dishes to remain in fume hood overnight to allow excess toluene to evaporate.

1.2.9. Transfer capsules and filters to parchment paper inside of an oven set at 70˚ C. Leave capsules and filters in oven for 25 hours to stabilize.

1.2.10. After 25 hours, remove capsules and filters and place into prototype housings, then label for sampling.

1.3. Pre-calibration of samplers:

1.3.1. Obtain prototype labeled “Calibration” sampler – only to be used for calibration purposes and remove its plastic inlet cap.

1.3.2. Obtain SKC Multi-Purpose Calibration Jar and Bios DryCal.

1.3.3. Twist open calibration jar lid and attach metal outlet of PHISH to adapter tubing inside SKC calibration jar.

1.3.4. Place the attached prototype inside of the calibration jar. Reattach the jar lid and turn until tightly sealed.

1.3.5. On lid of SKC calibration jar, attach the barbed elbow fitting inlet with tubing to the Bios DryCal suction inlet.

1.3.6. On lid of calibration jar, attach the outlet tubing to the Gilian 12 pump inlet.

1.4. Gilian 12 pump:

1.4.1. Press and hold down the “Power” button until display appears

1.4.1.1. *To set the flow rate:*

1.4.1.1.1. Press the “Set” button once. “FLO” is displayed.

1.4.1.1.2. Press “Enter” button to begin setting the flow rate.

1.4.1.1.3. Press and hold the up arrow to increase the flow rate set point or the down arrow to decrease the flow rate set point.

1.4.1.1.4. Press “Enter” when 10 LPM is reached.

1.4.1.2. *To calibrate the Gilian pump with Bios DryCal:*

1.4.1.2.1. Press the “Set/Cal” button twice. Display will show “CAL”

1.4.1.2.2. Press the “Enter” button to enter Calibration Mode. “SCAL” is displayed for 10 seconds before the pump motor will start running. The set flow rate is displayed.

1.4.1.2.3. Follow calibrator operation below.

1.4.1.2.4. To turn off, hold “Power” button until “OFF” is displayed on the screen. It will turn off after 10 seconds.

1.5. Bios DryCal calibrator operation:

1.5.1. Hold the power button to turn the calibrator on.

1.5.2. Highlight “Measure” with the arrows and press enter.

1.5.3. Highlight “Cont.” for continuous measurements (in sets of 10) and press enter.

1.5.4. Attach the Gilian 12 pump to the calibrator via appropriate tubing and follow 1.4.1.2 above to place pump in calibration mode.

1.5.5. To adjust the Gilian 12 calibration flowrate, press the “Set/Cal” button, then scroll using the up and down arrows to input the average reading from the Bios DryCal, then press “Set/Cal.”

1.5.5.1. Let pump run through several sets of measurements to allow flow rate settling.

1.5.6. Refer back to the calibrator average to get the flow rate as close to desired reading as possible (Prototype pumps 8 – 10 LPM and IOM pumps – 2 LPM).

1.6. Lab Analysis

1.6.1. Once back to lab, alcohol wipe each outer surface of the prototype samplers.

1.6.2. Prepare samples for laboratory shipment and fill out corresponding chain of custody forms.

2. <u>IOM</u>

2.3. Preparing substrates:

2.3.1. Obtain IOM cassette capsule and gently remove the cassette from the capsule without touching the sides – touch the red cap or larger bottom lip to push/pull the cassette out.

2.3.2. Gently holding the cassette by the rubber cover, remove the cassette bottom.

2.3.3. Use tweezers to place the filter on the bottom.

2.3.4. Put the cassette top and bottom back together – a clip noise should be heard.

2.3.5. Slide the cassette back into the capsule without touching the sides of the cassette.

2.4. Pre-Calibration:

2.4.1. Obtain IOM Sampler adaptor and push the IOM "Calibration" Sampler through the hinged bracket and place inlet against adapter's foam ring.

2.4.2. Clamp IOM in place by using the screw-plastic clamp until foam ring compresses by 1 mm – ensure that IOM Sampler remains on the middle of the foam.

2.4.3. Use tubing to connect bottom calibrator hose barb to Bios DryCal calibrator inlet.

2.4.4. Use tubing to connect IOM outlet to the inlet of GilAir Plus or SKC 224-PCXR4 pump.

2.4.5. Calibrate IOM pumps to 2 LPM following Bios DryCal calibration operating instructions below (Follow step 1.5 for Bios DryCal operation).

2.4.5.1. *GilAir Plus Calibration operation:*

2.4.5.1.1. Press and hold down the checkmark/power symbol button until display appears.

2.4.5.1.2. Ensure that the Bios DryCal calibrator is turned on.

2.4.5.1.3. On the pump, use the down arrow to highlight "Calibrate," then press the checkmark button.

2.4.5.1.4. Refer to the Bios DryCal display for actual flow; adjust the pump as needed.

2.4.5.2. *SKC 224-PCXR4 Pre-calibration operation:*

2.4.5.2.1. Flip switch on pump face to "ON".

2.4.5.2.2. Use small screw driver to adjust screw on pump face to increase/decrease the flow rate to obtain a flow of 2 LPM.

2.4.5.2.3. Follow steps 1.5 for Bios DryCal operation.

2.4.5.2.4. Once adequate flow rate is achieved, flip switch "OFF".

2.5 Lab Analysis:

2.5.1 Once back to lab or in clean area, alcohol wipe each outer surface of the IOM samplers.

2.5.2 Remove IOMs from their holders and place them into their transport cases.

2.5.3 Prepare samples for laboratory shipment and prepare corresponding chain of custody form.


SOP1612.01 Field Protocol for Prototype and IOM Sampler Operation

1. Purpose and Applicability

This document outlines a procedure for assembling, operating, and disassembling both the prototype and IOM Samplers in the field.

2. Safety and Operating Precautions

Take care when activating samplers to ensure caps are off – prototype filters rip easily.

3. Equipment and Materials

Prototype samplers containing 37-mm 8.0 µm MCE filters
Personal sampling pumps, 10 LPM (Gilian 12)

IOM samplers containing 0.8 µm 25-mm MCE filters
Personal sampling pumps, 2 LPM (Gilian GilAir Plus or SKC 224-PCXR8)

Substrate holders – Ziploc bags
Tygon tubing
SKC Large Calibration Jar (No. 225-111)
Bios DryCal Defender Model 520 calibrator
IOM Calibration adapter
Personal sampling clips to attach samplers to worker's lapel

4. Reference

SOP1602.01 Lab Protocol: Prototype and IOM preparation

5. Definitions

IOM: Institute of Occupational Medicine Sampler
MCE filter: Mixed cellulose ester filter

6. Procedures

1. Prototype

1.1. Assembly

1.1.1.Sampler Set Up (area or personal):

1.1.1.1. Select prototype and IOM samplers that have the correct day's label.

1.1.1.2. Connect bottom metal outlet of prototype with tubing to Gilian 12 pump outlet, use tubing adapters to adapt larger pump tubing to smaller tubing to attach to prototype outlet.

1.1.1.3. If barbed bottom outlet of IOM has a cover, remove it and place in a Ziploc bag.

1.1.1.4. Attach tubing to barbed bottom outlet of sampler to the GilAir Plus or SKC 224-PCXR4 pump.

1.1.1.5. For area sampling, clip prototype and IOM vertically with metal clasp on cart, to have the inlets facing outward, oriented toward the particle source.

1.1.1.6. For personal sampling, clip prototype and IOM vertically with metal clasp onto sampler holder.

1.1.1.7. Clip sampler holder onto workers lapel – ask what their preference of shoulder is.

1.1.1.8. Attach sampling pumps on the backside of the worker onto belt – provide belts if they are not wearing one.

1.1.1.9. Remove the sampler's rubber inlet covers and place in a Ziploc bag.

1.1.1.10. On Gilian 12 pump press and hold down the "Power/Enter" button until display appears, press "Power/Enter" to allow pump to activate.

1.1.1.11. On the GilAir Plus, press and hold the button with a checkmark and power symbol to activate the pump. Then press the checkmark button again to select "Run".

1.1.1.12. On the SKC 224-PCXR4 pump, switch the sampling pump to the "ON" position.

1.1.1.13. Record sampling start time.

1.2. End of Sampling Period (BEFORE CART MOVES!)

1.2.1. Turn pumps on "hold". For the Gilian 12 pump, press and hold down the "Run/Stop" button, record the "clock end time" on the field sheet.

1.2.2. On the GilAir Plus, press the checkmark button and "pause" sampling.

1.2.3. On the SKC 224-PCXR4, press the "hold" button.

1.2.4. Place inlet covers over sampler inlets,(BEFORE CART MOVES and before removing samplers)

1.2.5. Remove pumps from workers and samplers from tubings.

1.2.6. Store samplers in labeled sample box for that day.

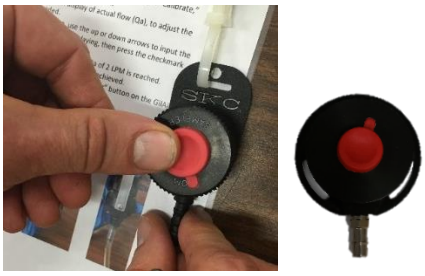

1.3. Prototype sampling pump post-calibration

1.3.1. Within 30-minutes of end of sampling period, handle the correct day's "field blank," take it out of the bag, remove the inlet cover, put the inlet cover into the bag, retrieve an inlet cover, then seal the field blank back up (IMPORTANT – so that we know our hands on the caps are not transferring metals onto our samples).

1.3.2. Obtain prototype labeled "Calibration" sampler and remove its plastic inlet cap.

1.3.3. Obtain SKC Multi-Purpose Calibration Jar and Bios DryCal.

1.3.4. Twist open calibration jar lid and attach metal outlet of prototype to adapter tubing inside SKC calibration jar.

1.3.5. Place the attached prototype inside of the calibration jar. Reattach the jar lid and turn until tightly sealed.

1.3.6. Connect proper tubing on calibration jar to the "suction" inlet of the Bios DryCal.

1.3.7. On lid of calibration jar, attach the outlet tubing to the Gilian 12 pump inlet.

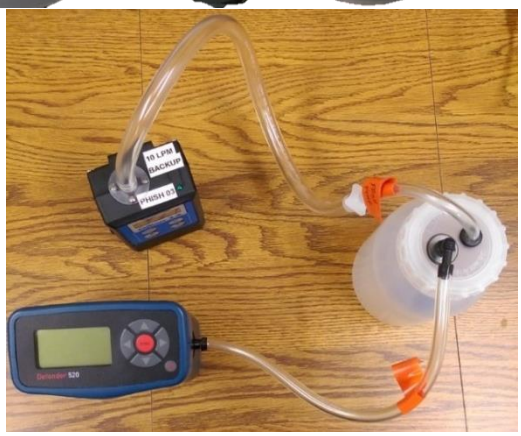

1.3.7.1. *Bios DryCal calibrator operation:*

1.3.7.1.1. Hold the power button to turn the calibrator on.

1.3.7.1.2. Highlight "Measure" with the arrows and press enter.

1.3.7.1.3. Highlight "Cont." for continuous measurements (in sets of 10) and press enter.

1.3.7.1.4. Attach the Gilian 12 pump to the calibrator via appropriate tubing and follow 1.4. from the SOP "SOP1602.01 Lab Protocol for Prototype and IOM Samplers" to place pump in calibration mode.

1.3.7.1.5. To adjust the Gilian 12 calibration flowrate, press the "Set/Cal" button, then scroll using the up and down arrows to input the average reading from the Bios DryCal, then press "Set/Cal."

1.3.7.1.5.1. Let pump run through several sets of measurements to allow flow rate settling.

1.3.7.1.6. Refer back to the calibrator average to get the flow rate as close to desired reading as possible (prototype 8 – 10 LPM and IOM – 2 LPM).

1.3.7.2. *Gilian 12 pump calibration operation:*

1.3.7.2.1. Ensure that the Bios DryCal calibrator is turned on (see section above).

1.3.7.2.2. Press and hold the "Run/Stop" button to reactivate the pump.

1.3.7.2.3. Record post-sampling flow rate averages from the DryCal display.

1.3.7.2.4. Once calibration is complete, hold down the "Power" button on the Gilian 12 pump to turn the pump off.

1.5 IOM sampling pump post-calibration

1.5.1 Within 30-minutes of end of sampling period, again handle the field blank by taking it out of the bag, removing the cover, putting the cover into the Ziploc bag, then retrieve the cover, and seal it back up (IMPORTANT – so that we know our hands on the caps are not transferring metals onto our samples).

1.5.2 Obtain IOM Sampler adaptor and push the IOM "Calibration" Sampler through the hinged bracket and place inlet against adapter's foam ring.

1.5.3 Clamp IOM in place by using the screw-plastic clamp until foam ring compresses by 1 mm – ensure that IOM Sampler remains on the middle of the foam.

1.5.4 Use tubing to connect bottom calibrator hose barb to Bios DryCal calibrator outlet.

1.5.5 Use tubing to connect IOM outlet to the inlet of GilAir Plus pump.

1.5.5.1 *GilAir Plus Calibration operation:*

1.5.5.1.1 Ensure that the Bios DryCal calibrator is turned on (see 1.3.7.1).

1.5.5.1.2 On the pump, press the checkmark button to reactivate the pump.

1.5.5.1.3 Refer to the DryCal display for actual flow, do not adjust pump, just record the flow averages for post-calibration.

1.5.5.1.4 Once calibration is complete, hold down the "Power" button on the GilAir Plus pump.

1.5.5.1.5 Place calibration equipment back in designated box.

1.5.5.2 *SKC 224-PCXR4 Calibration operation:*

1.5.5.2.1 Ensure that the Bios DryCal calibrator is turned on (see 1.3.7.1).

1.5.5.2.2 On the pump face, press the hold button to reactivate the pump.

1.5.5.2.3 Refer to the DryCal display for actual flow, do not adjust pump, just record the flow averages for post-calibration.

1.5.5.2.4 Once calibration is complete, flip the power switch to “off” on the pump face.

APPENDIX B: LABORATORY LIMITS OF DETECTION AND QUANTIFICATION

Metal analytes and corresponding limits of detection and quantification for American Industrial Hygiene Association (AIHA) accredited laboratory (101574), (ALS Global, Salt Lake City, UT). Analyzed using the NIOSH Manual of Analytical Methods, modified Method 7300, a 15-metal scan.

Analyte	LOD (ug/sample)	RL (ug/sample)
Aluminum	1.5	5.0
Arsenic	0.75	2.5
Beryllium	0.0038	0.013
Cadmium	0.023	0.075
Calcium	4.5	15
Chromium	0.38	1.3
Copper	0.15	0.50
Iron	1.5	5.0
Lead	0.38	1.3
Manganese	0.038	0.13
Nickel	0.089	0.30
Selenium	0.75	2.5
Silver	0.075	0.25
Sodium	1.1	3.8
Zinc	0.15	0.50

APPENDIX C: RAW DATA

All paired prototype and IOM data set, Part 1:

Paircat	PairID	Date	QI	TI	Process	Sample Type	AnName	Iflags	Imass	Icon	LnIcon	QP	TP	Pflags	Pmass	Pcon	LnPcon	P/I	Ln P/I	RatioCat
+/- PHISH, -IOM	01-D	10/17/2016	1.99	389	W	A	Aluminum	<	1.5000	0.00194	-6.24625	9.93	389	()	1.9000	0.00049	-7.61729	0.2538	-1.3710	A
+/- PHISH, -IOM	12-D	11/9/2016	1.98	494	W	A	Aluminum	<	1.5000	0.00153	-6.48017	9.90	494	()	4.4000	0.00090	-7.01296	0.5870	-0.5328	A
+/- PHISH, -IOM	26-D	12/5/2016	1.98	433	W	A	Aluminum	<	1.5000	0.00175	-6.34584	9.93	433	()	1.5000	0.00035	-7.96083	0.1989	-1.6150	A
+/- PHISH, -IOM	28-D	12/7/2016	2.02	435	W	A	Aluminum	<	1.5000	0.00171	-6.37298	10.10	435	()	2.1000	0.00048	-7.64594	0.2800	-1.2730	A
+/- PHISH, -IOM	A-03	5/19/2016	1.99	417	W	A	Aluminum	<	1.5000	0.00181	-6.31324	7.93	417	()	3.0000	0.00091	-7.00450	0.5009	-0.6913	A
+/- PHISH, -IOM	C-P3	11/21/2016	2.01	499	G	P	Beryllium	<	0.0038	0.00000370	-12.50718	8.87	497	()	0.0057	0.000001	-13.55855	0.3495	-1.0514	A
+/- PHISH, -IOM	C-P4	11/21/2016	1.99	478	P	P	Beryllium	<	0.0038	0.00000400	-12.42922	8.81	482	()	0.0070	0.000002	-13.31511	0.4123	-0.8859	A
+/- PHISH, -IOM	C-P6	11/22/2016	2.00	361	P	P	Beryllium	<	0.0038	0.00000520	-12.16685	7.92	361	()	0.0068	0.000002	-12.94847	0.4577	-0.7816	A
+/- PHISH, -IOM	C-P7	11/22/2016	2.01	366	S	P	Beryllium	<	0.0038	0.00000510	-12.18627	7.96	363	()	0.0056	0.000002	-13.15319	0.3803	-0.9669	A
+/- PHISH, -IOM	C-P2	11/21/2016	2.02	490	G	P	Beryllium	<	0.0038	0.00000370	-12.50718	8.93	494	()	0.0078	0.000002	-13.24558	0.4779	-0.7384	A
+/- PHISH, -IOM	C-P5	11/22/2016	2.00	357	S	P	Beryllium	<	0.0038	0.00000370	-12.50718	7.95	355	()	0.0080	0.000003	-12.77297	0.7666	-0.2658	A
+/- PHISH, -IOM	C-P8	11/22/2016	1.99	362	T	P	Beryllium	<	0.0038	0.00000370	-12.50718	7.96	364	()	0.0090	0.000003	-12.68211	0.8395	-0.1749	A
+/- PHISH, -IOM	01-D	10/17/2016	1.99	389	W	A	Cadmium	<	0.0230	0.00003	-10.42398	9.93	389	()	0.0270	0.00001	-11.87106	0.2353	-1.4471	A
+/- PHISH, -IOM	08-D	10/31/2016	1.99	396	TG	A	Cadmium	<	0.0230	0.00003	-10.43929	10.06	396	()	0.0330	0.00001	-11.70123	0.2831	-1.2619	A
+/- PHISH, -IOM	27-D	12/6/2016	1.96	488	SO	A	Cadmium	<	0.0230	0.00002	-10.63552	9.77	488	()	0.0540	0.00001	-11.38789	0.4712	-0.7524	A
+/- PHISH, -IOM	28-D	12/7/2016	2.02	435	W	A	Cadmium	<	0.0230	0.00003	-10.55070	10.10	435	()	0.0570	0.00001	-11.25259	0.4957	-0.7019	A
+/- PHISH, -IOM	03-D	10/18/2016	1.98	427	W	A	Calcium	<	4.5000	0.00532	-5.23580	9.91	427	()	6.2000	0.00147	-6.52527	0.2754	-1.2895	A
+/- PHISH, -IOM	05-D	10/26/2016	1.97	462	SO	A	Calcium	<	4.5000	0.00496	-5.30698	9.98	462	()	7.8000	0.00169	-6.38169	0.3414	-1.0747	A
+/- PHISH, -IOM	10-D	11/2/2016	1.97	422	SO	A	Calcium	<	4.5000	0.00541	-5.21896	9.81	422	()	8.9000	0.00215	-6.14185	0.3974	-0.9229	A
+/- PHISH, -IOM	27-D	12/6/2016	1.96	488	SO	A	Calcium	<	4.5000	0.00470	-5.35918	9.77	488	()	7.5000	0.00157	-6.45422	0.3345	-1.0950	A
+/- PHISH, -IOM	31-D	12/7/2016	2.00	279	SO	A	Calcium	<	4.5000	0.00806	-4.82028	9.91	279	()	6.1000	0.00221	-6.11596	0.2737	-1.2957	A
+/- PHISH, -IOM	32-D	12/8/2016	2.01	391	SO	A	Calcium	<	4.5000	0.00573	-5.16276	9.91	391	()	7.9000	0.00204	-6.19539	0.3561	-1.0326	A
+/- PHISH, -IOM	C-P2	11/21/2016	2.02	490	G	P	Chromium	<	0.3800	0.00038	-7.86261	8.93	494	()	0.3900	0.00009	-9.33356	0.2297	-1.4710	A
+/- PHISH, -IOM	C-P3	11/21/2016	2.01	499	G	P	Chromium	<	0.3800	0.00038	-7.87832	8.87	497	()	0.4600	0.00010	-9.16779	0.2754	-1.2895	A
+/- PHISH, -IOM	C-P5	11/22/2016	2.00	357	S	P	Chromium	<	0.3800	0.00053	-7.53596	7.95	355	()	0.4100	0.00015	-8.83626	0.2725	-1.3003	A
+/- PHISH, -IOM	C-P6	11/22/2016	2.00	361	P	P	Chromium	<	0.3800	0.00053	-7.54961	7.92	361	()	0.3800	0.00013	-8.92522	0.2527	-1.3756	A
+/- PHISH, -IOM	C-P7	11/22/2016	2.01	366	S	P	Chromium	<	0.3800	0.00052	-7.56586	7.96	363	()	0.6000	0.00021	-8.47903	0.4013	-0.9132	A
+/- PHISH, -IOM	C-P8	11/22/2016	1.99	362	T	P	Chromium	<	0.3800	0.00053	-7.54736	7.96	364	()	1.0000	0.00035	-7.97158	0.6543	-0.4242	A
+/- PHISH, -IOM	28-D	12/7/2016	2.02	435	W	A	Chromium	<	0.3800	0.00043	-7.74603	10.10	435	()	0.4700	0.00011	-9.14290	0.2474	-1.3969	A
+/- PHISH, -IOM	A-03	5/19/2016	1.99	417	W	A	Chromium	<	0.3800	0.00046	-7.68629	7.93	417	()	0.5700	0.00017	-8.66523	0.3757	-0.9789	A
+/- PHISH, -IOM	06-D	10/24/2016	1.99	381	W	A	Copper	<	0.1500	0.00020	-8.52554	9.89	381	()	0.2400	0.00006	-9.66144	0.3211	-1.1359	A
+/- PHISH, -IOM	01-D	10/17/2016	1.99	389	W	A	Iron	<	1.5000	0.00194	-6.24625	9.93	389	()	3.0000	0.00078	-7.16053	0.4008	-0.9143	A
+/- PHISH, -IOM	04-D	10/24/2016	1.99	381	TG	A	Iron	<	1.5000	0.00198	-6.22295	9.86	381	()	2.0000	0.00053	-7.53814	0.2684	-1.3152	A
+/- PHISH, -IOM	06-D	10/24/2016	1.99	381	W	A	Iron	<	1.5000	0.00198	-6.22295	9.89	381	()	3.6000	0.00096	-6.95339	0.4817	-0.7304	A
+/- PHISH, -IOM	08-D	10/31/2016	1.99	396	TG	A	Iron	<	1.5000	0.00191	-6.26157	10.06	396	()	4.6000	0.00115	-6.76393	0.6051	-0.5024	A
+/- PHISH, -IOM	04-D	10/24/2016	1.99	381	TG	A	Lead	<	0.3800	0.00050	-7.59600	9.86	381	()	0.8900	0.00024	-8.34782	0.4715	-0.7518	A
+/- PHISH, -IOM	06-D	10/24/2016	1.99	381	W	A	Lead	<	0.3800	0.00050	-7.59600	9.89	381	()	0.7500	0.00020	-8.52201	0.3961	-0.9260	A
+/- PHISH, -IOM	A-03	5/19/2016	1.99	417	W	A	Lead	<	0.3800	0.00046	-7.68629	7.93	417	()	0.5400	0.00016	-8.71929	0.3559	-1.0330	A
+/- PHISH, -IOM	08-D	10/31/2016	1.99	396	TG	A	Manganese	<	0.0380	0.00005	-9.93720	10.06	396	()	0.1100	0.00003	-10.49726	0.5712	-0.5601	A
+/- PHISH, -IOM	09-D	10/31/2016	1.99	396	W	A	Manganese	<	0.0380	0.00005	-9.93720	9.97	396	()	0.0730	0.00002	-10.89829	0.3825	-0.9611	A
+/- PHISH, -IOM	12-D	11/9/2016	1.98	494	W	A	Nickel	<	0.0890	0.00009	-9.30475	9.90	494	()	0.1700	0.00003	-10.26652	0.3822	-0.9618	A
+/- PHISH, -IOM	02-D	10/19/2016	2.02	415	G	A	Silver	<	0.0750	0.00009	-9.31916	10.02	415	()	0.0750	0.00002	-10.92315	0.2011	-1.6040	A
+/- PHISH, -IOM	C-P3	11/21/2016	2.01	499	G	P	Silver	<	0.0750	0.00007	-9.50101	8.87	497	()	0.1300	0.00003	-10.43149	0.3944	-0.9305	A
+/- PHISH, -IOM	C-P8	11/22/2016	1.99	362	T	P	Silver	<	0.0750	0.00010	-9.17005	7.96	364	()	0.0840	0.00003	-10.44852	0.2785	-1.2785	A
+/- PHISH, -IOM	27-D	12/6/2016	1.96	488	SO	A	Silver	<	0.0750	0.00008	-9.45353	9.77	488	()	0.0860	0.00002	-10.92253	0.2302	-1.4690	A
+/- PHISH, -IOM	31-D	12/7/2016	2.00	279	SO	A	Silver	<	0.0750	0.00013	-8.91463	9.91	279	()	0.0830	0.00003	-10.41317	0.2235	-1.4985	A
+/- PHISH, +/- IOM	10-D	11/2/2016	1.97	422	SO	A	Beryllium	()	0.0049	0.00001	-12.04156	9.81	422	()	0.0042	0.000001	-13.80057	0.1722	-1.7590	B
+/- PHISH, +/- IOM	08-D	10/31/2016	1.99	396	TG	A	Calcium	()	5.9000	0.00751	-4.89208	10.06	396	()	7.7000	0.00193	-6.24876	0.2575	-1.3567	B
+/- PHISH, +/- IOM	30-D	12/7/2016	2.08	451	SO	A	Calcium	()	5.0000	0.00533	-5.23440	10.10	451	()	9.5000	0.00209	-6.17222	0.3915	-0.9378	B
+/- PHISH, +/- IOM	09-D	10/31/2016	1.99	396	W	A	Calcium	()	5.6000	0.00712	-4.94427	9.97	396	()	9.8000	0.00248	-5.99861	0.3484	-1.0543	B
+/- PHISH, +/- IOM	02-D	10/19/2016	2.02	415	G	A	Calcium	()	5.5000	0.00658	-5.02415	10.02	415	()	11.0000	0.00265	-5.93499	0.4022	-0.9108	B
+/- PHISH, +/- IOM	04-D	10/24/2016	1.99	381	TG	A	Calcium	()	4.6000	0.00608	-5.10236	9.86	381	()	10.0000	0.00266	-5.92870	0.4376	-0.8263	B
+/- PHISH, +/- IOM	01-D	10/17/2016	1.99	389	W	A	Calcium	()	4.6000	0.00594	-5.12566	9.93	389	()	12.0000	0.00311	-5.77423	0.5228	-0.6486	B
+/- PHISH, +/- IOM	06-D	10/24/2016	1.99	381	W	A	Calcium	()	5.4000	0.00714	-4.94202	9.89	381	()	14.0000	0.00372	-5.59527	0.5204	-0.6533	B
+/- PHISH, +/- IOM	A-03	5/19/2016	1.99	417	W	A	Calcium	()	4.9000	0.00592	-5.12947	7.93	417	()	14.0000	0.00424	-5.46405	0.7156	-0.3346	B
+/- PHISH, +/- IOM	01-B-A	9/6/2016	2.04	254	F	A	Calcium	()	5.3000	0.01023	-4.58258	10.11	255	()	13.0000	0.00505	-5.28934	0.4932	-0.7068	B
+/- PHISH, +/- IOM	02-D	10/19/2016	2.02	415	G	A	Copper	()	0.2300	0.00028	-8.19857	10.02	415	()	0.4700	0.00011	-9.08790	0.4109	-0.8893	B
+/- PHISH, +/- IOM	10-D	11/2/2016	1.97	422	SO	A	Manganese	()	0.0380	0.00005	-9.99321	9.81	422	()	0.0530	0.00001	-11.26536	0.2802	-1.2722	B
+/- PHISH, +/- IOM	01-B-A	9/6/2016	2.04	254	F	A	Manganese	()	0.0780	0.00015	-8.80133	10.11	255	()	0.0670	0.00003	-10.55736	0.1727	-1.7560	B
+/- PHISH, +IOM	01-B-A	9/6/2016	2.04	254	F	A	Beryllium	()	0.0040	0.00001	-11.77174	10.11	255		0.0081	0.000003	-12.67019	0.4072	-0.8985	C
+PHISH, -IOM	11-D	11/9/2016	2.00	492	W	A	Aluminum	<	1.5000	0.00153	-6.48366	9.89	492		5.1000	0.00105	-6.86076	0.6858	-0.3771	D
+PHISH, -IOM	25-D	12/5/2016	1.98	432	TG	A	Chromium	<	0.3800	0.00044	-7.71911	9.91	432		3.2000	0.00075	-7.19831	1.6834	0.5208	D
+PHISH, -IOM	29-D	12/7/2016	2.01	434	TG	A	Copper	<	0.1500	0.00017	-8.66830	10.16	434		0.8300	0.00019	-8.57783	1.0947	0.0905	D
+PHISH, -IOM	28-D	12/7/2016	2.02	435	W	A	Copper	<	0.1500	0.00017	-8.67556	10.10	435		1.3000	0.00030	-8.12552	1.7333	0.5500	D
+PHISH, -IOM	32-D	12/8/2016	2.01	391	SO	A	Copper	<	0.1500	0.00019	-8.56396	9.91	391		1.3000	0.00034	-7.99989	1.7578	0.5641	D
+PHISH, -IOM	09-D	10/31/2016	1.99	396	W	A	Iron	<	1.5000	0.00191	-6.26157	9.97	396		5.0000	0.00127	-6.67156	0.6637	-0.4100	D

All paired prototype and IOM data set, Part 2:

Paircat	PairID	Date	QI	TI	Process	Sample Type	AnName	Iflags	Imass	Icon	LnIcon	QP	TP	Pflags	Pmass	Pcon	LnPcon	P/I	Ln P/I	RatioCat
+PHISH, -IOM	02-D	10/19/2016	2.02	415	G	A	Iron	<	1.5000	0.00179	-6.32343	10.02	415		9.3000	0.00224	-6.10287	1.2468	0.2206	D
+PHISH, -IOM	01-D	10/17/2016	1.99	389	W	A	Lead	<	0.3800	0.00049	-7.61930	9.93	389		1.3000	0.00034	-7.99678	0.6856	-0.3775	D
+PHISH, -IOM	26-D	12/5/2016	1.98	433	W	A	Nickel	<	0.0380	0.00004	-10.02148	9.93	433		0.2400	0.00006	-9.79341	1.2562	0.2281	D
+PHISH, -IOM	11-D	11/9/2016	2.00	492	W	A	Nickel	<	0.0890	0.00009	-9.30824	9.89	492		0.3300	0.00007	-9.59867	0.7479	-0.2904	D
+PHISH, -IOM	10-D	11/2/2016	1.97	422	SO	A	Silver	<	0.0750	0.00009	-9.31331	9.81	422		0.2900	0.00007	-9.56577	0.7769	-0.2525	D
+PHISH, +/- IOM	26-D	12/5/2016	1.98	433	W	A	Cadmium	()	0.0300	0.00004	-10.25786	9.93	433		0.0890	0.00002	-10.78542	0.5900	-0.5276	E
+PHISH, +/- IOM	C-P3	11/21/2016	2.01	499	G	P	Cadmium	()	0.0330	0.00003	-10.32199	8.87	497		0.1800	0.00004	-10.10606	1.2410	0.2159	E
+PHISH, +/- IOM	C-P7	11/22/2016	2.01	366	S	P	Cadmium	()	0.0470	0.00006	-9.65589	7.96	363		0.1500	0.00005	-9.86532	0.8110	-0.2094	E
+PHISH, +/- IOM	C-P2	11/21/2016	2.02	490	G	P	Cadmium	()	0.0490	0.00005	-9.91096	8.93	494		0.2300	0.00005	-9.86163	1.0506	0.0493	E
+PHISH, +/- IOM	C-P5	11/22/2016	2.00	357	S	P	Cadmium	()	0.0500	0.00007	-9.56411	7.95	355		0.1900	0.00007	-9.60539	0.9596	-0.0413	E
+PHISH, +/- IOM	29-D	12/7/2016	2.01	434	TG	A	Calcium	()	5.7000	0.00653	-5.03071	10.16	434		15.0000	0.00340	-5.68345	0.5206	-0.6527	E
+PHISH, +/- IOM	26-D	12/5/2016	1.98	433	W	A	Calcium	()	4.9000	0.00573	-5.16207	9.93	433		19.0000	0.00442	-5.42186	0.7712	-0.2598	E
+PHISH, +/- IOM	25-D	12/5/2016	1.98	432	TG	A	Calcium	()	7.7000	0.00900	-4.71030	9.91	432		25.0000	0.00584	-5.14259	0.6490	-0.4323	E
+PHISH, +/- IOM	12-D	11/9/2016	1.98	494	W	A	Calcium	()	7.7000	0.00787	-4.84441	9.90	494		29.0000	0.00593	-5.12727	0.7536	-0.2829	E
+PHISH, +/- IOM	28-D	12/7/2016	2.02	435	W	A	Calcium	()	6.8000	0.00774	-4.86152	10.10	435		33.0000	0.00751	-4.89137	0.9706	-0.0299	E
+PHISH, +/- IOM	11-D	11/9/2016	2.00	492	W	A	Calcium	()	13.0000	0.01324	-4.32417	9.89	492		44.0000	0.00904	-4.70581	0.6827	-0.3816	E
+PHISH, +/- IOM	05-D	10/26/2016	1.97	462	SO	A	Copper	()	0.3000	0.00033	-8.01503	9.98	462		1.3000	0.00028	-8.17345	0.8535	-0.1584	E
+PHISH, +/- IOM	30-D	12/7/2016	2.08	451	SO	A	Copper	()	0.4600	0.00049	-7.62036	10.10	451		1.3000	0.00029	-8.16114	0.5823	-0.5408	E
+PHISH, +/- IOM	25-D	12/5/2016	1.98	432	TG	A	Copper	()	0.4200	0.00049	-7.61902	9.91	432		1.6000	0.00037	-7.89146	0.7615	-0.2724	E
+PHISH, +/- IOM	27-D	12/6/2016	1.96	488	SO	A	Copper	()	0.2600	0.00027	-8.21033	9.77	488		1.9000	0.00040	-7.82727	1.4668	0.3831	E
+PHISH, +/- IOM	26-D	12/5/2016	1.98	433	W	A	Copper	()	0.3000	0.00035	-7.95528	9.93	433		1.9000	0.00044	-7.72444	1.2597	0.2308	E
+PHISH, +/- IOM	01-B-A	9/6/2016	2.04	254	F	A	Copper	()	0.4800	0.00093	-6.98425	10.11	255		1.4000	0.00054	-7.51782	0.5865	-0.5336	E
+PHISH, +/- IOM	31-D	12/7/2016	2.00	279	SO	A	Copper	()	0.1500	0.00027	-8.22148	9.91	279		1.9000	0.00069	-7.28240	2.5576	0.9391	E
+PHISH, +/- IOM	08-D	10/31/2016	1.99	396	TG	A	Lead	()	0.3800	0.00048	-7.63462	10.06	396		1.4000	0.00035	-7.95351	0.7270	-0.3189	E
+PHISH, +/- IOM	26-D	12/5/2016	1.98	433	W	A	Lead	()	1.1000	0.00129	-6.65600	9.93	433		4.8000	0.00112	-6.79768	0.8679	-0.1417	E
+PHISH, +/- IOM	01-D	10/17/2016	1.99	389	W	A	Manganese	()	0.0580	0.00007	-9.49903	9.93	389		0.1400	0.00004	-10.22525	0.4837	-0.7262	E
+PHISH, +/- IOM	04-D	10/24/2016	1.99	381	TG	A	Manganese	()	0.0860	0.00011	-9.08183	9.86	381		0.1800	0.00005	-9.94608	0.4214	-0.8643	E
+PHISH, +/- IOM	C-P4	11/21/2016	1.99	478	P	P	Nickel	()	0.2700	0.00028	-8.16456	8.81	482		0.5100	0.00012	-9.02661	0.4223	-0.8621	E
+PHISH, +/- IOM	02-D	10/19/2016	2.02	415	G	A	Nickel	()	0.0990	0.00012	-9.04153	10.02	415		0.5300	0.00013	-8.96776	1.0766	0.0738	E
+PHISH, +/- IOM	28-D	12/7/2016	2.02	435	W	A	Nickel	()	0.1000	0.00011	-9.08103	10.10	435		0.7300	0.00017	-8.70259	1.4600	0.3784	E
+PHISH, +/- IOM	A-03	5/19/2016	1.99	417	W	A	Nickel	()	0.1200	0.00014	-8.83897	7.93	417		0.5600	0.00017	-8.68293	1.1689	0.1560	E
+PHISH, +/- IOM	C-P6	11/22/2016	2.00	361	P	P	Nickel	()	0.2200	0.00030	-8.09615	7.92	361		0.6800	0.00024	-8.34330	0.7810	-0.2472	E
+PHISH, +/- IOM	C-P7	11/22/2016	2.01	366	S	P	Nickel	()	0.2900	0.00040	-7.83615	7.96	363		1.2000	0.00042	-7.78588	1.0516	0.0503	E
+PHISH, +/- IOM	26-D	12/5/2016	1.98	433	W	A	Zinc	()	0.2700	0.00032	-8.06064	9.93	433		0.5100	0.00012	-9.03964	0.3757	-0.9790	E
+PHISH, +/- IOM	28-D	12/7/2016	2.02	435	W	A	Zinc	()	0.1700	0.00019	-8.55040	10.10	435		0.7800	0.00018	-8.63634	0.9176	-0.0859	E
+PHISH, +/- IOM	30-D	12/7/2016	2.08	451	SO	A	Zinc	()	0.2200	0.00023	-8.35796	10.10	451		1.7000	0.00037	-7.89288	1.5921	0.4651	E
+PHISH, +IOM	C-P4	11/21/2016	1.99	478	P	P	Aluminum		34.0000	0.03583	-3.32887	8.81	482		41.0000	0.00966	-4.63969	0.2696	-1.3108	F
+PHISH, +IOM	C-P3	11/21/2016	2.01	499	G	P	Aluminum		16.0000	0.01595	-4.13815	8.87	497		89.0000	0.02019	-3.90263	1.2656	0.2355	F
+PHISH, +IOM	C-P8	11/22/2016	1.99	362	T	P	Aluminum		18.0000	0.02499	-3.68941	7.96	364		60.0000	0.02071	-3.87724	0.8288	-0.1878	F
+PHISH, +IOM	C-P2	11/21/2016	2.02	490	G	P	Aluminum		18.0000	0.01823	-4.00465	8.93	494		100.0000	0.02267	-3.78678	1.2434	0.2179	F
+PHISH, +IOM	C-P7	11/22/2016	2.01	366	S	P	Aluminum		23.0000	0.03134	-3.46278	7.96	363		70.0000	0.02424	-3.71971	0.7734	-0.2569	F
+PHISH, +IOM	C-P6	11/22/2016	2.00	361	P	P	Aluminum		18.0000	0.02493	-3.69165	7.92	361		73.0000	0.02555	-3.66718	1.0248	0.0245	F
+PHISH, +IOM	C-P5	11/22/2016	2.00	357	S	P	Aluminum		28.0000	0.03931	-3.23618	7.95	355		98.0000	0.03475	-3.35969	0.8838	-0.1235	F
+PHISH, +IOM	29-D	12/7/2016	2.01	434	TG	A	Cadmium		0.0980	0.00011	-9.09397	10.16	434		0.2600	0.00006	-9.73858	0.5249	-0.6446	F
+PHISH, +IOM	02-D	10/19/2016	2.02	415	G	A	Cadmium		0.0870	0.00010	-9.17074	10.02	415		0.3300	0.00008	-9.44154	0.7628	-0.2708	F
+PHISH, +IOM	25-D	12/5/2016	1.98	432	TG	A	Cadmium		0.1300	0.00015	-8.79174	9.91	432		0.4500	0.00011	-9.15997	0.6920	-0.3682	F
+PHISH, +IOM	C-P8	11/22/2016	1.99	362	T	P	Cadmium		0.1000	0.00014	-8.88236	7.96	364		0.3700	0.00013	-8.96584	0.9199	-0.0835	F
+PHISH, +IOM	C-P4	11/21/2016	1.99	478	P	P	Cadmium		0.4700	0.00050	-7.61025	8.81	482		0.5500	0.00013	-8.95110	0.2616	-1.3409	F
+PHISH, +IOM	C-P6	11/22/2016	2.00	361	P	P	Cadmium		0.1500	0.00021	-8.47915	7.92	361		0.5700	0.00020	-8.51976	0.9602	-0.0406	F
+PHISH, +IOM	C-P4	11/21/2016	1.99	478	P	P	Calcium		28.0000	0.02951	-3.52303	8.81	482		38.0000	0.00895	-4.71568	0.3034	-1.1927	F
+PHISH, +IOM	C-P3	11/21/2016	2.01	499	G	P	Calcium		16.0000	0.01595	-4.13815	8.87	497		80.0000	0.01815	-4.00924	1.1376	0.1289	F
+PHISH, +IOM	C-P8	11/22/2016	1.99	362	T	P	Calcium		19.0000	0.02637	-3.63534	7.96	364		57.0000	0.01967	-3.92853	0.7459	-0.2932	F
+PHISH, +IOM	C-P7	11/22/2016	2.01	366	S	P	Calcium		21.0000	0.02862	-3.55375	7.96	363		63.0000	0.02182	-3.82507	0.7624	-0.2713	F
+PHISH, +IOM	C-P6	11/22/2016	2.00	361	P	P	Calcium		18.0000	0.02493	-3.69165	7.92	361		64.0000	0.02240	-3.79875	0.8984	-0.1071	F
+PHISH, +IOM	C-P2	11/21/2016	2.02	490	G	P	Calcium		21.0000	0.02127	-3.85050	8.93	494		99.0000	0.02244	-3.79683	1.0551	0.0537	F
+PHISH, +IOM	C-P5	11/22/2016	2.00	357	S	P	Calcium		25.0000	0.03510	-3.34950	7.95	355		96.0000	0.03404	-3.38031	0.9697	-0.0308	F
+PHISH, +IOM	10-D	11/2/2016	1.97	422	SO	A	Copper		0.5600	0.00067	-7.30286	9.81	422		1.9000	0.00046	-7.68604	0.6817	-0.3832	F
+PHISH, +IOM	12-D	11/9/2016	1.98	494	W	A	Copper		0.8900	0.00091	-7.00217	9.90	494		3.8000	0.00078	-7.15956	0.8544	-0.1574	F
+PHISH, +IOM	11-D	11/9/2016	2.00	492	W	A	Copper		1.3000	0.00132	-6.62676	9.89	492		6.3000	0.00129	-6.64945	0.9776	-0.0227	F
+PHISH, +IOM	A-03	5/19/2016	1.99	417	W	A	Copper		2.1000	0.00254	-5.97677	7.93	417		9.2000	0.00278	-5.88391	1.0973	0.0929	F
+PHISH, +IOM	C-P4	11/21/2016	1.99	478	P	P	Copper		39.4600	0.04159	-3.17994	8.81	482		67.0000	0.01579	-4.14857	0.3796	-0.9686	F
+PHISH, +IOM	C-P6	11/22/2016	2.00	361	P	P	Copper		27.4600	0.03803	-3.26929	7.92	361		92.0000	0.03220	-3.43585	0.8466	-0.1666	F
+PHISH, +IOM	C-P2	11/21/2016	2.02	490	G	P	Copper		169.4600	0.17163	-1.76241	8.93	494		240.0000	0.05440	-2.91131	0.3170	-1.1489	F
+PHISH, +IOM	C-P8	11/22/2016	1.99	362	T	P	Copper		97.4600	0.13529	-2.00034	7.96	364		200.0000	0.06903	-2.67327	0.5102	-0.6729	F
+PHISH, +IOM	C-P7	11/22/2016	2.01	366	S	P	Copper		52.4600	0.07149	-2.63823	7.96	363		230.0000	0.07965	-2.53012	1.1142	0.1081	F
+PHISH, +IOM	C-P5	11/22/2016	2.00	357	S	P	Copper		329.4600	0.46259	-0.77092	7.95	355		330.0000	0.11700	-2.14557	0.2529	-1.3747	F
+PHISH, +IOM	C-P3	11/21/2016	2.01	499	G	P	Copper		549.4600	0.54782	-0.60180	8.87	497		840.0000	0.19055	-1.65786	0.3478	-1.0561	F

All paired prototype and IOM data set, Part 3:

Paircat	PairID	Date	QI	TI	Process	Sample Type	AnName	Iflags	Imass	Icon	LnIcon	QP	TP	Pflags	Pmass	Pcon	LnPcon	P/I	Ln P/I	RatioCat
+PHISH, +IOM	C-P4	11/21/2016	1.99	478	P	P	Iron		33.0000	0.03478	-3.35872	8.81	482		47.0000	0.01107	-4.50312	0.3184	-1.1444	F
+PHISH, +IOM	29-D	12/7/2016	2.01	434	TG	A	Iron		12.0000	0.01376	-4.28627	10.16	434		52.0000	0.01179	-4.44026	0.8573	-0.1540	F
+PHISH, +IOM	C-P3	11/21/2016	2.01	499	G	P	Iron		19.0000	0.01894	-3.96630	8.87	497		120.0000	0.02722	-3.60377	1.4370	0.3625	F
+PHISH, +IOM	C-P6	11/22/2016	2.00	361	P	P	Iron		19.0000	0.02632	-3.63759	7.92	361		80.0000	0.02800	-3.57561	1.0639	0.0620	F
+PHISH, +IOM	C-P2	11/21/2016	2.02	490	G	P	Iron		23.0000	0.02329	-3.75953	8.93	494		140.0000	0.03174	-3.45031	1.3624	0.3092	F
+PHISH, +IOM	C-P7	11/22/2016	2.01	366	S	P	Iron		27.0000	0.03679	-3.30244	7.96	363		94.0000	0.03255	-3.42491	0.8847	-0.1225	F
+PHISH, +IOM	11-D	11/9/2016	2.00	492	W	A	Iron		43.0000	0.04381	-3.12792	9.89	492		160.0000	0.03288	-3.41483	0.7506	-0.2869	F
+PHISH, +IOM	C-P8	11/22/2016	1.99	362	T	P	Iron		30.0000	0.04164	-3.17858	7.96	364		100.0000	0.03451	-3.36641	0.8288	-0.1878	F
+PHISH, +IOM	12-D	11/9/2016	1.98	494	W	A	Iron		42.0000	0.04294	-3.14796	9.90	494		200.0000	0.04092	-3.19625	0.9529	-0.0483	F
+PHISH, +IOM	25-D	12/5/2016	1.98	432	TG	A	Iron		37.0000	0.04326	-3.14060	9.91	432		180.0000	0.04207	-3.16851	0.9725	-0.0279	F
+PHISH, +IOM	C-P5	11/22/2016	2.00	357	S	P	Iron		28.0000	0.03931	-3.23618	7.95	355		120.0000	0.04255	-3.15717	1.0822	0.0790	F
+PHISH, +IOM	26-D	12/5/2016	1.98	433	W	A	Iron		41.0000	0.04794	-3.03773	9.93	433		210.0000	0.04884	-3.01919	1.0187	0.0185	F
+PHISH, +IOM	28-D	12/7/2016	2.02	435	W	A	Iron		83.0000	0.09446	-2.35960	10.10	435		590.0000	0.13429	-2.00776	1.4217	0.3518	F
+PHISH, +IOM	A-03	5/19/2016	1.99	417	W	A	Iron		120.0000	0.14497	-1.93121	7.93	417		570.0000	0.17248	-1.75747	1.1897	0.1737	F
+PHISH, +IOM	C-P4	11/21/2016	1.99	478	P	P	Lead		11.0000	0.01159	-4.45733	8.81	482		14.0000	0.00330	-5.71421	0.2845	-1.2569	F
+PHISH, +IOM	29-D	12/7/2016	2.01	434	TG	A	Lead		5.4000	0.00619	-5.08478	10.16	434		15.0000	0.00340	-5.68345	0.5495	-0.5987	F
+PHISH, +IOM	02-D	10/19/2016	2.02	415	G	A	Lead		4.6000	0.00550	-5.20284	10.02	415		19.0000	0.00457	-5.38844	0.8306	-0.1856	F
+PHISH, +IOM	C-P3	11/21/2016	2.01	499	G	P	Lead		4.1000	0.00409	-5.49975	8.87	497		24.0000	0.00544	-5.21321	1.3318	0.2865	F
+PHISH, +IOM	C-P7	11/22/2016	2.01	366	S	P	Lead		5.0000	0.00681	-4.98884	7.96	363		17.0000	0.00589	-5.13499	0.8640	-0.1462	F
+PHISH, +IOM	25-D	12/5/2016	1.98	432	TG	A	Lead		7.2000	0.00842	-4.77744	9.91	432		27.0000	0.00631	-5.06563	0.7496	-0.2882	F
+PHISH, +IOM	C-P2	11/21/2016	2.02	490	G	P	Lead		5.1000	0.00517	-5.26578	8.93	494		29.0000	0.00657	-5.02466	1.2727	0.2411	F
+PHISH, +IOM	C-P8	11/22/2016	1.99	362	T	P	Lead		6.2000	0.00861	-4.75523	7.96	364		21.0000	0.00725	-4.92706	0.8421	-0.1718	F
+PHISH, +IOM	C-P6	11/22/2016	2.00	361	P	P	Lead		5.3000	0.00734	-4.91432	7.92	361		21.0000	0.00735	-4.91312	1.0012	0.0012	F
+PHISH, +IOM	C-P5	11/22/2016	2.00	357	S	P	Lead		6.3000	0.00885	-4.72783	7.95	355		25.0000	0.00886	-4.72578	1.0020	0.0020	F
+PHISH, +IOM	01-B-A	9/6/2016	2.04	254	F	A	Lead		5.3000	0.01023	-4.58258	10.11	255		26.0000	0.01009	-4.59620	0.9865	-0.0136	F
+PHISH, +IOM	C-P4	11/21/2016	1.99	478	P	P	Manganese		0.3100	0.00033	-8.02641	8.81	482		0.4200	0.00010	-9.22076	0.3029	-1.1944	F
+PHISH, +IOM	C-P3	11/21/2016	2.01	499	G	P	Manganese		0.1500	0.00015	-8.80786	8.87	497		0.9200	0.00021	-8.47465	1.3954	0.3332	F
+PHISH, +IOM	C-P6	11/22/2016	2.00	361	P	P	Manganese		0.1600	0.00022	-8.41461	7.92	361		0.6700	0.00023	-8.35812	1.0581	0.0565	F
+PHISH, +IOM	06-D	10/24/2016	1.99	381	W	A	Manganese		0.1400	0.00019	-8.59453	9.89	381		0.9000	0.00024	-8.33968	1.2903	0.2549	F
+PHISH, +IOM	C-P7	11/22/2016	2.01	366	S	P	Manganese		0.2000	0.00027	-8.20772	7.96	363		0.6900	0.00024	-8.33927	0.8767	-0.1316	F
+PHISH, +IOM	02-D	10/19/2016	2.02	415	G	A	Manganese		0.2400	0.00029	-8.15601	10.02	415		1.0000	0.00024	-8.33288	0.8379	-0.1769	F
+PHISH, +IOM	C-P2	11/21/2016	2.02	490	G	P	Manganese		0.2000	0.00020	-8.50446	8.93	494		1.1000	0.00025	-8.29664	1.2310	0.2078	F
+PHISH, +IOM	C-P5	11/22/2016	2.00	357	S	P	Manganese		0.2000	0.00028	-8.17782	7.95	355		0.8800	0.00031	-8.07249	1.1111	0.1053	F
+PHISH, +IOM	C-P8	11/22/2016	1.99	362	T	P	Manganese		0.2700	0.00037	-7.88911	7.96	364		0.9400	0.00032	-8.03346	0.8656	-0.1444	F
+PHISH, +IOM	28-D	12/7/2016	2.02	435	W	A	Manganese		0.2600	0.00030	-8.12552	10.10	435		1.8000	0.00041	-7.80009	1.3846	0.3254	F
+PHISH, +IOM	29-D	12/7/2016	2.01	434	TG	A	Manganese		0.6600	0.00076	-7.18669	10.16	434		2.6000	0.00059	-7.43599	0.7793	-0.2493	F
+PHISH, +IOM	26-D	12/5/2016	1.98	433	W	A	Manganese		1.0000	0.00117	-6.75131	9.93	433		5.3000	0.00123	-6.69859	1.0541	0.0527	F
+PHISH, +IOM	25-D	12/5/2016	1.98	432	TG	A	Manganese		1.2000	0.00140	-6.56920	9.91	432		5.4000	0.00126	-6.67507	0.8995	-0.1059	F
+PHISH, +IOM	11-D	11/9/2016	2.00	492	W	A	Manganese		1.6000	0.00163	-6.41912	9.89	492		6.6000	0.00136	-6.60293	0.8321	-0.1838	F
+PHISH, +IOM	12-D	11/9/2016	1.98	494	W	A	Manganese		2.8000	0.00286	-5.85601	9.90	494		12.0000	0.00245	-6.00966	0.8576	-0.1537	F
+PHISH, +IOM	A-03	5/19/2016	1.99	417	W	A	Manganese		21.0000	0.02537	-3.67418	7.93	417		96.0000	0.02905	-3.53876	1.1450	0.1354	F
+PHISH, +IOM	29-D	12/7/2016	2.01	434	TG	A	Nickel		0.2000	0.00023	-8.38062	10.16	434		0.7200	0.00016	-8.72001	0.7122	-0.3394	F
+PHISH, +IOM	C-P2	11/21/2016	2.02	490	G	P	Nickel		0.8200	0.00083	-7.09348	8.93	494		1.3000	0.00029	-8.12959	0.3548	-1.0361	F
+PHISH, +IOM	C-P8	11/22/2016	1.99	362	T	P	Nickel		0.5500	0.00076	-7.17762	7.96	364		1.2000	0.00041	-7.78926	0.5425	-0.6116	F
+PHISH, +IOM	25-D	12/5/2016	1.98	432	TG	A	Nickel		0.3700	0.00043	-7.74577	9.91	432		2.0000	0.00047	-7.66832	1.0805	0.0775	F
+PHISH, +IOM	C-P5	11/22/2016	2.00	357	S	P	Nickel		1.5000	0.00211	-6.16291	7.95	355		1.7000	0.00060	-7.41403	0.2862	-1.2511	F
+PHISH, +IOM	C-P3	11/21/2016	2.01	499	G	P	Nickel		2.4000	0.00239	-6.03527	8.87	497		4.0000	0.00091	-7.00497	0.3792	-0.9697	F
+PHISH, +IOM	A-03	5/19/2016	1.99	417	W	A	Zinc		0.8000	0.00097	-6.94185	7.93	417		3.4000	0.00103	-6.87933	1.0645	0.0625	F
+PHISH, +IOM	27-D	12/6/2016	1.96	488	SO	A	Zinc		2.5000	0.00261	-5.94697	9.77	488		12.0000	0.00252	-5.98421	0.9634	-0.0372	F
+PHISH, +IOM	31-D	12/7/2016	2.00	279	SO	A	Zinc		2.3000	0.00412	-5.49145	9.91	279		7.1500	0.00259	-5.95714	0.6277	-0.4657	F
+PHISH, +IOM	06-D	10/24/2016	1.99	381	W	A	Zinc		2.5000	0.00331	-5.71213	9.89	381		11.1500	0.00296	-5.82288	0.8952	-0.1107	F
+PHISH, +IOM	C-P3	11/21/2016	2.01	499	G	P	Zinc		216.8000	0.21615	-1.53177	8.87	497		1095.1500	0.24842	-1.39262	1.1493	0.1392	F
+PHISH, +IOM	C-P7	11/22/2016	2.01	366	S	P	Zinc		236.8000	0.32269	-1.13106	7.96	363		745.1500	0.25805	-1.35462	0.7997	-0.2236	F
+PHISH, +IOM	C-P2	11/21/2016	2.02	490	G	P	Zinc		236.8000	0.23983	-1.42781	8.93	494		1195.1500	0.27092	-1.30592	1.1296	0.1219	F
+PHISH, +IOM	C-P5	11/22/2016	2.00	357	S	P	Zinc		246.8000	0.34652	-1.05980	7.95	355		935.1500	0.33156	-1.10395	0.9568	-0.0441	F
+PHISH, +IOM	C-P8	11/22/2016	1.99	362	T	P	Zinc		506.8000	0.70352	-0.35166	7.96	364		1098.3833	0.37909	-0.96999	0.5388	-0.6183	F
+PHISH, +IOM	C-P4	11/21/2016	1.99	478	P	P	Zinc		2198.9333	2.31752	0.84050	8.81	482		2198.3833	0.51800	-0.65779	0.2235	-1.4983	F
+PHISH, +IOM	C-P6	11/22/2016	2.00	361	P	P	Zinc		626.8000	0.86814	-0.14140	7.92	361		2398.3833	0.83938	-0.17509	0.9669	-0.0337	F
+PHISH, +IOM	32-D	12/8/2016	2.01	391	SO	A	Zinc		0.6600	0.00084	-7.08236	9.91	391		3.1000	0.00080	-7.13085	0.9527	-0.0485	F
-PHISH, -IOM	02-D	10/19/2016	2.02	415	G	A	Aluminum	<	1.5000	0.00179	-6.32343	10.02	415	<	1.5000	0.00036	-7.92742	0.2011	-1.6040	G
-PHISH, -IOM	03-D	10/18/2016	1.98	427	W	A	Aluminum	<	1.5000	0.00177	-6.33442	9.91	427	<	1.5000	0.00035	-7.94436	0.1999	-1.6099	G
-PHISH, -IOM	25-D	10/24/2016	1.99	381	TG	A	Aluminum	<	1.5000	0.00198	-6.22295	9.86	381	<	1.5000	0.00040	-7.82582	0.2013	-1.6029	G
-PHISH, -IOM	05-D	10/26/2016	1.97	462	SO	A	Aluminum	<	1.5000	0.00165	-6.40559	9.98	462	<	1.5000	0.00033	-8.03035	0.1970	-1.6248	G
-PHISH, -IOM	06-D	10/24/2016	1.99	381	W	A	Aluminum	<	1.5000	0.00198	-6.22295	9.89	381	<	1.5000	0.00040	-7.82886	0.2007	-1.6059	G
-PHISH, -IOM	08-D	10/31/2016	1.99	396	TG	A	Aluminum	<	1.5000	0.00191	-6.26157	10.06	396	<	1.5000	0.00038	-7.88452	0.1973	-1.6230	G
-PHISH, -IOM	09-D	10/31/2016	1.99	396	W	A	Aluminum	<	1.5000	0.00191	-6.26157	9.97	396	<	1.5000	0.00038	-7.87553	0.1991	-1.6140	G
-PHISH, -IOM	10-D	11/2/2016	1.97	422	SO	A	Aluminum	<	1.5000	0.00180	-6.31757	9.81	422	<	1.5000	0.00036	-7.92243	0.2009	-1.6049	G

All paired prototype and IOM data set, Part 4:

Paircat	PairID	Date	QI	TI	Process	Sample Type	AnName	Iflags	Imass	Icon	LnIcon	QP	TP	Pflags	Pmass	Pcon	LnPcon	P/I	Ln P/I	RatioCat
-PHISH, -IOM	25-D	12/5/2016	1.98	432	TG	A	Aluminum	<	1.5000	0.00175	-6.34606	9.91	432	<	1.5000	0.00035	-7.95600	0.1999	-1.6099	G
-PHISH, -IOM	27-D	12/6/2016	1.96	488	SO	A	Aluminum	<	1.5000	0.00157	-6.45779	9.77	488	<	1.5000	0.00031	-8.06365	0.2007	-1.6059	G
-PHISH, -IOM	29-D	12/7/2016	2.01	434	TG	A	Aluminum	<	1.5000	0.00172	-6.36571	10.16	434	<	1.5000	0.00034	-7.98604	0.1978	-1.6203	G
-PHISH, -IOM	30-D	12/7/2016	2.08	451	SO	A	Aluminum	<	1.5000	0.00160	-6.43837	10.10	451	<	1.5000	0.00033	-8.01804	0.2060	-1.5797	G
-PHISH, -IOM	31-D	12/7/2016	2.00	279	SO	A	Aluminum	<	1.5000	0.00269	-5.91889	9.91	279	<	1.5000	0.00054	-7.51879	0.2019	-1.5999	G
-PHISH, -IOM	32-D	12/8/2016	2.01	391	SO	A	Aluminum	<	1.5000	0.00191	-6.26138	9.91	391	<	1.5000	0.00039	-7.85679	0.2028	-1.5954	G
-PHISH, -IOM	01-D	10/17/2016	1.99	389	W	A	Arsenic	<	0.7500	0.00097	-6.93940	9.93	389	<	0.7500	0.00019	-8.54682	0.2004	-1.6074	G
-PHISH, -IOM	01-B-A	9/6/2016	2.04	254	F	A	Arsenic	<	0.7500	0.00145	-6.53797	10.11	255	<	0.7500	0.00029	-8.14198	0.2011	-1.6040	G
-PHISH, -IOM	02-D	10/19/2016	2.02	415	G	A	Arsenic	<	0.7500	0.00090	-7.01658	10.02	415	<	0.7500	0.00018	-8.62056	0.2011	-1.6040	G
-PHISH, -IOM	03-D	10/18/2016	1.98	427	W	A	Arsenic	<	0.7500	0.00089	-7.02756	9.91	427	<	0.7500	0.00018	-8.63751	0.1999	-1.6100	G
-PHISH, -IOM	04-D	10/24/2016	1.99	381	TG	A	Arsenic	<	0.7500	0.00099	-6.91610	9.86	381	<	0.7500	0.00020	-8.51897	0.2013	-1.6029	G
-PHISH, -IOM	05-D	10/26/2016	1.97	462	SO	A	Arsenic	<	0.7500	0.00083	-7.09874	9.98	462	<	0.7500	0.00016	-8.72350	0.1970	-1.6248	G
-PHISH, -IOM	06-D	10/24/2016	1.99	381	W	A	Arsenic	<	0.7500	0.00099	-6.91610	9.89	381	<	0.7500	0.00020	-8.52201	0.2007	-1.6059	G
-PHISH, -IOM	08-D	10/31/2016	1.99	396	TG	A	Arsenic	<	0.7500	0.00095	-6.95472	10.06	396	<	0.7500	0.00019	-8.57766	0.1973	-1.6229	G
-PHISH, -IOM	09-D	10/31/2016	1.99	396	W	A	Arsenic	<	0.7500	0.00095	-6.95472	9.97	396	<	0.7500	0.00019	-8.56868	0.1991	-1.6140	G
-PHISH, -IOM	10-D	11/2/2016	1.97	422	SO	A	Arsenic	<	0.7500	0.00090	-7.01072	9.81	422	<	0.7500	0.00018	-8.61558	0.2009	-1.6049	G
-PHISH, -IOM	11-D	11/9/2016	2.00	492	W	A	Arsenic	<	0.7500	0.00076	-7.17680	9.89	492	<	0.7500	0.00015	-8.77768	0.2017	-1.6009	G
-PHISH, -IOM	12-D	11/9/2016	1.98	494	W	A	Arsenic	<	0.7500	0.00077	-7.17331	9.90	494	<	0.7500	0.00015	-8.78225	0.2001	-1.6089	G
-PHISH, -IOM	C-P2	11/21/2016	2.02	490	G	P	Arsenic	<	0.7500	0.00076	-7.18271	8.93	494	<	0.7500	0.00017	-8.67963	0.2238	-1.4969	G
-PHISH, -IOM	C-P3	11/21/2016	2.01	499	G	P	Arsenic	<	0.7500	0.00075	-7.19842	8.87	497	<	0.7500	0.00017	-8.67895	0.2275	-1.4805	G
-PHISH, -IOM	C-P4	11/21/2016	1.99	478	P	P	Arsenic	<	0.7500	0.00079	-7.14291	8.81	482	<	0.7500	0.00018	-8.64095	0.2236	-1.4980	G
-PHISH, -IOM	C-P5	11/22/2016	2.00	357	S	P	Arsenic	<	0.7500	0.00105	-6.85606	7.95	355	<	0.7500	0.00027	-8.23234	0.2525	-1.3763	G
-PHISH, -IOM	C-P6	11/22/2016	2.00	361	P	P	Arsenic	<	0.7500	0.00104	-6.86971	7.92	361	<	0.7500	0.00026	-8.24532	0.2527	-1.3756	G
-PHISH, -IOM	C-P7	11/22/2016	2.01	366	S	P	Arsenic	<	0.7500	0.00102	-6.88596	7.96	363	<	0.7500	0.00026	-8.25589	0.2541	-1.3699	G
-PHISH, -IOM	C-P8	11/22/2016	1.99	362	T	P	Arsenic	<	0.7500	0.00104	-6.86746	7.96	364	<	0.7500	0.00026	-8.25926	0.2486	-1.3918	G
-PHISH, -IOM	25-D	12/5/2016	1.98	432	TG	A	Arsenic	<	0.7500	0.00088	-7.03920	9.91	432	<	0.7500	0.00018	-8.64915	0.1999	-1.6100	G
-PHISH, -IOM	26-D	12/5/2016	1.98	433	W	A	Arsenic	<	0.7500	0.00088	-7.03899	9.93	433	<	0.7500	0.00017	-8.65398	0.1989	-1.6150	G
-PHISH, -IOM	27-D	12/6/2016	1.96	488	SO	A	Arsenic	<	0.7500	0.00078	-7.15094	9.77	488	<	0.7500	0.00016	-8.75680	0.2007	-1.6059	G
-PHISH, -IOM	28-D	12/7/2016	2.02	435	W	A	Arsenic	<	0.7500	0.00085	-7.06613	10.10	435	<	0.7500	0.00017	-8.67556	0.2000	-1.6094	G
-PHISH, -IOM	29-D	12/7/2016	2.01	434	TG	A	Arsenic	<	0.7500	0.00086	-7.05886	10.16	434	<	0.7500	0.00017	-8.67919	0.1978	-1.6203	G
-PHISH, -IOM	30-D	12/7/2016	2.08	451	SO	A	Arsenic	<	0.7500	0.00080	-7.13152	10.10	451	<	0.7500	0.00016	-8.71119	0.2060	-1.5797	G
-PHISH, -IOM	31-D	12/7/2016	2.00	279	SO	A	Arsenic	<	0.7500	0.00134	-6.61204	9.91	279	<	0.7500	0.00027	-8.21193	0.2019	-1.5999	G
-PHISH, -IOM	32-D	12/8/2016	2.01	391	SO	A	Arsenic	<	0.7500	0.00095	-6.95452	9.91	391	<	0.7500	0.00019	-8.54993	0.2028	-1.5954	G
-PHISH, -IOM	A-03	5/19/2016	1.99	417	W	A	Arsenic	<	0.7500	0.00091	-7.00639	7.93	417	<	0.7500	0.00023	-8.39079	0.2505	-1.3844	G
-PHISH, -IOM	03-D	10/18/2016	1.98	427	W	A	Beryllium	<	0.0038	0.00000	-12.31264	9.91	427	<	0.0038	0.00000	-13.92258	0.1999	-1.6099	G
-PHISH, -IOM	05-D	10/26/2016	1.97	462	SO	A	Beryllium	<	0.0038	0.00000	-12.38381	9.98	462	<	0.0038	0.00000	-14.00857	0.1970	-1.6248	G
-PHISH, -IOM	06-D	10/24/2016	1.99	381	W	A	Beryllium	<	0.0038	0.00001	-12.20117	9.89	381	<	0.0038	0.00000	-13.80708	0.2007	-1.6059	G
-PHISH, -IOM	08-D	10/31/2016	1.99	396	TG	A	Beryllium	<	0.0038	0.00000	-12.23979	10.06	396	<	0.0038	0.00000	-13.86274	0.1973	-1.6230	G
-PHISH, -IOM	09-D	10/31/2016	1.99	396	W	A	Beryllium	<	0.0038	0.00000	-12.23979	9.97	396	<	0.0038	0.00000	-13.85375	0.1991	-1.6140	G
-PHISH, -IOM	11-D	11/9/2016	2.00	492	W	A	Beryllium	<	0.0038	0.00000	-12.46188	9.89	492	<	0.0038	0.00000	-14.06276	0.2017	-1.6009	G
-PHISH, -IOM	25-D	12/5/2016	1.98	432	TG	A	Beryllium	<	0.0038	0.00000	-12.32428	9.91	432	<	0.0038	0.00000	-13.93422	0.1999	-1.6099	G
-PHISH, -IOM	26-D	12/5/2016	1.98	433	W	A	Beryllium	<	0.0038	0.00000	-12.32406	9.93	433	<	0.0038	0.00000	-13.93905	0.1989	-1.6150	G
-PHISH, -IOM	27-D	12/6/2016	1.96	488	SO	A	Beryllium	<	0.0038	0.00000	-12.43601	9.77	488	<	0.0038	0.00000	-14.04187	0.2007	-1.6059	G
-PHISH, -IOM	28-D	12/7/2016	2.02	435	W	A	Beryllium	<	0.0038	0.00000	-12.35120	10.10	435	<	0.0038	0.00000	-13.96064	0.2000	-1.6094	G
-PHISH, -IOM	29-D	12/7/2016	2.01	434	TG	A	Beryllium	<	0.0038	0.00000	-12.34393	10.16	434	<	0.0038	0.00000	-13.96426	0.1978	-1.6203	G
-PHISH, -IOM	30-D	12/7/2016	2.08	451	SO	A	Beryllium	<	0.0038	0.00000	-12.41659	10.10	451	<	0.0038	0.00000	-13.99626	0.2060	-1.5797	G
-PHISH, -IOM	31-D	12/7/2016	2.00	279	SO	A	Beryllium	<	0.0038	0.00001	-11.89711	9.91	279	<	0.0038	0.00000	-13.49701	0.2019	-1.5999	G
-PHISH, -IOM	32-D	12/8/2016	2.01	391	SO	A	Beryllium	<	0.0038	0.00000	-12.23960	9.91	391	<	0.0038	0.00000	-13.83501	0.2028	-1.5954	G
-PHISH, -IOM	A-03	5/19/2016	1.99	417	W	A	Beryllium	<	0.0038	0.00000	-12.29146	7.93	417	<	0.0038	0.00000	-13.67586	0.2505	-1.3844	G
-PHISH, -IOM	03-D	10/18/2016	1.98	427	W	A	Cadmium	<	0.0230	0.00003	-10.51214	9.91	427	<	0.0230	0.00001	-12.12208	0.1999	-1.6099	G
-PHISH, -IOM	04-D	10/24/2016	1.99	381	TG	A	Cadmium	<	0.0230	0.00003	-10.40068	9.86	381	<	0.0230	0.00001	-12.00355	0.2013	-1.6029	G
-PHISH, -IOM	05-D	10/26/2016	1.97	462	SO	A	Cadmium	<	0.0230	0.00003	-10.58332	9.98	462	<	0.0230	0.00000	-12.20807	0.1970	-1.6248	G
-PHISH, -IOM	06-D	10/24/2016	1.99	381	W	A	Cadmium	<	0.0230	0.00003	-10.40068	9.89	381	<	0.0230	0.00001	-12.00658	0.2007	-1.6059	G
-PHISH, -IOM	09-D	10/31/2016	1.99	396	W	A	Cadmium	<	0.0230	0.00003	-10.43929	9.97	396	<	0.0230	0.00001	-12.05326	0.1991	-1.6140	G
-PHISH, -IOM	10-D	11/2/2016	1.97	422	SO	A	Cadmium	<	0.0230	0.00003	-10.49530	9.81	422	<	0.0230	0.00001	-12.10016	0.2009	-1.6049	G
-PHISH, -IOM	11-D	11/9/2016	2.00	492	W	A	Cadmium	<	0.0230	0.00002	-10.66138	9.89	492	<	0.0230	0.00000	-12.26226	0.2017	-1.6009	G
-PHISH, -IOM	12-D	11/9/2016	1.98	494	W	A	Cadmium	<	0.0230	0.00002	-10.65789	9.90	494	<	0.0230	0.00000	-12.26683	0.2001	-1.6089	G
-PHISH, -IOM	30-D	12/7/2016	2.08	451	SO	A	Cadmium	<	0.0230	0.00002	-10.61610	10.10	451	<	0.0230	0.00001	-12.19577	0.2060	-1.5797	G
-PHISH, -IOM	31-D	12/7/2016	2.00	279	SO	A	Cadmium	<	0.0230	0.00004	-10.09662	9.91	279	<	0.0230	0.00001	-11.69651	0.2019	-1.5999	G
-PHISH, -IOM	32-D	12/8/2016	2.01	391	SO	A	Cadmium	<	0.0230	0.00003	-10.43910	9.91	391	<	0.0230	0.00001	-12.03451	0.2028	-1.5954	G
-PHISH, -IOM	A-03	5/19/2016	1.99	417	W	A	Cadmium	<	0.0230	0.00003	-10.49097	7.93	417	<	0.0230	0.00001	-11.87537	0.2505	-1.3844	G
-PHISH, -IOM	01-D	10/17/2016	1.99	389	W	A	Chromium	<	0.3800	0.00049	-7.61930	9.93	389	<	0.3800	0.00010	-9.22672	0.2004	-1.6074	G
-PHISH, -IOM	01-B-A	9/6/2016	2.04	254	F	A	Chromium	<	0.3800	0.00073	-7.21787	10.11	255	<	0.3800	0.00015	-8.82188	0.2011	-1.6040	G
-PHISH, -IOM	02-D	10/19/2016	2.02	415	G	A	Chromium	<	0.3800	0.00045	-7.69648	10.02	415	<	0.3800	0.00009	-9.30047	0.2011	-1.6040	G
-PHISH, -IOM	03-D	10/18/2016	1.98	427	W	A	Chromium	<	0.3800	0.00045	-7.70746	9.91	427	<	0.3800	0.00009	-9.31741	0.1999	-1.6100	G
-PHISH, -IOM	04-D	10/24/2016	1.99	381	TG	A	Chromium	<	0.3800	0.00050	-7.59600	9.86	381	<	0.3800	0.00010	-9.19887	0.2013	-1.6029	G
-PHISH, -IOM	05-D	10/26/2016	1.97	462	SO	A	Chromium	<	0.3800	0.00042	-7.77864	9.98	462	<	0.3800	0.00008	-9.40340	0.1970	-1.6248	G

All paired prototype and IOM data set, Part 5:

Paircat	PairID	Date	QI	TI	Process	Sample Type	AnName	Iflags	Imass	Icon	LnIcon	QP	TP	Pflags	Pmass	Pcon	LnPcon	P/I	Ln P/I	RatioCat
-PHISH, -IOM	06-D	10/24/2016	1.99	381	W	A	Chromium	<	0.3800	0.00050	-7.59600	9.89	381	<	0.3800	0.00010	-9.20191	0.2007	-1.6059	G
-PHISH, -IOM	08-D	10/31/2016	1.99	396	TG	A	Chromium	<	0.3800	0.00048	-7.63462	10.06	396	<	0.3800	0.00010	-9.25757	0.1973	-1.6230	G
-PHISH, -IOM	09-D	10/31/2016	1.99	396	W	A	Chromium	<	0.3800	0.00048	-7.63462	9.97	396	<	0.3800	0.00010	-9.24858	0.1991	-1.6140	G
-PHISH, -IOM	10-D	11/2/2016	1.97	422	SO	A	Chromium	<	0.3800	0.00046	-7.69062	9.81	422	<	0.3800	0.00009	-9.29548	0.2009	-1.6049	G
-PHISH, -IOM	11-D	11/9/2016	2.00	492	W	A	Chromium	<	0.3800	0.00039	-7.85671	9.89	492	<	0.3800	0.00008	-9.45759	0.2017	-1.6009	G
-PHISH, -IOM	12-D	11/9/2016	1.98	494	W	A	Chromium	<	0.3800	0.00039	-7.85322	9.90	494	<	0.3800	0.00008	-9.46215	0.2001	-1.6089	G
-PHISH, -IOM	C-P4	11/21/2016	1.99	478	P	P	Chromium	<	0.3800	0.00040	-7.82281	8.81	482	<	0.3800	0.00009	-9.32085	0.2236	-1.4980	G
-PHISH, -IOM	26-D	12/5/2016	1.98	433	W	A	Chromium	<	0.3800	0.00044	-7.71889	9.93	433	<	0.3800	0.00009	-9.33388	0.1989	-1.6150	G
-PHISH, -IOM	27-D	12/6/2016	1.96	488	SO	A	Chromium	<	0.3800	0.00040	-7.83084	9.77	488	<	0.3800	0.00008	-9.43670	0.2007	-1.6059	G
-PHISH, -IOM	29-D	12/7/2016	2.01	434	TG	A	Chromium	<	0.3800	0.00044	-7.73876	10.16	434	<	0.3800	0.00009	-9.35909	0.1978	-1.6203	G
-PHISH, -IOM	30-D	12/7/2016	2.08	451	SO	A	Chromium	<	0.3800	0.00041	-7.81142	10.10	451	<	0.3800	0.00008	-9.39109	0.2060	-1.5797	G
-PHISH, -IOM	31-D	12/7/2016	2.00	279	SO	A	Chromium	<	0.3800	0.00068	-7.29194	9.91	279	<	0.3800	0.00014	-8.89184	0.2019	-1.5999	G
-PHISH, -IOM	32-D	12/8/2016	2.01	391	SO	A	Chromium	<	0.3800	0.00048	-7.63443	9.91	391	<	0.3800	0.00010	-9.22984	0.2028	-1.5954	G
-PHISH, -IOM	01-D	10/17/2016	1.99	389	W	A	Copper	<	0.1500	0.00019	-8.54883	9.93	389	<	0.1500	0.00004	-10.15626	0.2004	-1.6074	G
-PHISH, -IOM	03-D	10/18/2016	1.98	427	W	A	Copper	<	0.1500	0.00018	-8.63700	9.91	427	<	0.1500	0.00004	-10.24694	0.1999	-1.6099	G
-PHISH, -IOM	08-D	10/31/2016	1.99	396	TG	A	Copper	<	0.1500	0.00019	-8.56415	10.06	396	<	0.1500	0.00004	-10.18710	0.1973	-1.6230	G
-PHISH, -IOM	09-D	10/31/2016	1.99	396	W	A	Copper	<	0.1500	0.00019	-8.56415	9.97	396	<	0.1500	0.00004	-10.17811	0.1991	-1.6140	G
-PHISH, -IOM	01-B-A	9/6/2016	2.04	254	F	A	Iron	<	1.5000	0.00289	-5.84482	10.11	255	<	1.5000	0.00058	-7.44883	0.2011	-1.6040	G
-PHISH, -IOM	03-D	10/18/2016	1.98	427	W	A	Iron	<	1.5000	0.00177	-6.33442	9.91	427	<	1.5000	0.00035	-7.94436	0.1999	-1.6099	G
-PHISH, -IOM	05-D	10/26/2016	1.97	462	SO	A	Iron	<	1.5000	0.00165	-6.40559	9.98	462	<	1.5000	0.00033	-8.03035	0.1970	-1.6248	G
-PHISH, -IOM	10-D	11/2/2016	1.97	422	SO	A	Iron	<	1.5000	0.00180	-6.31757	9.81	422	<	1.5000	0.00036	-7.92243	0.2009	-1.6049	G
-PHISH, -IOM	27-D	12/6/2016	1.96	488	SO	A	Iron	<	1.5000	0.00157	-6.45779	9.77	488	<	1.5000	0.00031	-8.06365	0.2007	-1.6059	G
-PHISH, -IOM	30-D	12/7/2016	2.08	451	SO	A	Iron	<	1.5000	0.00160	-6.43837	10.10	451	<	1.5000	0.00033	-8.01804	0.2060	-1.5797	G
-PHISH, -IOM	31-D	12/7/2016	2.00	279	SO	A	Iron	<	1.5000	0.00269	-5.91889	9.91	279	<	1.5000	0.00054	-7.51879	0.2019	-1.5999	G
-PHISH, -IOM	32-D	12/8/2016	2.01	391	SO	A	Iron	<	1.5000	0.00191	-6.26138	9.91	391	<	1.5000	0.00039	-7.85679	0.2028	-1.5954	G
-PHISH, -IOM	03-D	10/18/2016	1.98	427	W	A	Lead	<	0.3800	0.00045	-7.70746	9.91	427	<	0.3800	0.00009	-9.31741	0.1999	-1.6100	G
-PHISH, -IOM	05-D	10/26/2016	1.97	462	SO	A	Lead	<	0.3800	0.00042	-7.77864	9.98	462	<	0.3800	0.00008	-9.40340	0.1970	-1.6248	G
-PHISH, -IOM	09-D	10/31/2016	1.99	396	W	A	Lead	<	0.3800	0.00048	-7.63462	9.97	396	<	0.3800	0.00010	-9.24858	0.1991	-1.6140	G
-PHISH, -IOM	10-D	11/2/2016	1.97	422	SO	A	Lead	<	0.3800	0.00046	-7.69062	9.81	422	<	0.3800	0.00009	-9.29548	0.2009	-1.6049	G
-PHISH, -IOM	11-D	11/9/2016	2.00	492	W	A	Lead	<	0.3800	0.00039	-7.85671	9.89	492	<	0.3800	0.00008	-9.45759	0.2017	-1.6009	G
-PHISH, -IOM	12-D	11/9/2016	1.98	494	W	A	Lead	<	0.3800	0.00039	-7.85322	9.90	494	<	0.3800	0.00008	-9.46215	0.2001	-1.6089	G
-PHISH, -IOM	27-D	12/6/2016	1.96	488	SO	A	Lead	<	0.3800	0.00040	-7.83084	9.77	488	<	0.3800	0.00008	-9.43670	0.2007	-1.6059	G
-PHISH, -IOM	28-D	12/7/2016	2.02	435	W	A	Lead	<	0.3800	0.00043	-7.74603	10.10	435	<	0.3800	0.00009	-9.35547	0.2000	-1.6094	G
-PHISH, -IOM	30-D	12/7/2016	2.08	451	SO	A	Lead	<	0.3800	0.00041	-7.81142	10.10	451	<	0.3800	0.00008	-9.39109	0.2060	-1.5797	G
-PHISH, -IOM	31-D	12/7/2016	2.00	279	SO	A	Lead	<	0.3800	0.00068	-7.29194	9.91	279	<	0.3800	0.00014	-8.89184	0.2019	-1.5999	G
-PHISH, -IOM	32-D	12/8/2016	2.01	391	SO	A	Lead	<	0.3800	0.00048	-7.63443	9.91	391	<	0.3800	0.00010	-9.22984	0.2028	-1.5954	G
-PHISH, -IOM	03-D	10/18/2016	1.98	427	W	A	Manganese	<	0.0380	0.00004	-10.01005	9.91	427	<	0.0380	0.00001	-11.61999	0.1999	-1.6099	G
-PHISH, -IOM	05-D	10/26/2016	1.97	462	SO	A	Manganese	<	0.0380	0.00004	-10.08123	9.98	462	<	0.0380	0.00001	-11.70598	0.1970	-1.6248	G
-PHISH, -IOM	27-D	12/6/2016	1.96	488	SO	A	Manganese	<	0.0380	0.00004	-10.13343	9.77	488	<	0.0380	0.00001	-11.73929	0.2007	-1.6059	G
-PHISH, -IOM	30-D	12/7/2016	2.08	451	SO	A	Manganese	<	0.0380	0.00004	-10.11400	10.10	451	<	0.0380	0.00001	-11.69368	0.2060	-1.5797	G
-PHISH, -IOM	31-D	12/7/2016	2.00	279	SO	A	Manganese	<	0.0380	0.00007	-9.59453	9.91	279	<	0.0380	0.00001	-11.19442	0.2019	-1.5999	G
-PHISH, -IOM	32-D	12/8/2016	2.01	391	SO	A	Manganese	<	0.0380	0.00005	-9.93701	9.91	391	<	0.0380	0.00001	-11.53242	0.2028	-1.5954	G
-PHISH, -IOM	01-D	10/17/2016	1.99	389	W	A	Nickel	<	0.0380	0.00005	-9.92188	9.93	389	<	0.0380	0.00001	-11.52931	0.2004	-1.6074	G
-PHISH, -IOM	01-B-A	9/6/2016	2.04	254	F	A	Nickel	<	0.0890	0.00017	-8.66940	10.11	255	<	0.0890	0.00003	-10.27341	0.2011	-1.6040	G
-PHISH, -IOM	03-D	10/18/2016	1.98	427	W	A	Nickel	<	0.0380	0.00004	-10.01005	9.91	427	<	0.0380	0.00001	-11.61999	0.1999	-1.6099	G
-PHISH, -IOM	04-D	10/24/2016	1.99	381	TG	A	Nickel	<	0.0890	0.00012	-9.04754	9.86	381	<	0.0890	0.00002	-10.65040	0.2013	-1.6029	G
-PHISH, -IOM	05-D	10/26/2016	1.97	462	SO	A	Nickel	<	0.0380	0.00004	-10.08123	9.98	462	<	0.0380	0.00001	-11.70598	0.1970	-1.6248	G
-PHISH, -IOM	06-D	10/24/2016	1.99	381	W	A	Nickel	<	0.0890	0.00012	-9.04754	9.89	381	<	0.0890	0.00002	-10.65344	0.2007	-1.6059	G
-PHISH, -IOM	08-D	10/31/2016	1.99	396	TG	A	Nickel	<	0.0380	0.00005	-9.93720	10.06	396	<	0.0380	0.00001	-11.56015	0.1973	-1.6230	G
-PHISH, -IOM	09-D	10/31/2016	1.99	396	W	A	Nickel	<	0.0380	0.00005	-9.93720	9.97	396	<	0.0380	0.00001	-11.55116	0.1991	-1.6140	G
-PHISH, -IOM	10-D	11/2/2016	1.97	422	SO	A	Nickel	<	0.0890	0.00011	-9.14216	9.81	422	<	0.0890	0.00002	-10.74702	0.2009	-1.6049	G
-PHISH, -IOM	27-D	12/6/2016	1.96	488	SO	A	Nickel	<	0.0380	0.00004	-10.13343	9.77	488	<	0.0380	0.00001	-11.73929	0.2007	-1.6059	G
-PHISH, -IOM	30-D	12/7/2016	2.08	451	SO	A	Nickel	<	0.0380	0.00004	-10.11400	10.10	451	<	0.0380	0.00001	-11.69368	0.2060	-1.5797	G
-PHISH, -IOM	31-D	12/7/2016	2.00	279	SO	A	Nickel	<	0.0380	0.00007	-9.59453	9.91	279	<	0.0380	0.00001	-11.19442	0.2019	-1.5999	G
-PHISH, -IOM	32-D	12/8/2016	2.01	391	SO	A	Nickel	<	0.0380	0.00005	-9.93701	9.91	391	<	0.0380	0.00001	-11.53242	0.2028	-1.5954	G
-PHISH, -IOM	01-D	10/17/2016	1.99	389	W	A	Selenium	<	0.7500	0.00097	-6.93940	9.93	389	<	0.7500	0.00019	-8.54682	0.2004	-1.6074	G
-PHISH, -IOM	01-B-A	9/6/2016	2.04	254	F	A	Selenium	<	0.7500	0.00145	-6.53797	10.11	255	<	0.7500	0.00029	-8.14198	0.2011	-1.6040	G
-PHISH, -IOM	02-D	10/19/2016	2.02	415	G	A	Selenium	<	0.7500	0.00090	-7.01658	10.02	415	<	0.7500	0.00018	-8.62056	0.2011	-1.6040	G
-PHISH, -IOM	03-D	10/18/2016	1.98	427	W	A	Selenium	<	0.7500	0.00089	-7.02756	9.91	427	<	0.7500	0.00018	-8.63751	0.1999	-1.6100	G
-PHISH, -IOM	04-D	10/24/2016	1.99	381	TG	A	Selenium	<	0.7500	0.00099	-6.91610	9.86	381	<	0.7500	0.00020	-8.51897	0.2013	-1.6029	G
-PHISH, -IOM	05-D	10/26/2016	1.97	462	SO	A	Selenium	<	0.7500	0.00083	-7.09874	9.98	462	<	0.7500	0.00016	-8.72350	0.1970	-1.6248	G
-PHISH, -IOM	06-D	10/24/2016	1.99	381	W	A	Selenium	<	0.7500	0.00099	-6.91610	9.89	381	<	0.7500	0.00020	-8.52201	0.2007	-1.6059	G
-PHISH, -IOM	08-D	10/31/2016	1.99	396	TG	A	Selenium	<	0.7500	0.00095	-6.95472	10.06	396	<	0.7500	0.00019	-8.57766	0.1973	-1.6229	G
-PHISH, -IOM	09-D	10/31/2016	1.99	396	W	A	Selenium	<	0.7500	0.00095	-6.95472	9.97	396	<	0.7500	0.00019	-8.56868	0.1991	-1.6140	G
-PHISH, -IOM	10-D	11/2/2016	1.97	422	SO	A	Selenium	<	0.7500	0.00090	-7.01072	9.81	422	<	0.7500	0.00018	-8.61558	0.2009	-1.6049	G
-PHISH, -IOM	11-D	11/9/2016	2.00	492	W	A	Selenium	<	0.7500	0.00076	-7.17680	9.89	492	<	0.7500	0.00015	-8.77768	0.2017	-1.6009	G
-PHISH, -IOM	12-D	11/9/2016	1.98	494	W	A	Selenium	<	0.7500	0.00077	-7.17331	9.90	494	<	0.7500	0.00015	-8.78225	0.2001	-1.6089	G

All paired prototype and IOM data set, Part 6:

Paircat	PairID	Date	QI	TI	Process	Sample Type	AnName	Iflags	Imass	Icon	LnIcon	QP	TP	Pflags	Pmass	Pcon	LnPcon	P/I	Ln P/I	RatioCat
-PHISH, -IOM	C-P2	11/21/2016	2.02	490	G	P	Selenium	<	0.7500	0.00076	-7.18271	8.93	494	<	0.7500	0.00017	-8.67963	0.2238	-1.4969	G
-PHISH, -IOM	C-P3	11/21/2016	2.01	499	G	P	Selenium	<	0.7500	0.00075	-7.19842	8.87	497	<	0.7500	0.00017	-8.67895	0.2275	-1.4805	G
-PHISH, -IOM	C-P4	11/21/2016	1.99	478	P	P	Selenium	<	0.7500	0.00079	-7.14291	8.81	482	<	0.7500	0.00018	-8.64095	0.2236	-1.4980	G
-PHISH, -IOM	C-P5	11/22/2016	2.00	357	S	P	Selenium	<	0.7500	0.00105	-6.85606	7.95	355	<	0.7500	0.00027	-8.23234	0.2525	-1.3763	G
-PHISH, -IOM	C-P6	11/22/2016	2.00	361	P	P	Selenium	<	0.7500	0.00104	-6.86971	7.92	361	<	0.7500	0.00026	-8.24532	0.2527	-1.3756	G
-PHISH, -IOM	C-P7	11/22/2016	2.01	366	S	P	Selenium	<	0.7500	0.00102	-6.88596	7.96	363	<	0.7500	0.00026	-8.25589	0.2541	-1.3699	G
-PHISH, -IOM	C-P8	11/22/2016	1.99	362	T	P	Selenium	<	0.7500	0.00104	-6.86746	7.96	364	<	0.7500	0.00026	-8.25926	0.2486	-1.3918	G
-PHISH, -IOM	25-D	12/5/2016	1.98	432	TG	A	Selenium	<	0.7500	0.00088	-7.03920	9.91	432	<	0.7500	0.00018	-8.64915	0.1999	-1.6100	G
-PHISH, -IOM	26-D	12/5/2016	1.98	433	W	A	Selenium	<	0.7500	0.00088	-7.03899	9.93	433	<	0.7500	0.00017	-8.65398	0.1989	-1.6150	G
-PHISH, -IOM	27-D	12/6/2016	1.96	488	SO	A	Selenium	<	0.7500	0.00078	-7.15094	9.77	488	<	0.7500	0.00016	-8.75680	0.2007	-1.6059	G
-PHISH, -IOM	28-D	12/7/2016	2.02	435	W	A	Selenium	<	0.7500	0.00085	-7.06613	10.10	435	<	0.7500	0.00017	-8.67556	0.2000	-1.6094	G
-PHISH, -IOM	29-D	12/7/2016	2.01	434	TG	A	Selenium	<	0.7500	0.00086	-7.05886	10.16	434	<	0.7500	0.00017	-8.67919	0.1978	-1.6203	G
-PHISH, -IOM	30-D	12/7/2016	2.08	451	SO	A	Selenium	<	0.7500	0.00080	-7.13152	10.10	451	<	0.7500	0.00016	-8.71119	0.2060	-1.5797	G
-PHISH, -IOM	31-D	12/7/2016	2.00	279	SO	A	Selenium	<	0.7500	0.00134	-6.61204	9.91	279	<	0.7500	0.00027	-8.21193	0.2019	-1.5999	G
-PHISH, -IOM	32-D	12/8/2016	2.01	391	SO	A	Selenium	<	0.7500	0.00095	-6.95452	9.91	391	<	0.7500	0.00019	-8.54993	0.2028	-1.5954	G
-PHISH, -IOM	A-03	5/19/2016	1.99	417	W	A	Selenium	<	0.7500	0.00091	-7.00639	7.93	417	<	0.7500	0.00023	-8.39079	0.2505	-1.3844	G
-PHISH, -IOM	01-D	10/17/2016	1.99	389	W	A	Silver	<	0.0750	0.00010	-9.24198	9.93	389	<	0.0750	0.00002	-10.84941	0.2004	-1.6074	G
-PHISH, -IOM	01-B-A	9/6/2016	2.04	254	F	A	Silver	<	0.0750	0.00014	-8.84055	10.11	255	<	0.0750	0.00003	-10.44456	0.2011	-1.6040	G
-PHISH, -IOM	03-D	10/18/2016	1.98	427	W	A	Silver	<	0.0750	0.00009	-9.33015	9.91	427	<	0.0750	0.00002	-10.94009	0.1999	-1.6099	G
-PHISH, -IOM	04-D	10/24/2016	1.99	381	TG	A	Silver	<	0.0750	0.00010	-9.21869	9.86	381	<	0.0750	0.00002	-10.82155	0.2013	-1.6029	G
-PHISH, -IOM	05-D	10/26/2016	1.97	462	SO	A	Silver	<	0.0750	0.00008	-9.40132	9.98	462	<	0.0750	0.00002	-11.02608	0.1970	-1.6248	G
-PHISH, -IOM	06-D	10/24/2016	1.99	381	W	A	Silver	<	0.0750	0.00010	-9.21869	9.89	381	<	0.0750	0.00002	-10.82459	0.2007	-1.6059	G
-PHISH, -IOM	08-D	10/31/2016	1.99	396	TG	A	Silver	<	0.0750	0.00010	-9.25730	10.06	396	<	0.0750	0.00002	-10.88025	0.1973	-1.6230	G
-PHISH, -IOM	09-D	10/31/2016	1.99	396	W	A	Silver	<	0.0750	0.00010	-9.25730	9.97	396	<	0.0750	0.00002	-10.87126	0.1991	-1.6140	G
-PHISH, -IOM	11-D	11/9/2016	2.00	492	W	A	Silver	<	0.0750	0.00008	-9.47939	9.89	492	<	0.0750	0.00002	-11.08027	0.2017	-1.6009	G
-PHISH, -IOM	12-D	11/9/2016	1.98	494	W	A	Silver	<	0.0750	0.00008	-9.47590	9.90	494	<	0.0750	0.00002	-11.08483	0.2001	-1.6089	G
-PHISH, -IOM	C-P2	11/21/2016	2.02	490	G	P	Silver	<	0.0750	0.00008	-9.48529	8.93	494	<	0.0750	0.00002	-10.98222	0.2238	-1.4969	G
-PHISH, -IOM	C-P4	11/21/2016	1.99	478	P	P	Silver	<	0.0750	0.00008	-9.44550	8.81	482	<	0.0750	0.00002	-10.94353	0.2236	-1.4980	G
-PHISH, -IOM	C-P5	11/22/2016	2.00	357	S	P	Silver	<	0.0750	0.00011	-9.15865	7.95	355	<	0.0750	0.00003	-10.53493	0.2525	-1.3763	G
-PHISH, -IOM	C-P6	11/22/2016	2.00	361	P	P	Silver	<	0.0750	0.00010	-9.17229	7.92	361	<	0.0750	0.00003	-10.54790	0.2527	-1.3756	G
-PHISH, -IOM	C-P7	11/22/2016	2.01	366	S	P	Silver	<	0.0750	0.00010	-9.18854	7.96	363	<	0.0750	0.00003	-10.55847	0.2541	-1.3699	G
-PHISH, -IOM	25-D	12/5/2016	1.98	432	TG	A	Silver	<	0.0750	0.00009	-9.34179	9.91	432	<	0.0750	0.00002	-10.95173	0.1999	-1.6099	G
-PHISH, -IOM	26-D	12/5/2016	1.98	433	W	A	Silver	<	0.0750	0.00009	-9.34157	9.93	433	<	0.0750	0.00002	-10.95657	0.1989	-1.6150	G
-PHISH, -IOM	28-D	12/7/2016	2.02	435	W	A	Silver	<	0.0750	0.00009	-9.36871	10.10	435	<	0.0750	0.00002	-10.97815	0.2000	-1.6094	G
-PHISH, -IOM	29-D	12/7/2016	2.01	434	TG	A	Silver	<	0.0750	0.00009	-9.36145	10.16	434	<	0.0750	0.00002	-10.98177	0.1978	-1.6203	G
-PHISH, -IOM	30-D	12/7/2016	2.08	451	SO	A	Silver	<	0.0750	0.00008	-9.43410	10.10	451	<	0.0750	0.00002	-11.01377	0.2060	-1.5797	G
-PHISH, -IOM	32-D	12/8/2016	2.01	391	SO	A	Silver	<	0.0750	0.00010	-9.25711	9.91	391	<	0.0750	0.00002	-10.85252	0.2028	-1.5954	G
-PHISH, -IOM	A-03	5/19/2016	1.99	417	W	A	Silver	<	0.0750	0.00009	-9.30897	7.93	417	<	0.0750	0.00002	-10.69338	0.2505	-1.3844	G
-PHISH, -IOM	03-D	10/18/2016	1.98	427	W	A	Zinc	<	0.1500	0.00018	-8.63700	9.91	427	<	0.0000	0.00003	-10.28915	0.1916	-1.6522	G
-PHISH, -IOM	25-D	12/5/2016	1.98	432	TG	A	Zinc	<	0.1500	0.00018	-8.64864	9.91	432	<	0.0000	0.00003	-10.28915	0.1939	-1.6405	G
-PHISH, -IOM	29-D	12/7/2016	2.01	434	TG	A	Zinc	<	0.1500	0.00017	-8.66830	10.16	434	<	0.1500	0.00003	-10.28915	0.1977	-1.6209	G
-PHISH, -IOM	02-D	10/19/2016	2.02	415	G	A	Zinc	<	0.1500	0.00018	-8.62602	10.02	415	<	0.0000	0.00003	-10.28915	0.1895	-1.6631	G
-PHISH, +/- IOM	01-B-A	9/6/2016	2.04	254	F	A	Aluminum	()	1.5000	0.00289	-5.84482	10.11	255	<	1.5000	0.00058	-7.44883	0.2011	-1.6040	H
-PHISH, +/- IOM	01-D	10/17/2016	1.99	389	W	A	Beryllium	()	0.0039	0.00001	-12.19849	9.93	389	<	0.0038	0.00000	-13.83189	0.1953	-1.6334	H
-PHISH, +/- IOM	02-D	10/19/2016	2.02	415	G	A	Beryllium	()	0.0038	0.00000	-12.30165	10.02	415	<	0.0038	0.00000	-13.90564	0.2011	-1.6040	H
-PHISH, +/- IOM	04-D	10/24/2016	1.99	381	TG	A	Beryllium	()	0.0100	0.00001	-11.23359	9.86	381	<	0.0038	0.00000	-13.80404	0.0765	-2.5705	H
-PHISH, +/- IOM	12-D	11/9/2016	1.98	494	W	A	Beryllium	()	0.0110	0.00001	-11.39549	9.90	494	<	0.0038	0.00000	-14.06732	0.0691	-2.6718	H
-PHISH, +/- IOM	01-B-A	9/6/2016	2.04	254	F	A	Cadmium	()	0.0230	0.00004	-10.02255	10.11	255	<	0.0230	0.00001	-11.62655	0.2011	-1.6040	H
-PHISH, +/- IOM	04-D	10/24/2016	1.99	381	TG	A	Copper	()	0.2800	0.00037	-7.90138	9.86	381	<	0.1500	0.00004	-10.12841	0.1078	-2.2270	H
-PHISH, +/- IOM	01-D	10/17/2016	1.99	389	W	A	Zinc	()	0.1600	0.00021	-8.48430	9.93	389	<	0.0000	0.00003	-10.28915	0.1645	-1.8049	H
-PHISH, +/- IOM	08-D	10/31/2016	1.99	396	TG	A	Zinc	()	0.4800	0.00061	-7.40100	10.06	396	<	0.0000	0.00003	-10.28915	0.0557	-2.8882	H
-PHISH, +/- IOM	11-D	11/9/2016	2.00	492	W	A	Zinc	()	0.3900	0.00040	-7.83073	9.89	492	<	0.0000	0.00003	-10.28915	0.0856	-2.4584	H
-PHISH, +/- IOM	01-B-A	9/6/2016	2.04	254	F	A	Zinc	()	0.3600	0.00069	-7.27194	10.11	255	<	0.00000	0.00003	-10.28915	0.0489	-3.0172	H
-PHISH, +IOM	04-D	10/24/2016	1.99	381	TG	A	Zinc		2.1000	0.00278	-5.88648	9.86	381	<	0.0000	0.00003	-10.28915	0.0122	-4.4027	I
-PHISH, +IOM	05-D	10/26/2016	1.97	462	SO	A	Zinc		0.5800	0.00064	-7.35578	9.98	462	<	0.0000	0.00003	-10.28915	0.0532	-2.9334	I
-PHISH, +IOM	09-D	10/31/2016	1.99	396	W	A	Zinc		0.5600	0.00071	-7.24685	9.97	396	<	0.0000	0.00003	-10.28915	0.0477	-3.0423	I
-PHISH, +IOM	10-D	11/2/2016	1.97	422	SO	A	Zinc		1.8000	0.00217	-6.13525	9.81	422	<	0.0000	0.00003	-10.28915	0.0157	-4.1539	I
-PHISH, +IOM	12-D	11/9/2016	1.98	494	W	A	Zinc		0.7100	0.00073	-7.22812	9.90	494	<	0.0000	0.00008	-9.43348	0.1102	-2.2054	I

APPENDIX D: SHAPIRO-WILK NORMALITY TEST RESULTS

The results of the UNIVARAIATE Procedure to generate descriptive statistics and assess whether or not prototype and IOM concentrations were normally or log-normally distributed. This test was run using SAS v.9.3. (SAS Institute Inc., Cary, NC). SAS outputs are included below.

The UNIVARIATE Procedure

Variable: P_I (P/I)

RatioCat=A (±Prototype, -IOM)

Tests for Normality

Test	Statistic		p Value	
Shapiro-Wilk	**W**	0.900968	**Pr < W**	0.0009
Kolmogorov-Smirnov	**D**	0.146777	**Pr > D**	0.0142
Cramer-von Mises	**W-Sq**	0.182787	**Pr > W-Sq**	0.0085
Anderson-Darling	**A-Sq**	1.217518	**Pr > A-Sq**	<0.0050

The UNIVARIATE Procedure

Variable: P_I (P/I)

RatioCat=B (±Prototype, ±IOM)

Tests for Normality

Test	Statistic		p Value	
Shapiro-Wilk	**W**	0.95933	**Pr < W**	0.7433
Kolmogorov-Smirnov	**D**	0.123094	**Pr > D**	>0.1500
Cramer-von Mises	**W-Sq**	0.028453	**Pr > W-Sq**	>0.2500
Anderson-Darling	**A-Sq**	0.225355	**Pr > A-Sq**	>0.2500

The UNIVARIATE Procedure

Variable: P_I (P/I)

RatioCat=C (±Prototype, +IOM)

Tests for Normality

Test	Statistic		p Value	
Shapiro-Wilk	W	.	Pr < W	.
Kolmogorov-Smirnov	D	.	Pr > D	.
Cramer-von Mises	W-Sq	.	Pr > W-Sq	.
Anderson-Darling	A-Sq	.	Pr > A-Sq	.

The UNIVARIATE Procedure

Variable: P_I (P/I)

RatioCat=D (+Prototype, -IOM)

Tests for Normality

Test	Statistic		p Value	
Shapiro-Wilk	W	0.843126	Pr < W	0.0347
Kolmogorov-Smirnov	D	0.235112	Pr > D	0.0877
Cramer-von Mises	W-Sq	0.0974	Pr > W-Sq	0.1084
Anderson-Darling	A-Sq	0.67231	Pr > A-Sq	0.0588

The UNIVARIATE Procedure

Variable: P_I (P/I)

RatioCat=E (+Prototype, ±IOM)

Tests for Normality

Test	Statistic		p Value	
Shapiro-Wilk	W	0.8562	Pr < W	0.0007
Kolmogorov-Smirnov	D	0.132451	Pr > D	>0.1500
Cramer-von Mises	W-Sq	0.144957	Pr > W-Sq	0.0258
Anderson-Darling	A-Sq	0.970479	Pr > A-Sq	0.0136

The UNIVARIATE Procedure

Variable: P_I (P/I)

RatioCat=F (+Prototype, +IOM)

Tests for Normality

Test	Statistic		p Value	
Shapiro-Wilk	**W**	0.953794	**Pr < W**	0.0031
Kolmogorov-Smirnov	**D**	0.118009	**Pr > D**	<0.0100
Cramer-von Mises	**W-Sq**	0.193779	**Pr > W-Sq**	0.0063
Anderson-Darling	**A-Sq**	1.295342	**Pr > A-Sq**	<0.0050

The UNIVARIATE Procedure

Variable: P_I (P/I)

RatioCat=G (-Prototype, -IOM)

Tests for Normality

Test	Statistic		p Value	
Shapiro-Wilk	**W**	0.548814	**Pr < W**	<0.0001
Kolmogorov-Smirnov	**D**	0.387336	**Pr > D**	<0.0100
Cramer-von Mises	**W-Sq**	7.086387	**Pr > W-Sq**	<0.0050
Anderson-Darling	**A-Sq**	36.13158	**Pr > A-Sq**	<0.0050

The UNIVARIATE Procedure

Variable: P_I (P/I)

RatioCat=H (-Prototype, ±IOM)

Tests for Normality

Test	Statistic		p Value	
Shapiro-Wilk	**W**	0.827752	**Pr < W**	0.0218
Kolmogorov-Smirnov	**D**	0.215304	**Pr > D**	>0.1500
Cramer-von Mises	**W-Sq**	0.124125	**Pr > W-Sq**	0.0457
Anderson-Darling	**A-Sq**	0.77629	**Pr > A-Sq**	0.0311

The UNIVARIATE Procedure

Variable: P_I (P/I)

RatioCat=I (-Prototype, +IOM)

Tests for Normality

Test	Statistic		p Value	
Shapiro-Wilk	**W**	0.884519	**Pr < W**	0.3303
Kolmogorov-Smirnov	**D**	0.24556	**Pr > D**	>0.1500
Cramer-von Mises	**W-Sq**	0.055214	**Pr > W-Sq**	>0.2500
Anderson-Darling	**A-Sq**	0.348938	**Pr > A-Sq**	>0.2500

The UNIVARIATE Procedure

Variable: Ln_P_I (Ln P/I)

RatioCat=A (±Prototype, -IOM)

Tests for Normality

Test	Statistic		p Value	
Shapiro-Wilk	**W**	0.971311	**Pr < W**	0.3096
Kolmogorov-Smirnov	**D**	0.12448	**Pr > D**	0.0739
Cramer-von Mises	**W-Sq**	0.063785	**Pr > W-Sq**	>0.2500
Anderson-Darling	**A-Sq**	0.407741	**Pr > A-Sq**	>0.2500

The UNIVARIATE Procedure

Variable: Ln_P_I (Ln P/I)

RatioCat=B (±Prototype, ±IOM)

Tests for Normality

Test	Statistic		p Value	
Shapiro-Wilk	**W**	0.932926	**Pr < W**	0.3720
Kolmogorov-Smirnov	**D**	0.180931	**Pr > D**	>0.1500
Cramer-von Mises	**W-Sq**	0.062642	**Pr > W-Sq**	>0.2500
Anderson-Darling	**A-Sq**	0.398061	**Pr > A-Sq**	>0.2500

The UNIVARIATE Procedure

Variable: Ln_P_I (Ln P/I)

RatioCat=C (±Prototype, +IOM)

Tests for Normality

Test	Statistic		p Value	
Shapiro-Wilk	**W**	.	**Pr < W**	.
Kolmogorov-Smirnov	**D**	.	**Pr > D**	.
Cramer-von Mises	**W-Sq**	.	**Pr > W-Sq**	.
Anderson-Darling	**A-Sq**	.	**Pr > A-Sq**	.

The UNIVARIATE Procedure

Variable: Ln_P_I (Ln P/I)

RatioCat=D (+Prototype, -IOM)

Tests for Normality

Test	Statistic		p Value	
Shapiro-Wilk	**W**	0.855333	**Pr < W**	0.0501
Kolmogorov-Smirnov	**D**	0.225318	**Pr > D**	0.1184
Cramer-von Mises	**W-Sq**	0.09251	**Pr > W-Sq**	0.1280
Anderson-Darling	**A-Sq**	0.619068	**Pr > A-Sq**	0.0827

The UNIVARIATE Procedure

Variable: Ln_P_I (Ln P/I)

RatioCat=E (+Prototype, ±IOM)

Tests for Normality

Test	Statistic		p Value	
Shapiro-Wilk	**W**	0.985072	**Pr < W**	0.9324
Kolmogorov-Smirnov	**D**	0.051893	**Pr > D**	>0.1500
Cramer-von Mises	**W-Sq**	0.014944	**Pr > W-Sq**	>0.2500
Anderson-Darling	**A-Sq**	0.130941	**Pr > A-Sq**	>0.2500

The UNIVARIATE Procedure

Variable: Ln_P_I (Ln P/I)

RatioCat=F (+Prototype, +IOM)

Tests for Normality

Test	Statistic		p Value	
Shapiro-Wilk	**W**	0.854829	**Pr < W**	<0.0001
Kolmogorov-Smirnov	**D**	0.201471	**Pr > D**	<0.0100
Cramer-von Mises	**W-Sq**	0.836074	**Pr > W-Sq**	<0.0050
Anderson-Darling	**A-Sq**	4.818325	**Pr > A-Sq**	<0.0050

The UNIVARIATE Procedure

Variable: Ln_P_I (Ln P/I)

RatioCat=G (-Prototype, -IOM)

Tests for Normality

Test	Statistic		p Value	
Shapiro-Wilk	**W**	0.567348	**Pr < W**	<0.0001
Kolmogorov-Smirnov	**D**	0.380771	**Pr > D**	<0.0100
Cramer-von Mises	**W-Sq**	6.749575	**Pr > W-Sq**	<0.0050
Anderson-Darling	**A-Sq**	34.51826	**Pr > A-Sq**	<0.0050

The UNIVARIATE Procedure

Variable: Ln_P_I (Ln P/I)

RatioCat=H (-Prototype, ±IOM)

Tests for Normality

Test	Statistic		p Value	
Shapiro-Wilk	**W**	0.862977	**Pr < W**	0.0629
Kolmogorov-Smirnov	**D**	0.209295	**Pr > D**	>0.1500
Cramer-von Mises	**W-Sq**	0.093815	**Pr > W-Sq**	0.1228
Anderson-Darling	**A-Sq**	0.60319	**Pr > A-Sq**	0.0899

The UNIVARIATE Procedure

Variable: Ln_P_I (Ln P/I)

RatioCat=I (-Prototype, +IOM)

Tests for Normality

Test	Statistic		p Value	
Shapiro-Wilk	**W**	0.924162	**Pr < W**	0.5571
Kolmogorov-Smirnov	**D**	0.230953	**Pr > D**	>0.1500
Cramer-von Mises	**W-Sq**	0.04747	**Pr > W-Sq**	>0.2500
Anderson-Darling	**A-Sq**	0.281793	**Pr > A-Sq**	>0.2500

APPENDIX E: NONPARAMETRIC ANALYSIS OF CONCENTRATIONS COLLECTED BETWEEN SAMPLERS

The NPAR1WAY Procedure was used to perform a Wilcoxon Rank-Sum test to assess differences between samplers by aggregate concentrations collected, ratio of concentrations by sample type and by particle size. These tests were run using SAS v.9.3. (SAS Institute Inc., Cary, NC). SAS outputs are included below.

Nonparametric test: Does Prototype=IOM aggregate concentrations (zinc outlier removed)

The NPAR1WAY Procedure

Wilcoxon Scores (Rank Sums) for Variable TotC Classified by Variable Sampler

Sampler	N	Sum of Scores	Expected Under H0	Std Dev Under H0	Mean Score
I	21	469.0	451.50	39.752358	22.333333
P	21	434.0	451.50	39.752358	20.666667

Wilcoxon Two-Sample Test

Statistic (S)	469.0000
Normal Approximation	
Z	0.4276
One-Sided Pr > Z	0.3345
Two-Sided Pr > |Z|	0.6689
t Approximation	
One-Sided Pr > Z	0.3356
Two-Sided Pr > |Z|	0.6711
Exact Test	
One-Sided Pr >= S	0.3360
Two-Sided Pr >= |S - Mean|	0.6721

Z includes a continuity correction of 0.5.

Nonparametric test: Prototype:IOM concentrations by sample type

(0=personal 1=area; zinc outlier removed)

The NPAR1WAY Procedure

Wilcoxon Scores (Rank Sums) for Variable P_I
Classified by Variable TypeCode

TypeCode	N	Sum of Scores	Expected Under H0	Std Dev Under H0	Mean Score
0	55	2398.0	2475.0	118.426689	43.600000
1	34	1607.0	1530.0	118.426689	47.264706

Average scores were used for ties.

Wilcoxon Two-Sample Test

Statistic (S)	1607.0000
Normal Approximation	
Z	0.6460
One-Sided Pr > Z	0.2591
Two-Sided Pr > |Z|	0.5183
t Approximation	
One-Sided Pr > Z	0.2600
Two-Sided Pr > |Z|	0.5200
Exact Test	
One-Sided Pr >= S	0.2595
Two-Sided Pr >= |S - Mean|	0.5190

Z includes a continuity correction of 0.5.

Nonparametric test: Prototype:IOM concentrations by particle size

(0=small 1=large; zinc outlier removed)

The NPAR1WAY Procedure

Wilcoxon Scores (Rank Sums) for Variable P_I Classified by Variable PROCode

PROCode	N	Sum of Scores	Expected Under H0	Std Dev Under H0	Mean Score
0	45	1922.0	2025.0	121.860057	42.711111
1	44	2083.0	1980.0	121.860057	47.340909

Average scores were used for ties.

Wilcoxon Two-Sample Test

Statistic (S)	2083.0000
Normal Approximation	
Z	0.8411
One-Sided Pr > Z	0.2001
Two-Sided Pr > |Z|	0.4003
t Approximation	
One-Sided Pr > Z	0.2013
Two-Sided Pr > |Z|	0.4026
Exact Test	
One-Sided Pr >= S	0.2005
Two-Sided Pr >= |S - Mean|	0.4010

Z includes a continuity correction of 0.5.

APPENDIX F: LINEAR REGRESSION ANALYSIS

The REG Procedure was used to perform a linear regression analysis to determine the relationship of the prototype concentrations collected to the IOM concentrations collected. This test was run using SAS v.9.3. (SAS Institute, Cary, NC). SAS outputs are included below.

Proc Reg by aggregate metal concentrations (zinc outlier removed, with intercept)

Proc Reg

The REG Procedure

Model: MODEL1

Dependent Variable: Pcon Pcon

Analysis of Variance

Source	DF	Sum of Squares	Mean Square	F Value	Pr > F
Model	1	0.92192	0.92192	415.50	<.0001
Error	87	0.19304	0.00222		
Corrected Total	88	1.11496			

Root MSE	0.04710	**R-Square**	0.8269
Dependent Mean	0.04504	**Adj R-Sq**	0.8249
Coeff Var	104.58595		

Parameter Estimates

Variable	Label	DF	Parameter Estimate	Standard Error	t Value	Pr > |t|	95% Confidence Limits	
Intercept	Intercept	1	0.00313	0.00540	0.58	0.5639	-0.00760	0.01386
Icon	Icon	1	0.69934	0.03431	20.38	<.0001	0.63115	0.76753

Proc Reg by aggregate metal concentrations (zinc outlier and intercept removed)

The REG Procedure

Model: MODEL1

Dependent Variable: Pcon Pcon

Analysis of Variance

Source	DF	Sum of Squares	Mean Square	F Value	Pr > F
Model	1	1.10172	1.10172	500.31	<.0001
Error	88	0.19378	0.00220		
Uncorrected Total	89	1.29550			

Root MSE	0.04693	**R-Square**	0.8504
Dependent Mean	0.04504	**Adj R-Sq**	0.8487
Coeff Var	104.1903		

Parameter Estimates

Variable	Label	DF	Parameter Estimate	Standard Error	t Value	Pr > |t|	95% Confidence Limits	
Icon	Icon	1	0.70691	0.03160	22.37	<.0001	0.64410	0.76971

Proc Reg by sample type (zinc outlier removed, with intercept)

Proc Reg

The REG Procedure

Model: MODEL1

Dependent Variable: Pcon Pcon

Sample Type=A (area)

Analysis of Variance

Source	DF	Sum of Squares	Mean Square	F Value	Pr > F
Model	1	0.04556	0.04556	1334.88	<.0001
Error	32	0.00109	0.00003413		
Corrected Total	33	0.04665			

Root MSE	0.00584	**R-Square**	0.9766
Dependent Mean	0.01649	**Adj R-Sq**	0.9759
Coeff Var	35.4357		

Parameter Estimates

Variable	Label	DF	Parameter Estimate	Standard Error	t Value	Pr > |t|	95% Confidence Limits	
Intercept	Intercept	1	-0.00176	0.00112	-1.57	0.1259	-0.00404	0.00052100
Icon	Icon	1	1.20753	0.03305	36.54	<.0001	1.14021	1.27485

Proc Reg by sample type (zinc outlier removed, with intercept)

The REG Procedure

Model: MODEL1

Dependent Variable: Pcon Pcon

Sample Type=P (personal)

Analysis of Variance

Source	DF	Sum of Squares	Mean Square	F Value	Pr > F
Model	1	0.84006	0.84006	242.76	<.0001
Error	53	0.18340	0.00346		
Corrected Total	54	1.02346			

Root MSE	0.05883	**R-Square**	0.8208
Dependent Mean	0.06269	**Adj R-Sq**	0.8174
Coeff Var	93.8359		

Parameter Estimates

Variable	Label	DF	Parameter Estimate	Standard Error	t Value	Pr > |t|	95% Confidence Limits	
Intercept	Intercept	1	0.00185	0.00884	0.21	0.8346	-0.01588	0.01959
Icon	Icon	1	0.69418	0.04455	15.58	<.0001	0.60482	0.78354

Proc Reg by sample type (zinc outlier and intercept removed)

The REG Procedure

Model: MODEL1

Dependent Variable: Pcon Pcon

Sample Type=A (area)

Analysis of Variance

Source	DF	Sum of Squares	Mean Square	F Value	Pr > F
Model	1	0.05472	0.05472	1534.81	<.0001
Error	33	0.00118	0.00003565		
Uncorrected Total	34	0.05590			

Root MSE	0.00597	**R-Square**	0.9790
Dependent Mean	0.01649	**Adj R-Sq**	0.9783
Coeff Var	36.21628		

Parameter Estimates

Variable	Label	DF	Parameter Estimate	Standard Error	t Value	Pr > |t|	95% Confidence Limits	
Icon	Icon	1	1.18436	0.03023	39.18	<.0001	1.12285	1.24586

Proc Reg by sample type (zinc outlier and intercept removed)

The REG Procedure

Model: MODEL1

Dependent Variable: Pcon Pcon

Sample Type=P (personal)

Analysis of Variance

Source	DF	Sum of Squares	Mean Square	F Value	Pr > F
Model	1	1.05605	1.05605	310.68	<.0001
Error	54	0.18355	0.00340		
Uncorrected Total	55	1.23960			

Root MSE	0.05830	**R-Square**	0.8519
Dependent Mean	0.06269	**Adj R-Sq**	0.8492
Coeff Var	93.00160		

Parameter Estimates

Variable	Label	DF	Parameter Estimate	Standard Error	t Value	Pr > |t|	95% Confidence Limits	
Icon	Icon	1	0.69831	0.03962	17.63	<.0001	0.61888	0.77773

Proc Reg by particle size (zinc outlier removed, with intercept)

The REG Procedure

Model: MODEL1

Dependent Variable: Pcon Pcon

PROCode=0 (small particles)

Analysis of Variance

Source	DF	Sum of Squares	Mean Square	F Value	Pr > F
Model	1	0.75704	0.75704	505.15	<.0001
Error	43	0.06444	0.00150		
Corrected	44	0.82148			

Root MSE	0.03871	**R-Square**	0.9216
Dependent Mean	0.04500	**Adj R-Sq**	0.9197
Coeff Var	86.03220		

Parameter Estimates

Variable	Label	DF	Parameter Estimate	Standard Error	t Value	Pr > |t|	95% Confidence Limits	
Intercept	Intercept	1	0.00005391	0.00611	0.01	0.9930	-0.01226	0.01237
Icon	Icon	1	0.80285	0.03572	22.48	<.0001	0.73081	0.87489

Proc Reg by particle size (zinc outlier removed, with intercept)

The REG Procedure

Model: MODEL1

Dependent Variable: Pcon Pcon

PROCode=1 (large particles)

Analysis of Variance

Source	DF	Sum of Squares	Mean Square	F Value	Pr > F
Model	1	0.19865	0.19865	87.98	<.0001
Error	42	0.09483	0.00226		
Corrected Total	43	0.29348			

Root MSE	0.04752	**R-Square**	0.676
Dependent	0.04508	**Adj R-Sq**	0.669
Coeff Var	105.40298		

Parameter Estimates

Variable	Label	DF	Parameter Estimate	Standard Error	t Value	Pr > |t|	95% Confidence Limits	
Intercept	Intercept	1	0.01122	0.00802	1.40	0.1691	-0.00496	0.0274
Icon	Icon	1	0.52928	0.05643	9.38	<.0001	0.41540	0.64315

Proc Reg by particle size (zinc outlier and intercept removed)

The REG Procedure

Model: MODEL1

Dependent Variable: Pcon Pcon

PROCode=0 (small particles)

Analysis of Variance

Source	DF	Sum of Squares	Mean Square	F Value	Pr > F
Model	1	0.84815	0.84815	579.11	<.0001
Error	44	0.06444	0.00146		
Uncorrected Total	45	0.91259			

Root MSE	0.03827	**R-Square**	0.9294
Dependent Mean	0.04500	**Adj R-Sq**	0.9278
Coeff Var	85.04901		

Parameter Estimates

Variable	Label	DF	Parameter Estimate	Standard Error	t Value	Pr > |t|	95% Confidence Limits	
Icon	Icon	1	0.80295	0.03337	24.06	<.0001	0.73571	0.87020

Proc Reg by particle size (zinc outlier and intercept removed)

The REG Procedure

Model: MODEL1

Dependent Variable: Pcon Pcon

PROCode=1 (large particles)

Analysis of Variance

Source	DF	Sum of Squares	Mean Square	F Value	Pr > F
Model	1	0.28365	0.28365	122.89	<.0001
Error	43	0.09925	0.00231		
Uncorrected Total	44	0.38290			

Root MSE	0.04804	**R-Square**	0.7408
Dependent Mean	0.04508	**Adj R-Sq**	0.7348
Coeff Var	106.57066		

Parameter Estimates

Variable	Label	DF	Parameter Estimate	Standard Error	t Value	Pr > |t|	95% Confidence Limits	
Icon	Icon	1	0.56481	0.05095	11.09	<.0001	0.46206	0.66756

Metals Exposure/Air Quality Sampling Plan for Facility

Researchers at The University of Iowa, Colorado State University and Utah State have developed a new high-flow dust sampler to improve the quantification of low concentrations of inhalable dust. We have begun field testing in agricultural and metal refinery operations but want to evaluate their performance in additional processes that generate airborne metal concentrations.

Study:

- Sample (area or personal) the air using both the standard IOM and the new prototype sampler
- Compare the concentrations measured by both devices (gravimetric, ICP scan of 15 metals, table below), with analysis conducted by accredited labs (AIHA #17; AIHA PAT participant)
- Evaluate whether the new sampler improves our knowledge of airborne metal concentrations

Aluminum	Arsenic	Beryllium	Cadmium
Calcium	Chromium (total)	Copper	Iron
Lead	Manganese	Nickel	Selenium
Silver	Sodium	Zinc	

15-metal scan (NIOSH 7300/7303 Modified)

Additional metals as requested by participating location.

Equipment:

- The left image shows the two samplers that will be used to evaluate inhalable dust and metals; each sample will require both samplers
- The two pumps needed to sample the air are identified, with a total weight of 3.4 pounds, positioned on a worker hip (personal sampling) or on a cart (area)

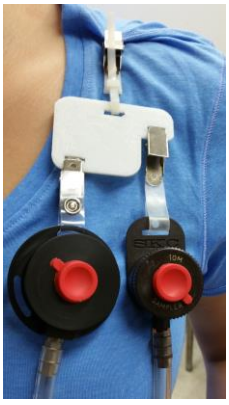

Inhalable Samplers: Prototype (left) and IOM (right)
red caps will be removed

The Gilian 12 (20.5 oz) will pull 10 Lpm of air through the prototype sampler, and the GilAir plus (20.5 oz) will pull 2 Lpm through the IOM.

Procedure:

- Conduct full-shift monitoring (at least 8 hours)
- Arrive to position monitors on workers/in areas at beginning of a shift; remove at end of shift
- We can deploy 4 paired monitors during one visit – (2 area, 2 personal or 3 personal, 1 area)

Timeline:

- Sampling to be performed during Summer/Fall of 2016
- Provide facility with concentration results
- Use sampler performance data in publication (non-disclosure of company, work area, worker details; present range of concentrations by manufacturing process)

REFERENCES

ACGIH. (2017). 2017 TLVs and BEIs Based on the Documentation of the Threshold Limit Values for chemical Substances and Physical Agents and Biological Exposure Indices. Cincinnati, OH: American Conference of Governmental Industrial Hygienists.

Aizenberg, V., Grinshpun, S. A., Willeke, K., Smith, J., & Baron, P. A. (2000). Performance Characteristics of the Button Personal Inhalable Aerosol Sampler. *AIHAJ - American Industrial Hygiene Association, 61*(3), 398-404. doi:10.1080/15298660008984550

Anthony, T. R., Cai, C., Mehaffy, J., Sleeth, D., & Volckens, J. (2017). Performance of prototype high-flow inhalable dust sampler in a livestock production facility. *J Occup Environ Hyg, 14*(5), 313-322. doi:10.1080/15459624.2016.1240872

Anthony, T. R., Landazuri, A. C., Van Dyke, M., & Volckens, J. (2010). Design and computational fluid dynamics investigation of a personal, high flow inhalable sampler. *Ann Occup Hyg, 54*(4), 427-442. doi:10.1093/annhyg/meq029

Anthony, T. R., Sleeth, D., & Volckens, J. (2016). Sampling efficiency of modified 37-mm sampling cassettes using computational fluid dynamics. *J Occup Environ Hyg, 13*(2), 148-158. doi:10.1080/15459624.2015.1091961

Ashley, K., & Harper, M. (2013). Closed-face filter cassette (CFC) sampling-guidance on procedures for inclusion of material adhering to internal sampler surfaces. *J Occup Environ Hyg, 10*(3), D29-33. doi:10.1080/15459624.2012.750554

ATSDR. (2007). ToxGuide™ for Lead Pb. [Pamphlet]. Atlanta, GA: Agency for Toxic Substances and Disease Registry.

ATSDR. (2008). Case Studies in Environmental Medicine (CSEM) Chromium Toxicity.

ATSDR. (2012). ToxGuide™ for Cadmium Cd. [Pamphlet]. Atlanta, GA: Agency for Toxic Substances and Disease Registry.

AWS. (1979). Fumes and Gases in the Welding Environment: A Research Report on Fumes and Gases Generated During Welding Operations (F. Y. Speight Ed.). Miami, FL.

Baron, P. A. (2003). *NIOSH Manual of Analytical Methods: Chapter O*. Cincinnati, OH: National Institute for Occupational Safety and Health.

BLS. (2008). Fatal occupational injuries by occupation and event or exposure, All United States. Retrieved from https://www.bls.gov/iif/oshwc/cfoi/cftb0236.pdf

BLS. (2012). Incidence rates of nonfatal occupational injuries and illnesses by industry and case types. Retrieved from https://www.bls.gov/iif/oshwc/osh/os/ostb3581.pdf

BLS. (2014). Fatal occupational injuries by occupation and event or exposure, all United States. Retrieved from https://www.bls.gov/iif/oshwc/cfoi/cftb0290.pdf

BLS. (2015). Industry Injury and Illness Data. *Injuries, Illnesses, and Fatalities.* Retrieved from https://www.bls.gov/iif/oshsum.htm#15Summary_Tables

BLS. (2016, March 31, 2017). May 2016 National Occupational Employment and Wage Estimates United States. *Occupational Employment Statistics.* Retrieved from https://www.bls.gov/oes/current/oes_nat.htm#51-0000

BLS. (2017). Industries at a Glance: Manufacturing. Retrieved from https://www.bls.gov/iag/tgs/iag31-33.htm

Brisson, M. J., & Archuleta, M. M. (2009). The real issue with wall deposits in closed filter cassettes--what's the sample? *J Occup Environ Hyg, 6*(12), 783-788. doi:10.1080/15459620903261427

Burgess, W. A. (1995). Recognition of Health Hazards in Industry: A Review of Materials Processes (2 ed.): Wiley-Interscience.

Ceballos, D., King, B., Beaucham, C., & Brueck, S. E. (2015). Comparison of a Wipe Method With and Without a Rinse to Recover Wall Losses in Closed Face 37-mm Cassettes used for Sampling Lead Dust Particulates. *J Occup Environ Hyg, 12*(10), D225-231. doi:10.1080/15459624.2015.1009991

CEN. (1993). Workplace Atmospheres - Size Fraction Definitions for Measurement of Airborne Particles (Vol. European Standard EN 481). Brussels: European Standardization Committee (CEN).

Cheng, Y. H., Chao, Y. C., Wu, C. H., Tsai, C. J., Uang, S. N., & Shih, T. S. (2008). Measurements of ultrafine particle concentrations and size distribution in an iron foundry. *J Hazard Mater, 158*(1), 124-130. doi:10.1016/j.jhazmat.2008.01.036

Cheng, Y. S., Zhou, Y., Irvin, C. M., Pierce, R. H., Naar, J., Backer, L. C., . . . Baden, D. G. (2005). Characterization of Marine Aerosol for Assessment of Human Exposure to Brevetoxins. *Environmental Health Perspectives, 113*(5), 638-643. doi:10.1289/ehp.7496

Chung, K. Y. K., & Scott, R. M. (1997). Particle-size Analysis of Welding Fume [Abstract]. *J. Aerosol Sci., 28*(2), 339.

Clinkenbeard, R. E., England, E. C., Johnson, D. L., Esmen, N. A., & Hall, T. A. (2002). A field comparison of the IOM inhalable aerosol sampler and a modified 37-mm cassette. *Appl Occup Environ Hyg, 17*(9), 622-627. doi:10.1080/10473220290095943

Cohen, H. J., & Powers, B. J. (2000). Particle Size Characterizations of Copper and Zinc Oxide Exposures of Employees Working in a Nonferrous Foundry Using Cascade Impactors. *AIHAJ - American Industrial Hygiene Association, 61*(3), 422-430. doi:10.1080/15298660008984554

Demange, M., Gorner, P., Elcabache, J. M., & Wrobel, R. (2002). Field comparison of 37-mm closed-face cassettes and IOM samplers. *Appl Occup Environ Hyg, 17*(3), 200-208. doi:10.1080/104732202753438289

EPA. (2012). What is Particulate Matter? Retrieved from https://www3.epa.gov/region1/eco/uep/particulatematter.html

Evans, D. E., Heitbrink, W. A., Slavin, T. J., & Peters, T. M. (2008). Ultrafine and respirable particles in an automotive grey iron foundry. *Ann Occup Hyg, 52*(1), 9-21. doi:10.1093/annhyg/mem056

Gao, P., Chen, B. T., Baron, P. A., & Soderholm, S. C. (2002). A Numerical Study of the Performance of an Aerosol Sampler with a Curved, Blunt, Multi-Orificed Inlet. *Aerosol Science and Technology, 36*(5), 540-553. doi:10.1080/02786820252883784

Glinsmann, P. W., & Rosenthal, F. S. (1985). Evaluation of an aerosol photometer for monitoring welding fume levels in a shipyard. *Am Ind Hyg Assoc J, 46*(7), 391-395. doi:10.1080/15298668591395030

Gomes, J., Lloyd, O., & Norman, N. (2002). The health of the workers in a rapidly developing country: effects of occupational exposure to noise and heat. *Occup. Med., 52*(3), 121-128.

Gomes, J., Lloyd, O. L., Norman, N. J., & Pahwa, P. (2001). Dust exposure and impairment of lung function at a small iron foundry in a rapidly developing country. *Occup Environ Med, 58*, 656-662. doi:10.1136/oem.58.10.656

Guha, N., Loomis, D., Guyton, K. Z., Grosse, Y., El Ghissassi, F., Bouvard, V., . . . Straif, K. (2017). Carcinogenicity of welding, molybdenum trioxide, and indium tin oxide. *The Lancet Oncology, 18*(5), 581-582. doi:10.1016/s1470-2045(17)30255-3

Harper, M., & Demange, M. (2007). Concerning sampler wall deposits in the chemical analysis of airborne metals. *J Occup Environ Hyg, 4*(9), D81-86. doi:10.1080/15459620701493149

Harper, M., Pacolay, B., Hintz, P., & Andrew, M. E. (2006). A comparison of portable XRF and ICP-OES analysis for lead on air filter samples from a lead ore concentrator mill and a lead-acid battery recycler. *J Environ Monit, 8*(3), 384-392. doi:10.1039/b518075a

Hauck, B. C., Grinshpun, S. A., Reponen, A., Reponen, T., Willeke, K., & Bornschein, R. L. (1997). Field Testing of New Aerosol Sampling Method With a Porous Curved Surface as Inlet. *American Industrial Hygiene Association Journal, 58*(10), 713-719.

Hendricks, W., Stones, F., & Lillquist, D. (2009). On wiping the interior walls of 37-mm closed-face cassettes: an OSHA perspective. *J Occup Environ Hyg, 6*(12), 732-734. doi:10.1080/15459620903012028

Hobson, A., Seixas, N., Sterling, D., & Racette, B. A. (2011). Estimation of particulate mass and manganese exposure levels among welders. *Ann Occup Hyg, 55*(1), 113-125. doi:10.1093/annhyg/meq069

IARC. (1990). IARC Monographs on the Evaluation of Carcinogenic Risks To Humans: Chromium, Nickel and Welding. *49*, 455-476.

Kennedy, E. R., Fischbach, T. J., Song, R., Elller, P. M., & Shulman, S. A. (Eds.). (1995). Cincinnati, OH: U.S. Department of Health and Human Services.

Kenny, L. C., Aitken, R. J., Baldwin, P. E. J., Beaumont, G. C., & Maynard, A. D. (1999). The Sampling Efficiency of Personal Inhalable Aerosol Samplers in Low Air Movement Environments *J. Aerosol Sci., 30*(5), 627-638.

Kenny, L. C., Aitken, T. R., Chalmers, J. C., Fabries, J. F., Gonzalez-Fernandez, E., Kromhout, F. H., . . . Prodi, V. (1997). A Collaborative European Study of Personal Inhalable Aerosol Sampler Performance *Ann. Occup. Hyg., 41*(2), 135-153.

Koehler, K. A., Anthony, T. R., Van Dyke, M., & Volckens, J. (2012). Solid versus liquid particle sampling efficiency of three personal aerosol samplers when facing the wind. *Ann Occup Hyg, 56*(2), 194-206. doi:10.1093/annhyg/mer077

Koehler, K. A., & Peters, T. M. (2015). New Methods for Personal Exposure Monitoring for Airborne Particles. *Curr Environ Health Rep, 2*(4), 399-411. doi:10.1007/s40572-015-0070-z

L'Orange, C., Anderson, K., Sleeth, D., Anthony, T. R., & Volckens, J. (2016). A Simple and Disposable Sampler for Inhalable Aerosol. *Ann Occup Hyg, 60*(2), 150-160. doi:10.1093/annhyg/mev065

Landazuri, A. C., Saez, A. E., & Anthony, T. R. (2016). Three-dimensional computational fluid dynamics modeling of particle uptake by an occupational air sampler using manually-scaled and adaptive grids. *J Aerosol Sci, 95*, 54-66. doi:10.1016/j.jaerosci.2016.01.004

Lehnert, M., Pesch, B., Lotz, A., Pelzer, J., Kendzia, B., Gawrych, K., . . . Weldox Study, G. (2012). Exposure to inhalable, respirable, and ultrafine particles in welding fume. *Ann Occup Hyg, 56*(5), 557-567. doi:10.1093/annhyg/mes025

Liden, G., Melin, B., Lidblom, A., Lindberg, K., & Noren, J. O. (2000). Personal sampling in parallel with open-face filter cassettes and IOM samplers for inhalable dust--implications for occupational exposure limits. *Appl Occup Environ Hyg, 15*(3), 263-276. doi:10.1080/104732200301584

Malmqvist, K., Johansson, G., Bohgard, M., & Akselsson, R. (1986). *Process-dependent Characteristics of Welding Fume Particles.* Paper presented at the International Conference on Health Hazards and Biological effects of Welding Fumes and Gases.

Mark, D. (1990). The Use of Dust-Collecting Cassettes in Dust Samplers *Ann. Occup. Hyg., 34*(3), 281-291. doi:10.1093/annhyg/34.3.281

Mark, D., & Vincent, J. H. (1986). A New Personal Sampler for Airborne Total Dust in Workplace *Ann. Occup. Hyg., 30*(1), 89-102. doi:10.1093/annhyg/30.1.89

Michaud, D., Baril, M., Dion, C., & Perrault, G. (1996). Characterization of Airborne Dust from Two Nonferrous Foundries by Physico-chemical Methods and Multivariate Statistical Analyses. *J Air Waste Manag Assoc, 46*(5), 450-457. doi:10.1080/10473289.1996.10467478

NIOSH. (1985). Recommendations for Control of Occupational Safety and Health Hazards.... Foundries.

O'Connor, S., O'Connor, P. F., Feng, H. A., & Ashley, K. (2014). Gravimetric Analysis of Particulate Matter using Air Samplers Housing Internal Filtration Capsules. *Gefahrst Reinhalt Luft, 74*(10), 403-410.

OSHA. (1996). Permissible Exposure Limits (PELS) for Air Contaminants. Retrieved from https://www.osha.gov/pls/oshaweb/owadisp.show_document?p_id=4536&p_table=UNIFIED_AGENDA

OSHA. (2002). Welding, Cutting and Brazing. *OSHA Archive.* Retrieved from https://www.osha.gov/archive/oshinfo/priorities/welding.html

OSHA. (2004). Particulates Not Otherwise Regulated (Total Dust). Retrieved from https://www.osha.gov/dts/chemicalsampling/data/CH_259640.html

OSHA. (2008). OSHA Technical Manual: Section II: Chapter 2: Surface Contaminants, Skin Exposure, Biological Monitoring and Other Analyses. Retrieved from https://www.osha.gov/dts/osta/otm/otm_ii/otm_ii_2.html

OSHA. (2011). New OSHA National Emphasis Program will help protect workers from chemical and physical hazards in the primary metals industries. *OSHA Trade Release.* Retrieved from https://www.osha.gov/pls/oshaweb/owadisp.show_document?p_table=NEWS_RELEASES&p_id=19935

OSHA. (2015). OSHABrief: Hazard Communication Standard: Safety Data Sheets. Retrieved from https://www.osha.gov/Publications/OSHA3514.html

Phalen, R. F., Hinds, W. C., John, W., Lio, P. J., Lippmann, M., McCawley, M. A., . . . Stuart, B. O. (1988). Particle Size-selective Sampling in the Workplace: Rationale and Recommended Techniques *Ann. Occup. Hyg., 32*(1), 403-411. doi:0003-4878/88

Puskar, M. A., Harkins, J. M., Moomey, J. D., & Hecker, L. H. (1991). INTERNAL WALL LOSSES OF PHARMACEUTICAL DUCTS DURING CLOSED-FACE, 37-MM POLYSTYRENE CASSETTE SAMPLING. *American Industrial Hygiene Association Journal, 52*(7), 280-286. doi:10.1080/15298669191364730

Rodahl, K. (2003). Occupational Health Conditions in Extreme Environments. *The Annals of Occupational Hygiene*. doi:10.1093/annhyg/meg033

Rosenman, K. D., Reilly, M. J., Rice, C., Hertzberg, V., Tseng, C.-Y., & Anderson, H. A. (1996). Silicosis among Foundry Workers: Implication for the Need to Revise the OSHA Standard. *Am J Epidemiology, 144*(9), 890-900. doi:10.1093/oxfordjournals.aje.a009023

Soderholm, S. C. (1989). Proposed International Conventions for Particle Size-Selective Sampling *Ann. Occup. Hyg., 33*(3), 301-320. doi:10.1093/annhyg/33.3.301

Stellman, J. M. e. (1998). Metal Processing and Metal Working. In J. M. Stellman (Ed.), *Encyclopaedia of Occupational Health and Safety* (4 ed., Vol. 3, pp. 82.11-82.41). Geneva, Switzerland: International Labour Office.

Stewart, J., Sleeth, D. K., Handy, R. G., Pahler, L. F., Anthony, T. R., & Volckens, J. (2017). Assessment of increased sampling pump flow rates in a disposable, inhalable aerosol sampler. *J Occup Environ Hyg, 14*(3), 207-213. doi:10.1080/15459624.2016.1237028

USGS. (1999). ICP-AES Technique Description. Retrieved from https://minerals.cr.usgs.gov/gips/na/5process.html

Wake, D., Mark, D., & Northage, C. (2002). Ultrafine Aerosols in the Workplace. *Ann. Occup. Hyg., 46*(1), 235-238. doi:10.1093/annhyg/mef678

Westberg, H., Lofstedt, H., Selden, A., Lilja, B. G., & Naystrom, P. (2005). Exposure to Low Molecular Weight Isocyanates and Formaldehyde in Foundries Using Hot Box Core Binders. *Ann Occup Hyg, 49*(8), 719-725. doi:10.1093/annhyg/mei040

Zhang, J., J., B., & R., D. (1985). Elemental Composition and Source Investigation of Particulates Suspended in the Air of an Iron Foundry *The Science of the Total Environment, 41*, 13-28. doi:10.1016/0048-9697(85)90158-5

Zhou, Y., & Cheng, Y. S. (2010). Evaluation of IOM personal sampler at different flow rates. *J Occup Environ Hyg, 7*(2), 88-93. doi:10.1080/15459620903418746

Zimmer, A. T., & Maynard, A. D. (2002). Investigation of the Aerosols Produced by a High-speed, Hand-held Grinder Using Various Substrates. *The Annals of Occupational Hygiene, 46*(8), 663-672. doi:10.1093/annhyg/mef089

Zugasti, A., Montes, N., Rojo, J. M., & Quintana, M. J. (2012). Field comparison of three inhalable samplers (IOM, PGP-GSP 3.5 and Button) for welding fumes. *J Environ Monit, 14*(2), 375-382. doi:10.1039/c1em10616c